INFORMATION TO USERS

This manuscript has been reproduced from the microfilm master. UMI films the text directly from the original or copy submitted. Thus, some thesis and dissertation copies are in typewriter face, while others may be from any type of computer printer.

The quality of this reproduction is dependent upon the quality of the copy submitted. Broken or indistinct print, colored or poor quality illustrations and photographs, print bleedthrough, substandard margins, and improper alignment can adversely affect reproduction.

In the unlikely event that the author did not send UMI a complete manuscript and there are missing pages, these will be noted. Also, if unauthorized copyright material had to be removed, a note will indicate the deletion.

Oversize materials (e.g., maps, drawings, charts) are reproduced by sectioning the original, beginning at the upper left-hand corner and continuing from left to right in equal sections with small overlaps.

Photographs included in the original manuscript have been reproduced xerographically in this copy. Higher quality 6" x 9" black and white photographic prints are available for any photographs or illustrations appearing in this copy for an additional charge. Contact UMI directly to order.

ProQuest Information and Learning
300 North Zeeb Road, Ann Arbor, MI 48106-1346 USA
800-521-0600

SOME EXACT AND APPROXIMATE INVERSE BOUNDARY AND SCATTERING PROBLEMS

BY

KHALID MASOOD

A Dissertation Presented to the

DEANSHIP OF GRADUATE STUDIES

KING FAHD UNIVERSITY OF PETROLEUM & MINERALS

DHAHRAN, SAUDI ARABIA

In Partial Fulfillment of the
Requirements for the Degree of

DOCTOR OF PHILOSOPHY

In

MATHEMATICAL SCIENCES

March 2002

Some Exact and Approximate Inverse Boundary and Scattering Problems

by

KHALID MASOOD

King Fahd University Of Petroleum & Minerals
Dhahran, Saudi Arabia
March 2002

KING FAHD UNIVERSITY OF PETROLEUM & MINERALS
DHAHRAN 31261, SAUDI ARABIA

DEANSHIP OF GRADUATE STUDIES

This Dissertation, written by **KHALID MASOOD** under the direction of his dissertation advisor and approved by his dissertation committee, has been presented to and accepted by the Dean of Graduate Studies, in partial fulfillment of the requirements for the degree of **DOCTOR OF PHILOSOPHY IN MATHEMATICAL SCIENCES**.

Dissertation Committee

Dr. F. D. Zaman (Dissertation Advisor)

Dr. Haydar Akca (Member)

Dr. Khaled M. Furati (Member)

Dr. Khaled M. Furati
Department Chairman

Dr. Gabor Korvin (Member)

Dr. Osama A. Jannadi
Dean of Graduate Studies

Dr. Salim Messaoudi (Member)

22/4/2002
Date

Dedicated to

My Parents **for their care and continuous prayers for my success;**

My Wife **for her care, patience and support to complete this work;**

My lovely and intelligent daughter and son:

Rabia and Athar

ACKNOWLEDGEMENTS

First and foremost, all praise is to Almighty Allah Who gave me the courage and patience to carry out this work, and peace and blessings be upon our prophet Muhammad.

Acknowledgment is due to King Fahd University of Petroleum & Minerals for providing support to this work, particularly appreciation is due to the Department of Mathematical Sciences for its support.

I am grateful to my advisor, Dr. F. D. Zaman, for his guidance and inspiration on both my study and research at KFUPM. He encouraged me to try out my ideas and provided me with the perfect combination of freedom to explore, and guidance.

Thanks are also due to my dissertation committee members including Dr. Haydar Akca, Dr. Khaled M. Furati, Dr. Gabor Korvin and Dr. Salim Messaoudi for their interest, cooperation, advice and constructive criticism.

I would also like to acknowledge chairmen Department of Mathematical Sciences, previously Dr. Walid S. Al-Sabah and presently Dr. Khaled M. Furati, for allowing me to use facilities in the department and for making every effort to make the

department more conducive for studies and research.

Lastly, I would like to thank all my teachers here at KFUPM and at previous institutions, all faculty and staff members of the Department of Mathematical Sciences, my fellow graduate students, and all my friends from whom I learned and who made the long working hours pleasant.

Contents

List of Figures

Abstract

Name:	Khalid Masood
Title:	Some Exact and Approximate Inverse Boundary and Scattering Problems
Major Field:	Mathematical Sciences
Date of Degree:	March 2002

The inverse problems are important in seismic exploration and underground geology. The frequently used earth model for such a purpose is that of a homogeneous and isotropic medium. This may not be an accurate description of many practical situations. We consider a model that incorporates the effects of damping in the medium and develop an inversion procedure for this case. It is hoped that the results based upon this model will prove to be more realistic in some situations of interest.

We consider the inverse problem of recovering the initial disturbance from the information of the final data. The damped and undamped models are compared by performing some numerical experiments. An application of damped wave equation is also presented which involve the introduction of a damping parameter in such a way that it closely approximates the heat conduction model. It is shown that the modified model based on the damped wave equation behaves much better than the classical heat conduction model.

The Gelfand-Levitan and Marchenko (GLM) procedure is used for the development of inversion formalism for estimating parameter changes across inhomogeneities. We use this method to recover a one-dimensional shear velocity variation in the surface of the earth. The Love waves, traveling in a layer overlying a half space, incident upon delta function potential, are considered. The equation of motion for Love waves is transformed to the Schrödinger equation by assuming a small variation in shear velocity which leads to the potential term in the governing equation of Love waves.

We consider a problem of the identification of physical properties of the earth using the damped wave equation based on the linearized inversion associated with Born's inversion theory. We assume that damping and sound speed are well approximated by the background plus the perturbation. The application of the method leads to a linear integral equation involving variations in sound speed and damping. Our aim is to recover these variations in velocity and damping, which in turn yields a map of the interfaces in the interior of the earth.

Doctor of Philosophy Degree
King Fahd University Of Petroleum & Minerals
March 2002

ملخص

الاســـم : خالد مسعود

العنوان : بعض الحلول التامة و التقريبية لمسائل المعكوس الحدية والمشتتة

التخصص : العلوم الرياضية

تاريخ الشهادة : مارس 2002م

إن المسائل العكسية مهمة جداً في الاستكشافات الزلزالية والجيولوجيا التحت الأرضية فنموذج الأرض الأكثر إستخدام لهذا الغرض هو الأوسط المتجانس والمتوحد الخواص. هذا النموذج ليس دقيقا في حالات كثيرة. هنا نطبق نموذج يأخذ بعين الاعتبار آثار التضاؤل في الوسط ونطبق طريقة عكسية لهذه الحالة. " نتمني أن نتائج هذا النموذج تكون مطابقة للواقع "

نستخدم المسائلة العكسية لإستعاد التشويش الإبتدائي من المعطيات والبيانات النهائية. كمانقارن نماذج التضاؤل وعدم التضاؤل بإستخدام تجارب عددية. نقدم كذلك تطبيقا خاصًا بمعادلة الموجة المتضائلة والتي تتضمن مقدمة لبراميتر التضاؤل، والتي تشبه معادلة توصيل الحرارة. نبين أن هذا النموذج أحسن بكثير من النموذج الكلاسيكي لتوصيل الحرارة.

نستخدم طريقة Gelfand-Levitan and Marchenko (GLM) في تطوير التشكيلة العكسية في تقدير تغيرات البراميتر عبر المناطق الغير متجانسة. نستخدم هذه الطريقة في تحديد سرعة الإنكسارعند سطح الأرض (البعد الواحد). نأخذ بعين الإعتبار موجات Love الساقطة. نحول معادلة حركة الموجات Love إلى معادلة Schrödinger بإفتراض تغيرات صغيرة في سرعة الكسر والتي تؤدي الى جهد في عبارة معادلة موجات Love .

نعين الخواص الفيزيائية للأرض بأستخدام معادلة الموجة المتضائلة الناتجة عن الطريقة العكسية المرفقة للنظرية العكسية لـ Born. وفى هذه الحالة نفترض أن التضاؤل وسرعة الصوت يكونان مقربين بالخلفية والتشويش. إن تطبيق هذه الطريقة يؤدي إلى معادلة تكاملية خطية تحتوي على تغيرات في سرعة الصوت والتضاؤل. فهدفنا هو إستيعاد هذه التغيرات في السرعة والتضاؤل والتي تؤدي إلى خريطة لبطن الأرض .

درجة الدكتوراه في الفلسفة

جامعة الملك فهد للبترول والمعادن، الظهران، المملكة العربية السعودية

مارس 2002 م

Chapter 1

INTRODUCTION

The fundamental task of science is to probe the world around us. The ability to infer information from an object without direct contact expands man's sensory horizon. The most powerful method for accomplishing this goal is to direct energy, in the form of waves, at an object and to observe the waves after they have interacted with that object. This method constitutes an important class of inverse problems known as inverse scattering problems. For example, a conventional photograph is produced by directing light waves from the flash bulb to the object in question and recording the image formed by reflected waves on the film. The results of such an experiment can be easily understood by simply looking at the picture, while the waves (such as X-rays, microwaves, sound waves) which penetrate the medium being studied are less directly meaningful. A wave which penetrates deeply into a medium gives us the opportunity to see below the surface. Inverse problems can be encountered in diverse fields ranging from medical to engineering sciences. They occur in geophysics, plasma diagnostics, electrodynamics, optics and many other areas. Typical inverse problems include the interpretation of electrocardiograms, image processing and back-projection tomography [3,30,33].

There is, in most cases, quite a natural distinction between the direct and the

inverse problem. For instance, predicting the future behavior of a physical system from the knowledge of its present state is regarded as a direct problem. However, determining the past state of a system from present observations, or the identification of physical parameters from observations of probed data constitute inverse problems. Some of the important classes of such inverse problems are the determination of the initial state (temperature or displacement) from the observed data; the determination of physical parameters of the medium; and determination of the shape and the nature of the scattering object in a medium from the scattered data [13, 59]. These inverse problems are often improperly posed. This ill-posedness might be due to the nonuniqueness or due to the discontinuous dependence of solutions on the data [15, 28, 31]. Therefore, a solution often has to be chosen from many possible different solutions in solving inverse scattering problems. As an added complication, the scattered field is nonlinearly related to the scattering object. This nonlinear relationship exacerbates the difficulty of finding a closed form solution to inverse scattering problems. However, if the scattered field is approximated as a linear function of the object, it vastly simplifies the inverse problem.

The correct understanding and solution of many inverse problems depend on the rigorous and exact analysis that can be obtained by faithfully solving the governing equation. Inverse boundary value problems are a class of problems in which unknown coefficients or data of a partial differential equation represent internal parameters of a medium, and the known information consists of the boundary measurements of solutions [34, 71]. These problems can arise in heat conduction, crack and corrosion identification, determination of elastic parameters etc. Several approaches and math-

ematical methods can be applied to the governing equation that can lead to analytic reconstruction methods for these problems.

The objective of seismic inversion is to estimate earth parameters, such as velocity and density from seismic data. In a seismic experiment, a source is set off at a point on the surface of earth, and the upward propagating wave is then measured at an array of receivers near the source [14, 16]. The image of a subsurface, so constructed is important, either for theoretical purposes or for the purpose of interpretation by a geologist for the identification of likely subsurface regions for resource extraction. These inverse problems form a class of problems in which unknown coefficients of wave equation represent internal parameters of a medium and the known information consists of boundary measurements. As mentioned above, an inverse problem can be simplified if the scattered field is approximated as a linear function of the object. There are several conditions under which the problem can be linearized. These conditions, for example, are those of the Born and the Rytov approximations [19, 49, 66]. For instance, in the Born approximation, the scattered field amplitude is a linear function of the object, whereas in the Rytov approximation, the phase perturbation is its linear function. Furthermore, another way of obtaining a linearized relationship between data and the object is to use high frequency waves. In this case concepts of reflection and refraction of plane waves at the plane interface carry over to inhomogeneous media. If the primary concern is high frequency seismic inversion, then the real objective is to obtain a reflector map of the earth's interior and devise means for estimating the changes in earth parameters across those reflectors.

1.1 A Brief Historical Background

One of the first rigorously treated inverse problem was Abel's solution of the tautochrone problem, published in 1826 [1]. Abel's solution to this problem in classical mechanics is of importance in many areas of inverse scattering. The next major exposition of inverse scattering was instigated by investigations into the structure of the atom by Rutherford in 1911 [64]. Inverse scattering became a subject of paramount importance with the advent of wave mechanical formulation of Schrödinger in 1926. The Schrödinger wave equation provided a way of relating the state of a particle to the potential influencing it at any time [22].

It soon became apparent that the inverse solution of the Schrödinger equation presented a formidable task and appropriate approximate solutions were eagerly sought by numerous workers in the field. Born eventually showed in 1926 that provided the scattering interaction was sufficiently weak, a particularly simple relationship existed between the scattered field and the scattering potential. The exact inverse solution of Schrödinger equation was given by Gelfand and Levitan and independently by Marchenko in the early 1950's [36, 55]. Historically the first exact inverse scattering solution was developed for the Schrödinger equation rather than the wave equation. Nevertheless, the wave equation can be obtained from Schrödinger equation by transformation. The importance of Gelfand-Levitan and Marchenko solution is well established, however in practice obtaining an exact inversion is not necessarily the end of the story, mainly due to the nature of measured data. Although R. G. Newton generalized the Gelfand-Levitan and Marchenko integral equation to higher

dimensions [60–62], the method is computationally cumbersome and is restricted to certain types of potentials.

The mapping of the interior of the earth from observations on surface of the earth is also an inverse problem. Herglotz [48] constructed the velocity exactly from the measurements of the arrival time as a function of distance from the earthquake source. The Herglotz-Wiechert [48, 72] construction only gives a unique result when velocity increases monotonically with depth (Gerver and Markushevitch [39, 55]). Despite the mathematical elegance of the exact nonlinear inversion schemes, they are of limited applicability. In order to increase applicability to a wide variety of problems, many researchers used approximation techniques such as linearization and perturbation methods. In the last three decades, many researchers around the world worked on the seismic inverse problems, see for example Gerver [37], Bleistein and Cohen [15–17], Liner [53], Hanitzsch [46], among others.

1.2 Objectives

The purpose of this Thesis is three-fold. Firstly, to consider initial inverse problems for damped wave equations and applying it to the inverse problem in the heat conduction. Secondly, to consider inverse problem of shear velocity reconstruction for seismic problems involving Love wave propagation using the Gelfand-Levitan theory. Thirdly, to consider the velocity inversion procedure based on the Born approximation applied to seismic inverse problems. Moreover, we will try to tie these into three aspects of a single problem.

1.2.1 Initial Inverse Problems

The usual method of solving inverse problems of initial profile reconstruction for heat conduction and wave problems is by applying Picard's criterion to integral equation of the first kind with the associated singular system. The inversion procedure presented in this Thesis uses the damped wave equation model. Instead of initial profile reconstruction of the wave equation, we consider initial profile reconstruction of the damped wave equation because it more realistically models the medium of interest. Moreover, the damped wave equation model regularizes the classical heat conduction model.

1.2.2 Shear Velocity Inversion for Love Waves

In 1950 Marchenko, and Gelfand-Levitan independently in 1952, found an inverse solution to the Schrödinger equation. They were also able to establish necessary conditions for the potential to be uniquely determined. Because of the considerable power and theoretical importance of the method, it became a touchstone by which all other inversion schemes were gauged. From a mathematical stance, the Gelfand-Levitan and Marchenko method is underpinned by the ability to construct an integrating kernel possessing the desired properties. The class of reflection coefficients which allow such integrating kernel is small and even for most simple scatterer, one is usually forced to resort to a numerical solution. These restrictions make practical implementation of Gelfand-Levitan and Marchenko method most challenging. In this Thesis an inversion procedure for the shear velocity of Love waves is considered. The equation

of motion for Love waves is transformed to the Schrödinger equation and then the potential is recovered by applying Gelfand-Levitan and Marchenko procedure.

1.2.3 Velocity Inversion Procedure

The seismic inverse problem has a difficulty, inherent in the inverse problem, of being nonlinear. The model describing the propagation of waves inside the earth contains the product of the unknown field times the unknown earth parameters. To overcome this difficulty, a linearization of the problem is performed by introducing background earth parameter values. It is expected that the map obtained through such a process is an approximate image of the subsurface structures. Indeed, sophistication in the development of such a technique would naturally complicate the problem. In this Thesis we introduce a damping term in the wave equation and its effect on the velocity inversion as well as on the recovery of damping is investigated.

1.3 Organization of the Dissertation

In Chapter 2, the initial inverse problems of damped and undamped wave equations are presented. The procedure consists of transforming the problem into integral equation of the first kind. The Picard's criterion which ensures the existence as well as a unique solution to the initial inverse problem can be applied to integral equation of the first kind. We considered the damped wave equation instead of the wave equation because it more realistically models the medium of interest. The inversion procedure developed for one-dimensional problems is then extended to two-dimensional problems.

The inversion method for the shear velocity of Love waves is presented in Chapter 3. The method is based on Gelfand-Levitan and Marchenko technique, which can be applied to the Schrödinger equation. First, a transformation technique to convert governing equation of Love waves to the Schrödinger equation is developed. The basic assumption we made is by introducing background parameters, which is certainly permissible in many physical situations.

In Chapter 4, a procedure is presented for high frequency inversion of impulse response data. The starting point is an inverse scattering integral equation based on the Born's approximation for modeling of the direct scattering problem. The process is developed on the one-dimensional damped wave equation by considering constant background and zero-offset experiment. The insight gained from the one-dimensional problem is then extended to three dimensional problem. The aim of introducing damping term in the wave equation is to get increasingly better approximation to velocity variations, which in turn ensure a more accurate map of the earth's interior.

Finally, to ensure smooth reading of the thesis, complicated derivations and the mathematical tools needed are relegated to the appendices.

Chapter 2

INITIAL INVERSE PROBLEMS

2.0.1 Abstract

The initial inverse problem in damped and undamped wave equations arise when experimental measurements of disturbance at a particular time are used to calculate the disturbance at some particular time in the past. Such problems can be reduced to integral equations of the first kind and Picard's criterion can be applied to solve the inverse problem with the help of the associated singular system.

Usually, in the real world, the medium of propagation offers some resistance. so it is desirable to introduce a damping term in the wave equation. We consider the inverse problem of recovering the initial disturbance from the information of the final data. The damped and undamped models are compared by performing some numerical experiments. An application of damped wave equation is also presented which involve the introduction of a damping parameter in such a way that it closely approximates the heat conduction model. It is shown that the modified model based on the damped wave equation behaves much better than the classical heat conduction model.

2.1 Introduction

Initial inverse problems are much less encountered in the literature than some other types of inverse problems. However, one of the earliest studies on inverse problems by Fourier and Kelvin [21] were concerned with initial inverse problems. that is, they tried to estimate the initial temperature distribution of the earth from current temperature measurements. Recently Nakamura et al. [59] used transformation techniques to solve the initial inverse problem in heat conduction and Al-Khalidi [5] dealt with the problem numerically. For comprehensive review of the literature and summary of various approaches in the field of inverse heat conduction problems. one can consult the books by Beck et al. [9] and by Hensel [47]. The inverse heat conduction problems are ill-posed [34], so the slightest error in the measurements can give abrupt results. If the damping of the medium is not taken into account then the initial inverse problem may also give abrupt results. We consider the regularization of the heat conduction problem by introducing the model based upon the damped wave equation. The application of this idea to some interesting inverse problems in heat conduction have appeared in Zaman and Masood [74], Masood and Zaman [56], Masood, Messaoudi and Zaman [57].

In many physical applications, one encounters the situation where the usual wave equation does not serve as a realistic model. For instance, the wave equation does not model correctly the medium of propagation that offers resistance, so a damping term which is proportional to velocity is introduced in the wave equation [65,71]. The inverse problems in such damped waves can be of interest in some cases. For example.

if a signal of an explosion is received from a known location then our inverse problem may predict the magnitude of the initial explosion.

2.1.1 Organization of the Chapter

The basic definitions and mathematical tools needed for this chapter are relegated to Appendix-A. In the second section the method of initial inverse problems is described for the wave equation without introducing a damping term. In the third section, we consider the one-dimensional wave equation with a damping term and perform some numerical experiments for different values of the damping parameter by constructing some particular examples. We also consider the two-dimensional problem and perform the same analysis as for the one-dimensional problem. We also present an interesting application of the damped wave equation to the heat conduction model. Finally, in the last section conclusions are presented.

2.2 Initial Inverse Problems in the Wave Equation

In the first subsection the procedure to recover the initial profile from the final profile is described in detail for the one-dimensional wave equation. In the second subsection the procedure is applied to the two-dimensional wave equation.

2.2.1 Initial Inverse Problem in the One-dimensional Wave Equation

First, we consider the one-dimensional wave equation

$$\frac{\partial^2 u}{\partial t^2} = \frac{\partial^2 u}{\partial x^2}, \qquad x \in [0, \pi],\ t \geq 0, \tag{2.1}$$

with homogeneous Dirichlet boundary conditions

$$u(0, t) = u(\pi, t) = 0. \tag{2.2}$$

Assume the final distribution

$$f(x) \doteq u(x, T). \tag{2.3}$$

We want to determine the initial profile $v_0(x)$

$$v_0(x) \doteq u(x, 0), \tag{2.4}$$

subject to

$$\frac{\partial u}{\partial t}(x, 0) = 0. \tag{2.5}$$

The functions $\phi_n(x) \doteq \sqrt{\frac{2}{\pi}} \sin(nx)$ form a complete orthonormal system in $L^2[0, \pi]$ and eigenfunctions of $\frac{d^2}{dx^2}$ on $[0, \pi]$. Thus $v_0(x) \in L^2[0, \pi]$ can be expanded as

$$v_0(x) = \sum_{n=1}^{\infty} c_n \phi_n(x) \ , \ \ x \in [0, \pi], \tag{2.6}$$

where

$$c_n = \sqrt{\frac{2}{\pi}} \int_0^{\pi} v_0(\tau) \sin(n\tau) d\tau. \tag{2.7}$$

Now by separation of variables suppose solution of direct problem (2.1). (2.2) and (2.3) is of the form

$$u(x,t) \doteq \sum_{n=1}^{\infty} a_n(t) \phi_n(x), \qquad x \in [0, \pi], \tag{2.8}$$

where $a_n(t)$ have to solve the initial value problem

$$\frac{d^2 a_n(t)}{dt^2} = -n^2 a_n(t). \qquad t \geq 0. \tag{2.9}$$

where

$$a_n(0) = c_n, \tag{2.10}$$

and

$$\frac{da_n(0)}{dt} = 0. \tag{2.11}$$

Therefore (2.8) can be written as

$$u(x,t) = \sum_{n=1}^{\infty} c_n \cos(nt)\phi_n(x), \tag{2.12}$$

Using condition (2.3) we write

$$f(x) = \int_0^{\pi} k(x,\tau)v_0(\tau)d\tau, \tag{2.13}$$

with

$$k(x,\tau) \doteq \sum_{n=1}^{\infty} \cos(nT)\phi_n(\tau)\phi_n(x). \tag{2.14}$$

Thus the inverse problem is reduced to solving the integral equation of the first kind given by (2.13). The singular system for the integral operator in (2.13) is given by

$$\{\cos(nT);\ \ \phi_n(x),\ \ \phi_n(x)\}. \tag{2.15}$$

It now follows from Picard's theorem that our inverse problem is solvable iff

$$\sum_{n=1}^{\infty} \frac{|f_n|^2}{(\cos(nT))^2} < \infty. \tag{2.16}$$

where

$$f_n \doteq \int_0^{\pi} f(\tau)\, o_n(\tau) d\tau. \tag{2.17}$$

are classical Fourier coefficients of f. In this case the solution is given by

$$v_0(x) = \sum_{n=1}^{\infty} \frac{f_n o_n(x)}{\cos(nT)}. \tag{2.18}$$

Following the same procedure as above . the heat equation

$$\frac{\partial u}{\partial t} = \frac{\partial^2 u}{\partial x^2}. \tag{2.19}$$

together with (2.2) . (2.3) and (2.4) is solvable iff

$$\sum_{n=1}^{\infty} e^{2n^2} |f_n|^2 < \infty, \tag{2.20}$$

and the solution is given by

$$v_0(x) = \sqrt{\frac{2}{\pi}} \sum_{n=1}^{\infty} e^{n^2} f_n \sin(nx). \tag{2.21}$$

From (2.20) and (2.21) it is clear that the inverse problem of heat conduction is extremely ill-posed i.e. solution exist only if Fourier coefficients decay much faster than $\exp[-n^2]$. A small error in n-th Fourier coefficient is amplified by the factor $\exp[n^2]$. Thus, already an error of, say, 10^{-6} in the fifth Fourier coefficient of the data leads to an error of about 10^3 in the initial temperature. Thus, one can consider at most about three degrees of freedom in the data and neglect higher modes.

2.2.2 Initial Inverse Problem in the Two-dimensional Wave Equation

We consider a two-dimensional wave problem as follows:

$$\frac{\partial^2 u}{\partial t^2} = \frac{\partial^2 u}{\partial x^2} + \frac{\partial^2 u}{\partial y^2}, \qquad x, y \in R. \tag{2.22}$$

where R is the rectangle

$$R = \{(x, y) / x \in [0, a], y \in [0, b]\}, \tag{2.23}$$

with homogeneous Dirichlet boundary conditions

$$u(0.y.t) = u(a.y.t) = 0, \quad y \in [0.b]\,. \tag{2.24}$$

$$u(x.0.t) = u(x.b.t) = 0. \quad x \in [0.a]\,. \tag{2.25}$$

Assume the final distribution of the form

$$f(x.y) \doteq u(x.y.T). \tag{2.26}$$

Our aim is to determine the initial profile $v_0(x.y)$

$$v_0(x.y) \doteq u(x.y.0). \tag{2.27}$$

$$\frac{\partial u}{\partial t}(x.y.0) = 0. \tag{2.28}$$

The functions $\varphi_{n.m}(x.y) \doteq \sqrt{\frac{4}{ab}}\sin(\frac{m\pi x}{a})\sin(\frac{n\pi y}{b})$ form a complete orthonormal system in $L^2[R]$ and eigenfunctions of ∇^2 on the rectangle R. Thus $v_0(x.y) \in L^2[R]$ can be expanded as

$$v_0(x.y) = \sum_{n.m=1}^{\infty} c_{n.m}\varphi_{n.m}(x.y)\ .\ \ x.y \in R. \tag{2.29}$$

where

$$c_{n,m} = \int_0^a \int_0^b v_0(x,y)\phi_{n,m}(x,y)dxdy. \tag{2.30}$$

By separation of variables, we assume a solution of the form

$$u(x,y,t) = \sum_{n,m=1}^{\infty} a_{n,m}(t)\,\phi_{n,m}(x,y)\ ,\ \ x,y \in R, \tag{2.31}$$

and using (2.31) in (2.22) together with (2.27) and (2.28) leads to the ordinary differential equation

$$\frac{d^2 a_{n,m}(t)}{dt^2} + \left[\left(\frac{m\pi}{a}\right)^2 + \left(\frac{n\pi}{b}\right)^2\right] a_{n,m}(t) = 0. \qquad t > 0. \tag{2.32}$$

subject to

$$a_{n,m}(0) = c_{n,m}. \tag{2.33}$$

and

$$\frac{d}{dt}a_{n,m}(0) = 0. \tag{2.34}$$

where $c_{n,m}$ is given by (2.30). The solution of the problem (2.32) is given by

$$a_{n,m}(t) = c_{n,m}\cos(\lambda_{n,m}t), \tag{2.35}$$

where

$$\lambda_{n,m} = \sqrt{\left(\frac{m\pi}{a}\right)^2 + \left(\frac{n\pi}{b}\right)^2}. \tag{2.36}$$

Now we use condition (2.26) to write the final profile in the form

$$\begin{aligned} f(x,y) &= \sum_{n,m=1}^{\infty} c_{n,m}\cos(\lambda_{n,m}T)\,\varphi_{n,m}(x,y) \\ &= \int_0^a \int_0^b v_0(\tau,\eta)K(x,y,\tau,\eta)\,d\tau d\eta, \end{aligned} \tag{2.37}$$

where

$$K(x,y,\tau,\eta) = \sum_{n,m=1}^{\infty} \cos(\lambda_{n,m}T)\,\varphi_{n,m}(x,y)\;\varphi_{n,m}(\tau,\eta). \tag{2.38}$$

Thus the inverse problem is reduced to solving the integral equation of the first kind (2.13). The singular system for the integral operator in (2.13) is given by

$$\left\{\cos(\lambda_{n,m}T);\quad \phi_{n,m}(x,y),\quad \varphi_{n,m}(x,y)\right\} \tag{2.39}$$

It now follows from Picard's theorem that our inverse problem is solvable iff

$$\sum_{n,m=1}^{\infty} \frac{|f_{n,m}|^2}{[\cos(\lambda_{n,m}T)]^2} < \infty. \tag{2.40}$$

where

$$f_{n,m} \doteq \int_0^a \int_0^b f(\tau,\eta)\,\phi_{n,m}(\tau,\eta)d\tau d\eta. \tag{2.41}$$

are classical Fourier coefficients of f. In this case the solution is given by

$$v_0(x,y) = \sum_{n,m=1}^{\infty} \frac{f_{n,m}\varphi_{n,m}(x,y)}{\cos(\lambda_{n,m}T)}. \tag{2.42}$$

The solution obtained in this section for the wave equation will be analyzed and compared with the damped wave equation in the next section.

2.3 Initial Inverse Problems in Damped Wave Equations

In the first subsection the one-dimensional damped wave equation is considered. In the second subsection the same procedure is applied to the two-dimensional damped wave equation. To see the effect of damping, comparison between damped and undamped models is considered by constructing some particular examples in both one and two-dimensions.

2.3.1 Initial Inverse Problem in the One-dimensional Damped Wave Equation

We consider the damped wave equation

$$\frac{\partial^2 u}{\partial t^2} + \delta \frac{\partial u}{\partial t} - \frac{\partial^2 u}{\partial x^2} = 0. \qquad \delta > 0.\ x \in [0.\pi].\ t \geq 0. \tag{2.43}$$

with homogeneous Dirichlet boundary conditions

$$u(0,t) = u(\pi.t) = 0. \tag{2.44}$$

Equation (2.43) has a dissipation or damping term which is proportional to $\frac{\partial u}{\partial t}$. the constant of proportionality being δ. We assume that the final disturbance $f(x)$ is given by

$$f(x) \doteq u(x.T). \tag{2.45}$$

We will consider the inverse problem of finding initial disturbance $v_0(x)$ from the information of final profile $f(x)$ so that

$$v_0(x) = u(x,0), \tag{2.46}$$

$$\frac{\partial u}{\partial t}(x,0) = 0. \tag{2.47}$$

The eigenfunctions of $\frac{d^2}{dx^2}$ given by $\phi_n(x) \doteq \sqrt{\frac{2}{\pi}}\sin(nx)$ form a complete orthonormal system in $L^2[0,\pi]$. Thus $v_0(x) \in L^2[0,\pi]$ can be expanded as

$$v_0(x) = \sum_{n=1}^{\infty} c_n \phi_n(x) \ , \ x \in [0,\pi]. \tag{2.48}$$

where

$$c_n = \int_0^{\pi} v_0(\tau)\phi_n(\tau)d\tau. \tag{2.49}$$

Now suppose that solution of the direct problem given by equations (2.43), (2.44) and (2.45) is

$$u(x,t) \doteq \sum_{n=1}^{\infty} a_n(t)\phi_n(x). \qquad x \in [0,\pi]. \tag{2.50}$$

where $a_n(t)$ satisfies the initial value problem

$$\frac{d^2a_n(t)}{dt^2} + \delta\frac{da_n(t)}{dt} = -n^2 a_n(t), \qquad t \geq 0. \tag{2.51}$$

subject to

$$a_n(0) = c_n, \tag{2.52}$$

and

$$\frac{da_n(0)}{dt} = 0. \tag{2.53}$$

Equations (2.51) , (2.52) and (2.53) can be solved easily to yield the solution

$$a_n(t) = e^{-\frac{\delta}{2}t}\left\{c_n \cos(k_n t) + \frac{\delta c_n}{2k_n}\sin(k_n t)\right\}, \quad 4n^2 > \delta^2. \tag{2.54}$$

$$a_n(t) = e^{-\frac{\delta}{2}t}\left\{c_n \cosh(k_n t) + \frac{\delta c_n}{2k_n}\sinh(k_n t)\right\}, \quad 4n^2 < \delta^2. \tag{2.55}$$

$$a_n(t) = c_n\left(1 + \frac{\delta}{2}t\right)e^{-\frac{\delta}{2}t}, \quad 4n^2 = \delta^2. \tag{2.56}$$

where

$$k_n = \frac{\sqrt{|4n^2 - \delta^2|}}{2}. \tag{2.57}$$

We set

$$b_n(t) = \begin{cases} c_n \cosh(k_n t) + \frac{\delta c_n}{2k_n} \sinh(k_n t). & \text{for } n \text{ such that } 4n^2 < \delta^2; \\ c_n \left(1 + \frac{\delta}{2} t\right). & \text{for } n \text{ such that } 4n^2 = \delta^2; \\ c_n \cos(k_n t) + \frac{\delta c_n}{2k_n} \sin(k_n t). & \text{for } n \text{ such that } 4n^2 > \delta^2. \end{cases}$$

Therefore equation (2.50) can be written as

$$u(x,t) = \exp\left(-\frac{\delta}{2} t\right) \sum_{n=1}^{\infty} b_n(t)\, \phi_n(x). \tag{2.58}$$

The order of damping increases until $4n^2$ reaches δ^2 and higher modes are all damped to the same extent. This solution shows that higher modes are damped in an oscillatory manner and lower modes are damped monotonically.

We use condition (2.45) to write

$$f(x) = \int_0^{\pi} k(x,\tau) v_0(\tau) d\tau. \tag{2.59}$$

with

$$k(x,\tau) = \exp\left(-\frac{\delta}{2} T\right) \sum_{n=1}^{\infty} B_n(T)\, \phi_n(\tau) \phi_n(x). \tag{2.60}$$

Thus the inverse problem is reduced to solving an integral equation of the first kind.

The singular system for the integral operator in equation (2.59) is given by

$$\left\{\exp\left(-\frac{\delta}{2}T\right)B_n(T):\ \ o_n(x),\ o_n(x)\right\}. \tag{2.61}$$

where

$$B_n(T)=\begin{cases}\cosh(k_nT)+\frac{\delta}{2k_n}\sinh(k_nT). & \text{for } n \text{ such that } 4n^2<\delta^2;\\ \left(1+\frac{\delta}{2}T\right). & \text{for } n \text{ such that } 4n^2=\delta^2;\\ \cos(k_nT)+\frac{\delta}{2k_n}\sin(k_nT). & \text{for } n \text{ such that } 4n^2>\delta^2.\end{cases}$$

Now by Picard's criterion, using singular system (2.61), the inverse problem is solvable iff

$$\sum_{n=1}^{\infty}\frac{\exp(\delta T)}{[B_n(T)]^2}|f_n|^2<\infty. \tag{2.62}$$

where

$$f_n=\int_0^{\pi}f(\tau)\,\phi_n(\tau)d\tau. \tag{2.63}$$

are classical Fourier coefficients of $f(x)$. In this case, by Picard's theorem, the

solutions are given by

$$v_0(x) = \sum_{n=1}^{\infty} \frac{\exp\left(\frac{\delta}{2}T\right)}{B_n(T)} f_n \phi_n(x). \tag{2.64}$$

From equation (2.62). it is clear that f_n should decay faster in case of oscillatory damping as compared to monotonic damping. In case of oscillatory damping. f_n should be such that equation (2.62) is satisfied. This can be more easily achieved by restricting to lower modes only.

Example 1 *Let us consider the initial distribution of the form*

$$u(x.0) = v_0(x) = \sqrt{\frac{2}{\pi}} \sin(mx). \tag{2.65}$$

where m is some fixed integer. First we solve the direct problem (2.43) – (2.47). to find the final profile $f(x)$. The solution of the direct problem with $T = 1$ is

$$\begin{aligned} f(x) &= \sqrt{\frac{2}{\pi}} e^{-\frac{\delta}{2}} \left(\cos k_m + \frac{\delta \sin k_m}{2k_m}\right) \sin(mx). \qquad 4m^2 > \delta^2. && (2.66) \\ &= \sqrt{\frac{2}{\pi}} e^{-\frac{\delta}{2}} \left(\cosh k_m + \frac{\delta \sinh k_m}{2k_m}\right) \sin(mx). \qquad 4m^2 < \delta^2. && (2.67) \\ &= \sqrt{\frac{2}{\pi}} e^{-\frac{\delta}{2}} \left(1 + \frac{\delta}{2}\right) \sin(mx), \qquad 4m^2 = \delta^2. && (2.68) \end{aligned}$$

Our aim is to use the final profile given by (2.66) – (2.68) to recover back the initial disturbance given by (2.65). From equation (2.63) the Fourier coefficients are given

by

$$f_m = e^{-\frac{\epsilon}{2}} \left(\cos k_m + \frac{\delta \sin k_m}{2k_m} \right), \qquad 4m^2 > \delta^2. \tag{2.69}$$

$$f_m = e^{-\frac{\epsilon}{2}} \left(\cosh k_m + \frac{\delta \sinh k_m}{2k_m} \right). \qquad 4m^2 < \delta^2. \tag{2.70}$$

$$f_m = e^{-\frac{\epsilon}{2}} \left(1 + \frac{\delta}{2} \right). \qquad 4m^2 = \delta^2. \tag{2.71}$$

We use equations (2.69), (2.70) *and* (2.71) *in equation* (2.64) *to recover in each case the initial profile* (2.65).

2.3.1.1 Comparison of Damped and Undamped Models

We now use damped data given by equations (2.69), (2.70) and (2.71) in the undamped model given by equation (2.18) to recover the initial profile by setting $T = 1$. The recovered initial profile is given by

$$v_0(x) = \frac{e^{-\frac{\epsilon}{2}} \left(\cos k_m + \frac{\delta \sin k_m}{2k_m} \right) \phi_m(x)}{\cos(m)}, \qquad 4m^2 > \delta^2. \tag{2.72}$$

$$v_0(x) = \frac{e^{-\frac{\delta}{2}}\left(\cosh k_m + \frac{\delta \sinh k_m}{2k_m}\right)\phi_m(x)}{\cos(m)}, \qquad 4m^2 < \delta^2, \tag{2.73}$$

$$v_0(x) = \sqrt{\frac{2}{\pi}}\frac{e^{-\frac{\delta}{2}}\left(1+\frac{\delta}{2}\right)\phi_m(x)}{\cos(m)}. \qquad 4m^2 = \delta^2. \tag{2.74}$$

In the next three figures, the exact initial profile is compared with recovered initial profile when the damped data is used in the undamped model. The solid line is used for exact initial profile while the dotted line for recovered initial profile. Three cases, depending on the magnitude of damping, are considered separately.

Fig. 2.1 depicts the case $4m^2 > \delta^2$. This depiction shows the case when the medium under consideration has small values of damping. Figs. 2.2 and 2.3 demonstrate that how reconstruction behave as magnitude of damping increases. Furthermore, the recovered profile also depend on the time displacement T due to the factor $\exp\left(-\frac{\delta}{2}T\right)$. For instance, if we take $T = 2$ then the exponential factor in above expressions is $\exp(-\delta)$. This will lead to further deviation of the recovered profile from the exact initial profile. Since in the real world every medium of propagation offers some resistance, so it is natural to consider the damped wave equation. From the figures it is clear that the recovered initial profile is not correct if inversion formula of the undamped wave equation is used.

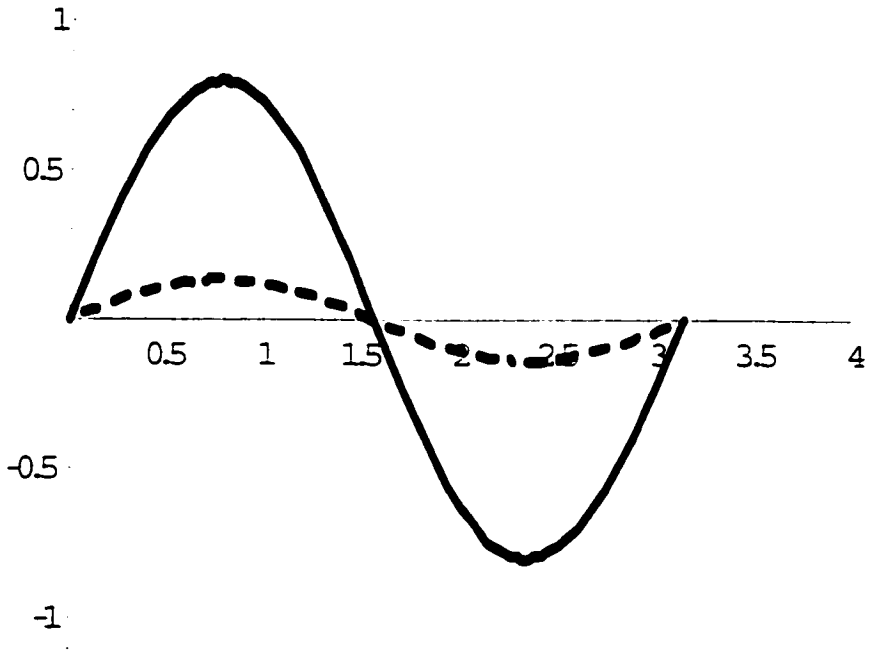

Figure 2.1: Response of the undamped model to the damped data in the case, $m = 2$ and $\delta = 1$ with $4m^2 > \delta^2$. The thick solid line represents the exact initial profile while the dashed line represents the recovered profile.

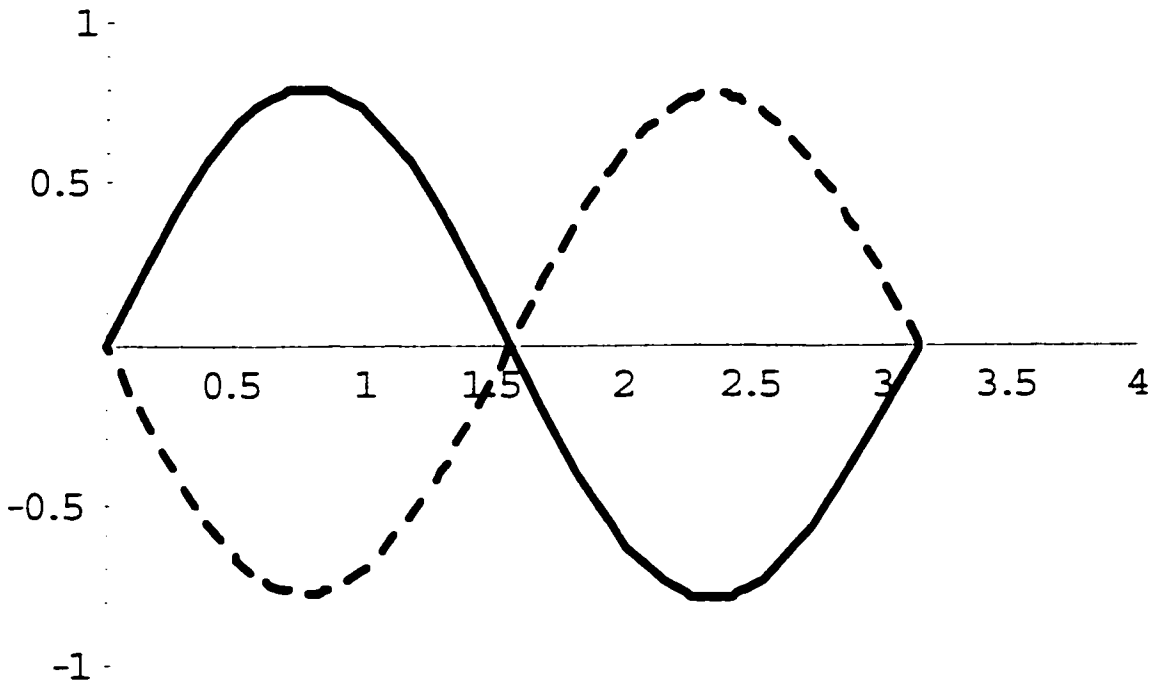

Figure 2.2: Response of the undamped model to the damped data in the case. $m = 2$ and $\delta = 4$ with $4m^2 = \delta^2$. The thick solid line represents the exact initial profile while the dashed line represents the recovered profile.

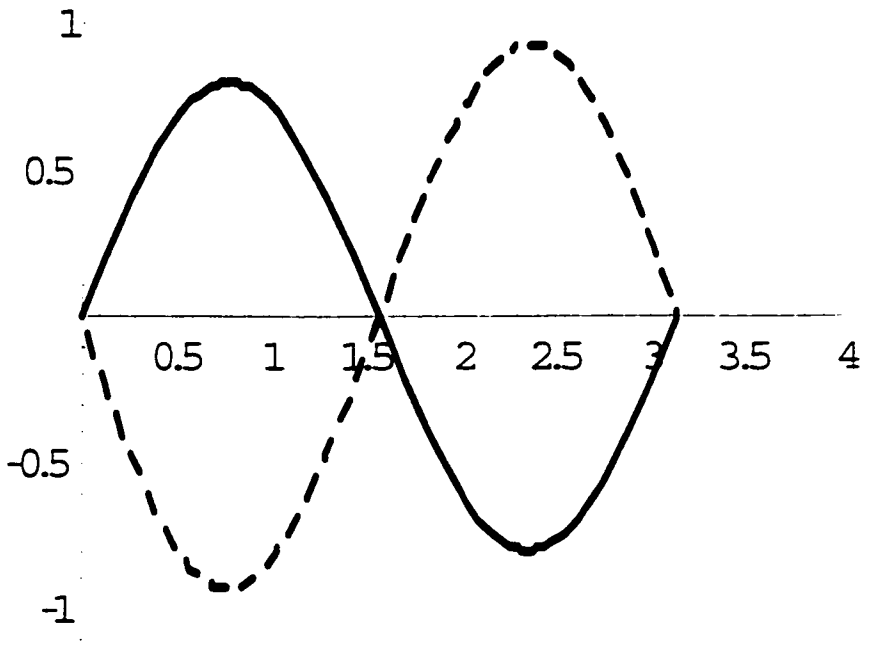

Figure 2.3: Response of the undamped model to the damped data in the case. $m = 2$ and $\delta = 5$ with $4m^2 < \delta^2$. The thick solid line represents the exact initial profile while the dashed line represents the recovered profile.

2.3.2 Initial Inverse Problem in the Two-dimensional Damped Wave Equation

We consider the two dimensional damped wave equation

$$\frac{\partial^2 u}{\partial t^2} + \delta \frac{\partial u}{\partial t} - \nabla^2 u = 0. \qquad x, y \in R,\ t \in [0, T]. \tag{2.75}$$

together with the conditions (2.24) – (2.28).where R is defined by (2.23). Following the same procedure as for the one-dimensional damped wave equation we can write the solution of (2.75) as

$$u(x, y, t) = \exp\left(-\frac{\delta}{2}t\right) \sum_{n,m=1}^{\infty} b_{n,m}(t)\, o_{n,m}(x, y). \tag{2.76}$$

where $\lambda_{n,m}$ is given by (2.36) and

$$b_{n,m}(t) = \begin{cases} c_{n,m} \cosh(k_{n,m}t) + \frac{\delta c_{n,m}}{2k_{n,m}} \sinh(k_{n,m}t). & 4\lambda_{n,m}^2 < \delta^2; \\ c_{n,m}\left(1 + \frac{\delta}{2}t\right), & 4\lambda_{n,m}^2 = \delta^2; \\ c_{n,m} \cos(k_{n,m}t) + \frac{\delta c_{n,m}}{2k_{n,m}} \sin(k_{n,m}t). & 4\lambda_{n,m}^2 < \delta^2, \end{cases}$$

where

$$k_{n,m} = \frac{\sqrt{|4\lambda_{n,m}^2 - \delta^2|}}{2}. \tag{2.77}$$

The singular system of the problem is given by

$$\left[\exp\left(-\frac{\delta}{2}T\right)B_{n.m}(T):\ \phi_{n.m}(x.y).\ \phi_{n.m}(x.y)\right] \tag{2.78}$$

where

$$B_{n.m}(T)=\begin{cases}\cosh(k_{n.m}T)+\frac{\delta}{2k_{n.m}}\sinh(k_{n.m}T). & 4\lambda_{n.m}^2<\delta^2:\\ \left(1+\frac{\delta}{2}T\right). & 4\lambda_{n.m}^2=\delta^2:\\ \cos(k_{n.m}T)+\frac{\delta}{2k_{n.m}}\sin(k_{n.m}T). & 4\lambda_{n.m}^2<\delta^2.\end{cases}$$

Now by Picard's criterion. by using the above singular systems. the solution exists iff

$$\sum_{n.m=1}^{\infty}\frac{\exp(\delta T)\,|f_{n.m}|^2}{[B_{n.m}(T)]^2}<\infty. \tag{2.79}$$

and the solution is given by

$$v_0(x.y)=\exp\left(\frac{\delta}{2}T\right)\sum_{n.m=1}^{\infty}\frac{f_{n.m}\ \phi_{n.m}(x.y)}{B_{n.m}(T)}. \tag{2.80}$$

Example 2 *Consider*

$$v_0(x.y)=\sin(\pi x)\sin(\pi y).\ \textit{with}\ a=b=2. \tag{2.81}$$

This example works in the same way as example 1. so there is no point to write the same type of details again.

2.3.2.1 Comparison of Damped and Undamped Models

For the two-dimensional model. we now use damped data in the undamped model to recover the initial profile. The recovered initial profile is given by

$$v_0(x.y) = \frac{e^{-\frac{\delta}{2}T}\left\{\cos(k_{n.m}T) + \frac{\delta}{2k_{n.m}}\sin(k_{n.m}T)\right\}\ \phi_{n.m}(x.y)}{\cos(\lambda_{n.m}T)}.\ \text{if}\ \ \delta^2 < 4\lambda_{n.m}^2. \quad (2.82)$$

$$v_0(x.y) = \frac{e^{-\frac{\delta}{2}T}\left\{\cosh(k_{n.m}T) + \frac{\delta}{2k_{n.m}}\sinh(k_{n.m}T)\right\}\ \phi_{n.m}(x.y)}{\cos(\lambda_{n.m}T)}.\ \text{if}\ \ \delta^2 > 4\lambda_{n.m}^2. \quad (2.83)$$

$$v_0(x.y) = \frac{e^{-\frac{\delta}{2}T}\ \left(1 + \frac{\delta}{2}T\right)\phi_{n.m}(x.y)}{\cos(\lambda_{n.m}T)}.\ \ \text{if}\ \ \delta^2 = 4\lambda_{n.m}^2. \quad (2.84)$$

In the following figures. the exact initial profile is compared with recovered initial profile when the damped data is used in the undamped model. We set $a = b = 2$ and $T = 1$.

Fig. 2.5 depicts the case $4\lambda_{n.m}^2 > \delta^2$. This depiction shows the case when the medium under consideration has small values of damping. Figs. 2.6 - 2.7 demonstrate that how the reconstruction behaves as the magnitude of damping increases.

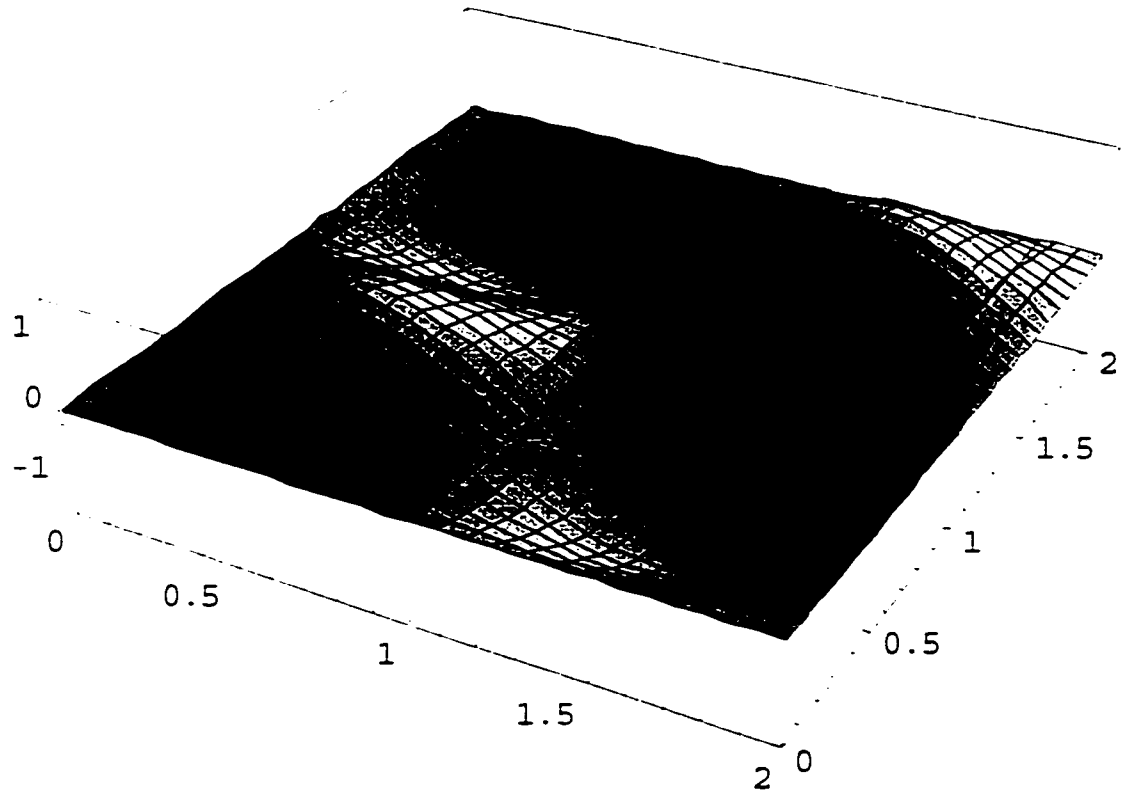

Figure 2.4: The exact initial profile.

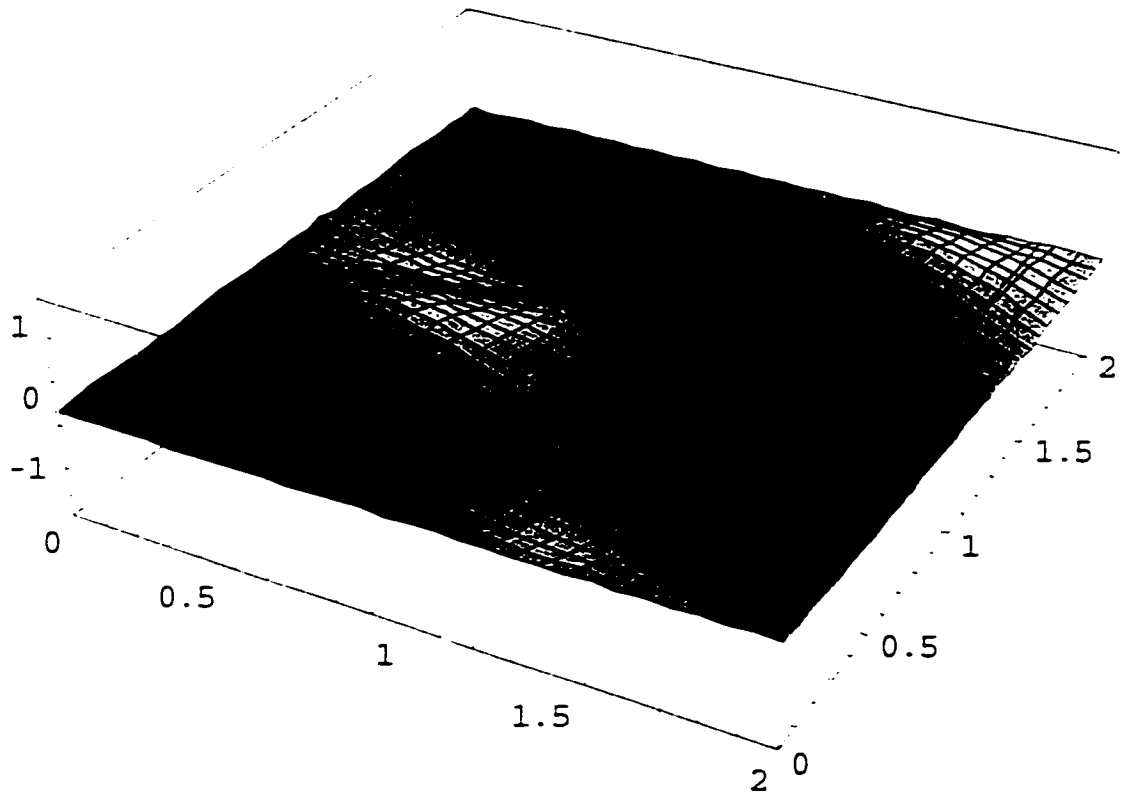

Figure 2.5: Response of the undamped model to the damped data in the case, $4\lambda_{n,m}^2 > \delta^2$, with $\delta = 3$.

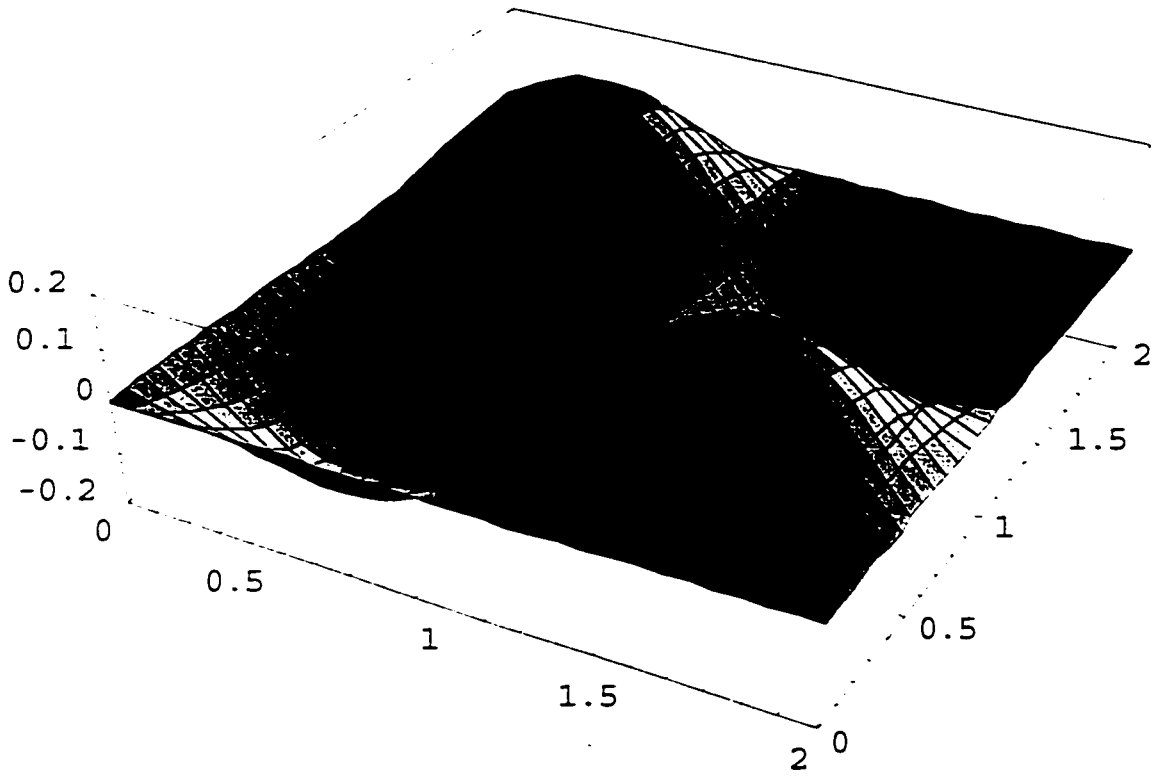

Figure 2.6: Response of the undamped model to the damped data in the case, $4\lambda_{n,m}^2 = \delta^2$, with $\delta = \sqrt{8}\pi$.

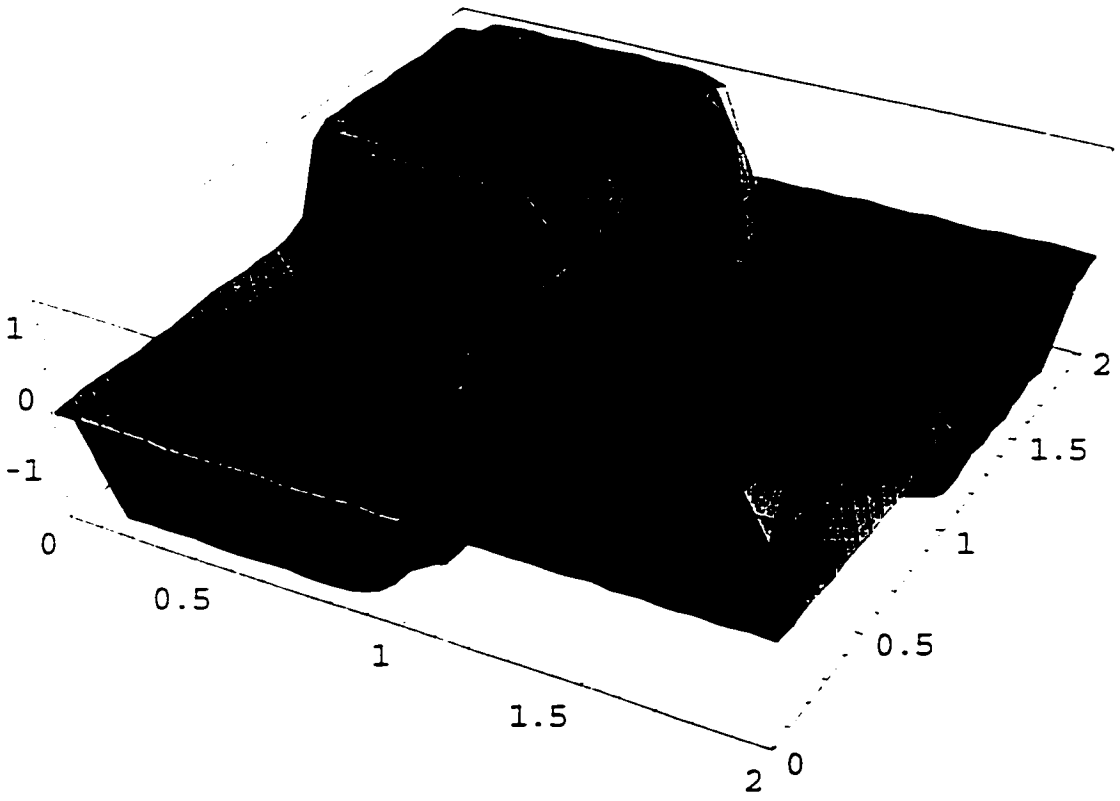

Figure 2.7: Response of the undamped model to the damped data in the case. $4\lambda_{n,m}^2 < \delta^2$, with $\delta = 9$.

2.3.3 Regularization of the Heat Conduction Model by the Damped Wave Equation

Inverse problems in the heat conduction arise quite naturally if one is interested in the unknown source giving rise to a measured heat flux. Such inverse problems in the heat conduction are extremely ill-posed [34], so small errors in the data give unacceptable results. There is an alternative approach to the heat conduction problem [32, 71], which consists of introducing a small damping parameter with the term $\frac{\partial^2 u}{\partial t^2}$. By controlling the size of the parameter we would like to obtain an approximate solution to the heat conduction problem. Also in some interesting situations the damping parameter is small due to properties of the material [41, 69]. So, we write the damped wave equation as

$$\delta \frac{\partial^2 u}{\partial t^2} + \frac{\partial u}{\partial t} = \frac{\partial^2 u}{\partial x^2}, \quad \delta > 0, \quad 0 < x < \pi, \tag{2.85}$$

together with conditions $(2.44 - 2.47)$. Following the same procedure as that for the one-dimensional wave equation and assuming solution of the form (2.50), for $\delta \to 0^+$we get the following ordinary differential equation

$$\delta \frac{d^2 a_n(t)}{dt^2} + \frac{da_n(t)}{dt} + n^2 a_n(t) = 0, \qquad \delta > 0, \quad t > 0, \tag{2.86}$$

subject to

$$a_n(0) = c_n. \tag{2.87}$$

and

$$\frac{da_n(0)}{dt} = 0. \tag{2.88}$$

This is a singular perturbation problem. so we seek the WKBJ (Wentzel, Kramers. Brillouin and Jeffreys) solution to this problem [10]. The WKBJ solution to (2.86) is

$$a_n(t) = \left(\frac{\delta n^2 - 1}{2\delta n^2 - 1}\right) c_n \exp\left[-n^2 t\right] - \left(\frac{\delta n^2 c_n}{2\delta n^2 - 1}\right) \exp\left[n^2 t - \frac{t}{\delta}\right]. \tag{2.89}$$

The singular system for this problem with $o_n(x) = \sqrt{\frac{2}{\pi}}\sin(nx)$ is

$$\left\{\left(\frac{\delta n^2 - 1}{2\delta n^2 - 1}\right) \exp\left[-n^2 T\right] + \left(\frac{\delta n^2}{2\delta n^2 - 1}\right) \exp\left[n^2 T - \frac{T}{\delta}\right] : o_n(x) \cdot o_n(x)\right\}. \tag{2.90}$$

By Picard's theorem the solution exists iff

$$\sum_{n=1}^{\infty} \frac{|f_n|^2}{\left\{\left(\frac{\delta n^2 - 1}{2\delta n^2 - 1}\right) \exp\left[-n^2 T\right] + \left(\frac{\delta n^2}{2\delta n^2 - 1}\right) \exp\left[n^2 T - \frac{T}{\delta}\right]\right\}^2} < \infty, \tag{2.91}$$

and the solution is given by

$$v_0(x) = \sum_{n=1}^{\infty} \frac{f_n \varnothing_n(x)}{\left\{\left(\frac{\delta n^2-1}{2\delta n^2-1}\right)\exp\left[-n^2T\right] + \left(\frac{\delta n^2}{2\delta n^2-1}\right)\exp\left[n^2T - \frac{T}{\delta}\right]\right\}}. \tag{2.92}$$

Letting $\delta \longrightarrow 0^+$ in expressions (2.91) and (2.92), we get the solution to the heat conduction problem

$$v_0(x) = \sum_{n=1}^{\infty} \exp\left(n^2T\right) f_n \varnothing_n(x). \tag{2.93}$$

Example 3 *Let us consider the initial temperature distribution of the form* $v_0(x) = \sqrt{\frac{2}{\pi}}\sin(mx)$. *where* m *is some fixed integer. then the final data for* (2.92) *and* (2.93) *can be given by*

$$f_m = \left(\frac{\delta m^2 - 1}{2\delta m^2 - 1}\right)\exp\left[-m^2T\right] + \left(\frac{\delta m^2}{2\delta m^2 - 1}\right)\exp\left[m^2T - \frac{T}{\delta}\right]. \tag{2.94}$$

and

$$f_m = \exp\left[-m^2T\right]. \tag{2.95}$$

Now it is routine to check analytically that these final profiles correspond to the initial profile $v_0(x)$.

2.3.3.1 Numerical Experiments

Now we use the final data for the damped wave equation given by (2.94) in the heat conduction solution (2.93) and compare it with the exact initial profile for different values of the damping parameter. Also we use the final data for the heat conduction model given by (2.95) in the damped wave solution (2.92) and compare it with the exact initial profile. These are represented by dashed, thin and thick solid lines respectively in Figs. 2.8-2.9. We consider the case $m = 2$ and $T = 1$. It is clear from Figs. 2.8-2.9 that the damped wave equation closely approximates the heat conduction model for $\delta \leq 0.01$.

Now we analyze the models by adding white Gaussian noise to the data (2.95). In Figs. 2.10-2.21, we use the noisy data (white Gaussian noise+(2.95)) in both heat conduction and damped wave models and see the mean behavior of 100 independent realizations. The noisy data used in the heat conduction solution (2.93) is represented by a dotted line and in the damped wave solution (2.92) by a thin solid line and the exact initial profile by a thick solid line.

We have considered the second mode, that is, $m = 2$ in Figs. 2.10-2.12 . Also we have retained first three terms ($N = 3$) in series (2.92) and (2.93). In Fig. 2.10, the signal to noise ratio (SNR) is equal to 50 dB (we have chosen SNR=50 dB to ensure that both the models appear clearly in the Figure, where SNR is defined as, SNR=10 log(variance of the signal/variance of the noise)dB) and $\delta = 0.04$. The damped wave model behaves better than the heat conduction model even for this low level of noise. We have increased the level of noise in Figs. 2.11-2.12 to SNR=20 dB.

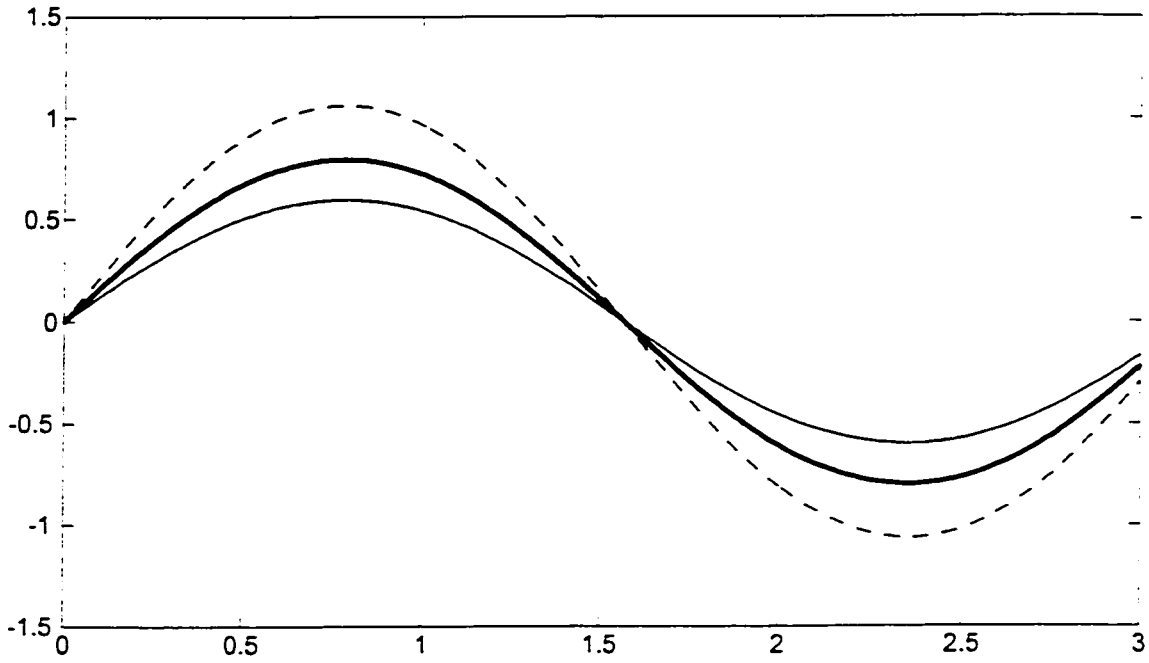

Figure 2.8: The case $m = 2, T = 1, \delta = 0.05$. The thick solid line represents the exact initial profile, the thin solid line represents the response of the damped model to the classical heat data and the dashed line represents the response of the classical heat model to the damped data.

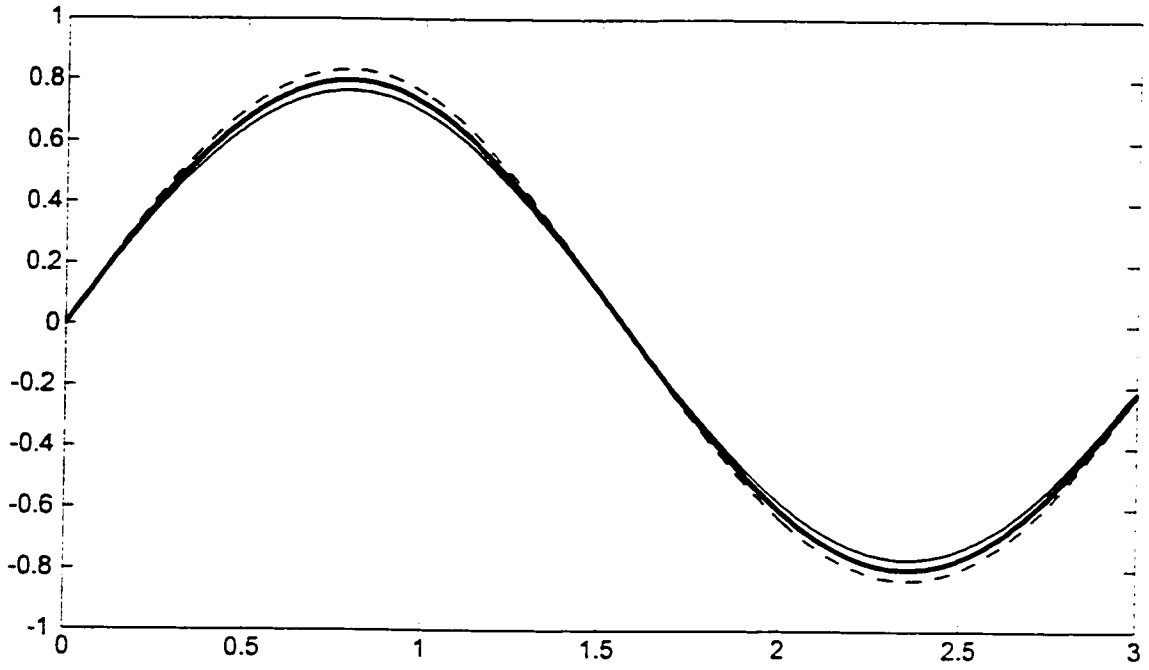

Figure 2.9: The case $m = 2, T = 1, \delta = 0.01$. The thick solid line represents the exact initial profile, the thin solid line represents the response of the damped model to the classical heat data and the dashed line represents the response of the classical heat model to the damped data.

In Fig. 2.11. the approximation of exact initial profile by the damped wave model is demonstrated with an appropriate choice of δ. How to choose δ is discussed in the last paragraph of this section. The inherent instability of the heat conduction model is clear from Fig. 2.12 by observing the range of the vertical axis.

In Figs. 2.13-2.15. we have considered $m = 4$ and $N = 4$. In Fig.2.13. we set SNR=100 dB. $\delta = 0.022$. and see the effects of this very low noise on both the models as compared to the exact profile. We decrease SNR to 20 dB and observe the behavior of heat conduction model in Fig. 2.15. noting that the vertical axis is given in units of 10^4. However for the damped wave model in Fig. 2.14 with SNR=20 dB and $\delta = 0.067$. some information of the initial profile may be recovered. So. from the above analysis of figures. we conclude that the damped wave model behaves much better than the heat conduction model in the case of noisy data. Even for lower modes. if the magnitude of noise increases. the heat conduction model becomes highly unstable.

The same analysis applies to higher modes, see Figs. 2.16-2.17. To see the effects of the size of parameter T in both models. we set $T = 2$ in Figs. 2.18-2.21. Comparing Figs. 2.18-2.19 with Figs. 2.11-2.12 and Figs. 2.20-2.21 with Figs. 2.14-2.15. For the heat conduction model. the error is more than double. However for the damped wave model, there is very little degradation.

To choose δ, we start from a higher value of δ for which there is no signal appearing on the graph. We gradually reduce the size and note the values of δ for which the signal starts to appear. We reduce the size further and note the values of δ for which the signal amplifies significantly. Then we take the mean of the two values of δ,

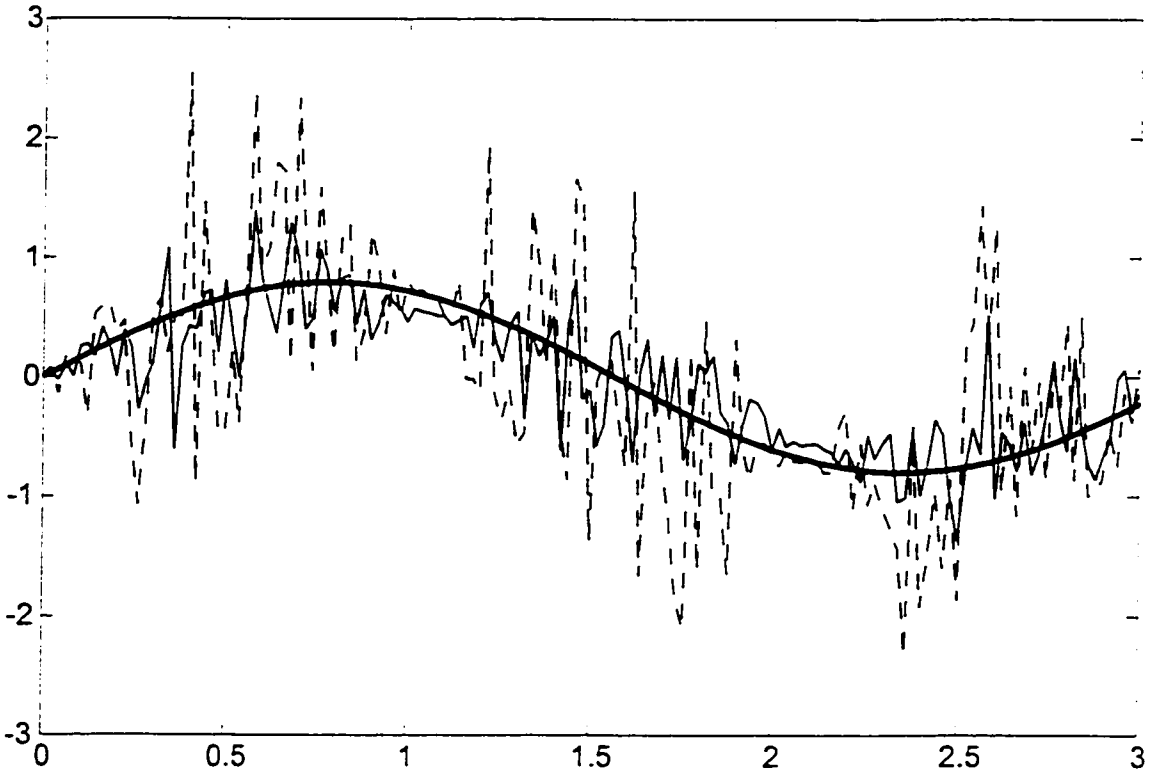

Figure 2.10: The case of noisy data with SNR=50 dB. $N = 3$. $m = 2$. $T = 1$. $\delta = 0.04$. The noisy data used in the heat conduction solution is represented by the dotted line and in the damped wave solution by the thin solid line and the exact initial profile by the thick solid line.

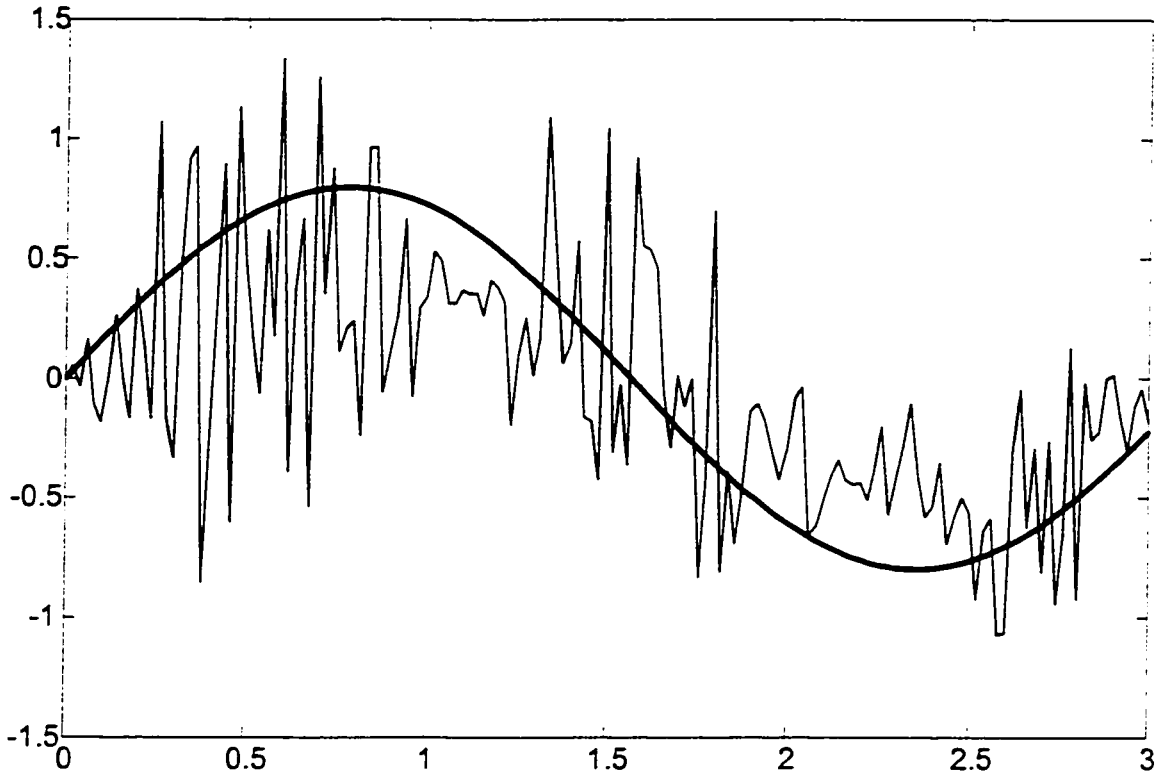

Figure 2.11: Response of the damped model in the case of noisy data with SNR=20 dB, $N = 3$, $m = 2, T = 1$, $\delta = 0.075$.

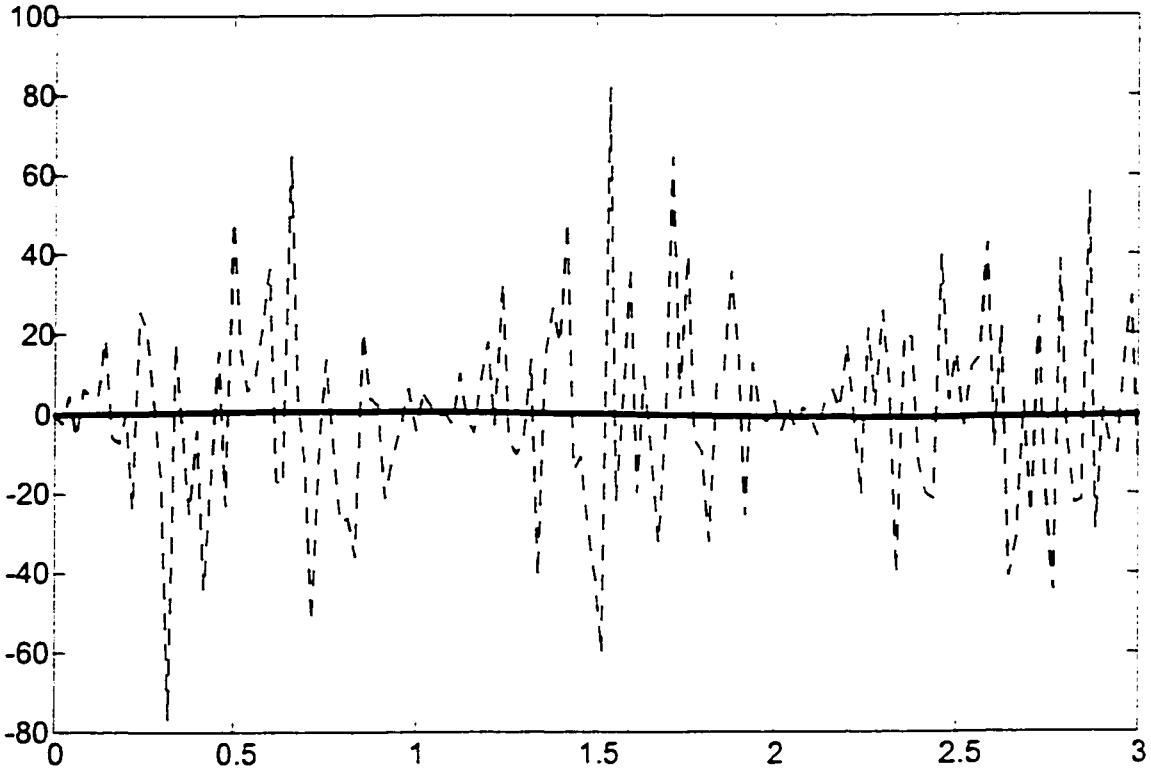

Figure 2.12: Response of the classical heat model in the case of noisy data with SNR=20 dB. $N = 3$, $m = 2, T = 1$.

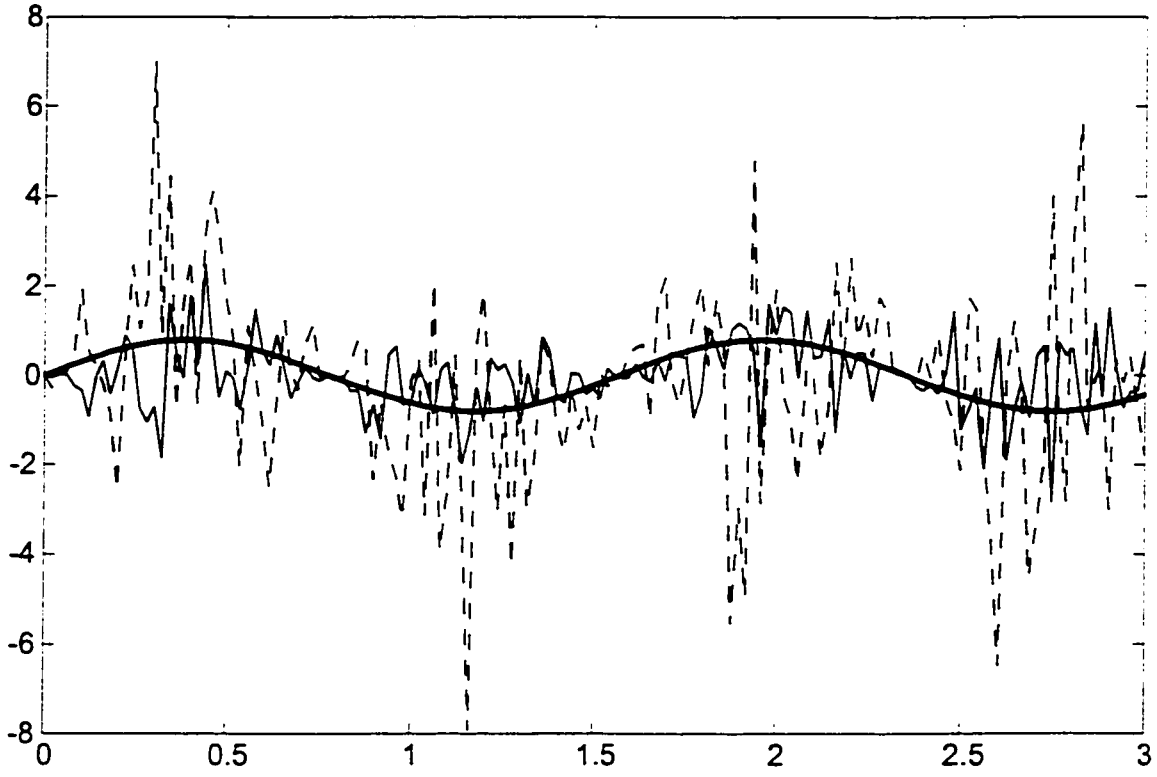

Figure 2.13: The case of noisy data with SNR=100 dB. $N = 4, T = 1, m = 4$. $\delta = 0.022$. The noisy data used in the heat conduction solution is represented by the dotted line and in the damped wave solution by the thin solid line and the exact initial profile by the thick solid line.

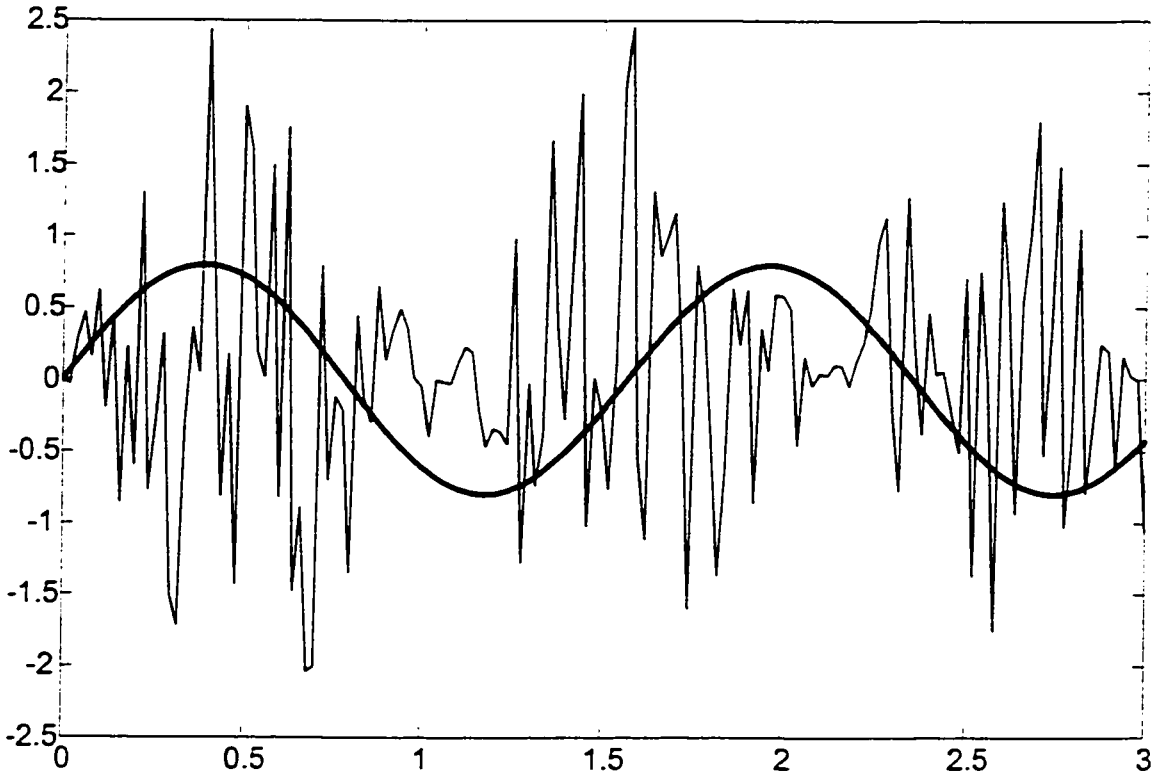

Figure 2.14: Response of the damped model in the case of noisy data with SNR=20 dB, $N = 4, T = 1, m = 4, \delta = 0.067$.

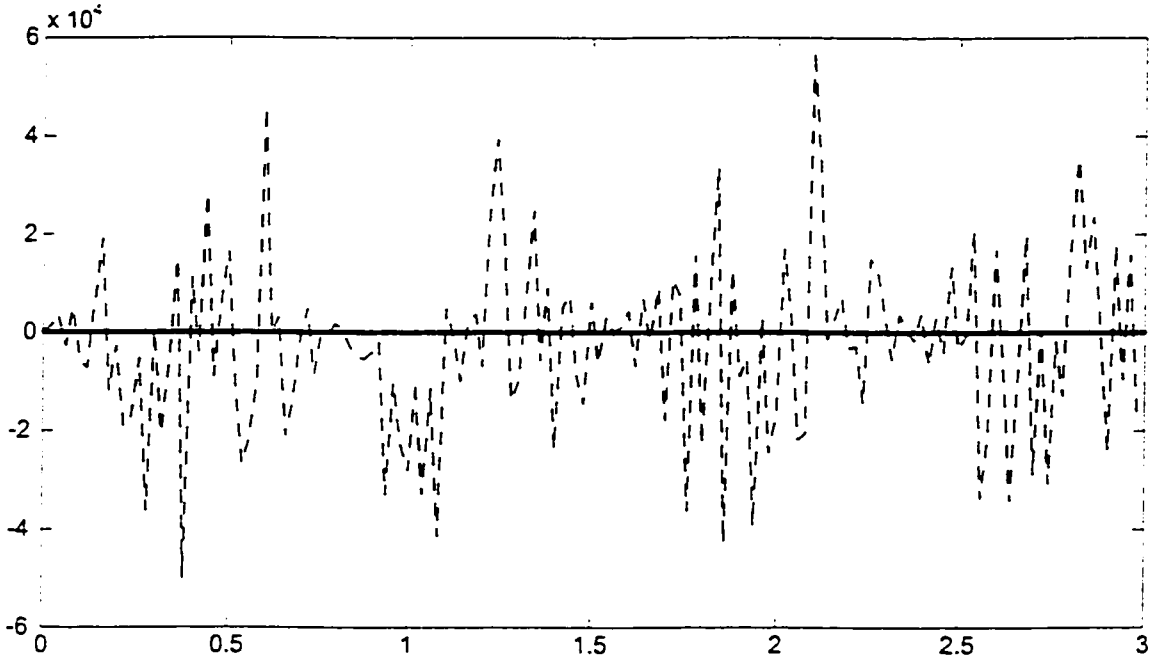

Figure 2.15: Response of the classical heat model in the case of noisy data with SNR=20 dB. $N = 4, T = 1, m = 4$.

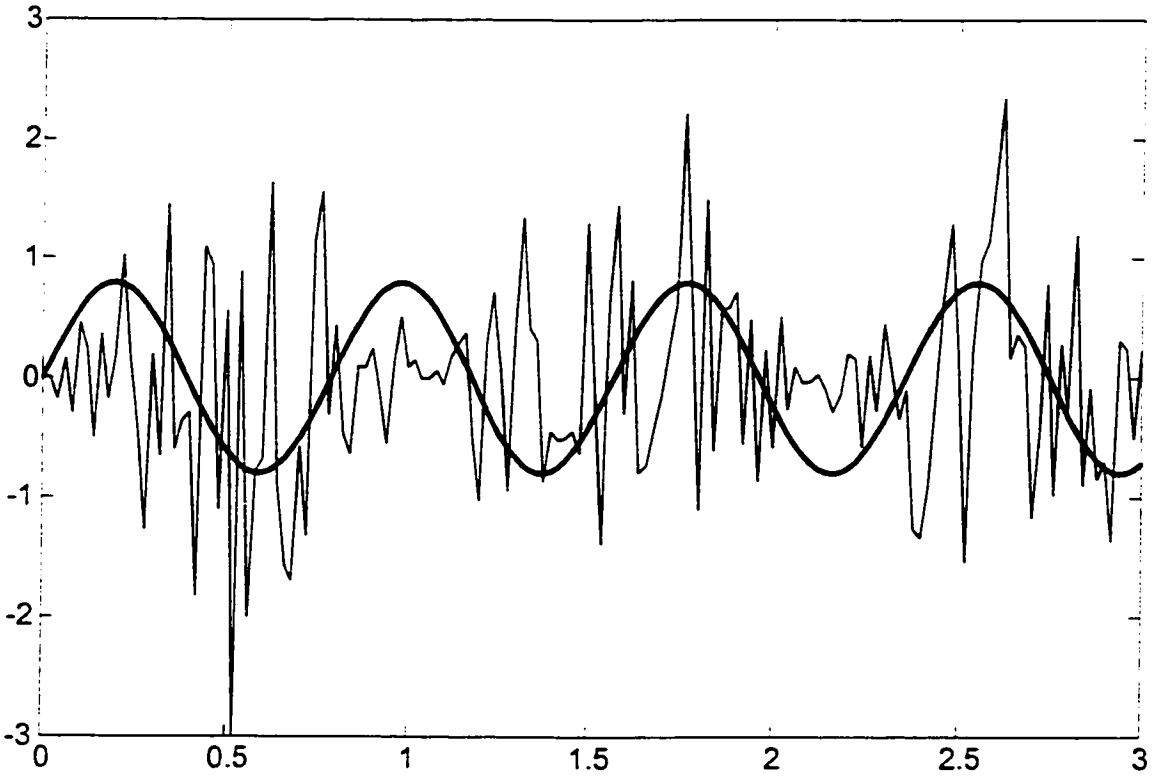

Figure 2.16: Response of the damped model in the case of noisy data with SNR=20 dB. $N = 8, T = 1, m = 8, \delta = 0.065$.

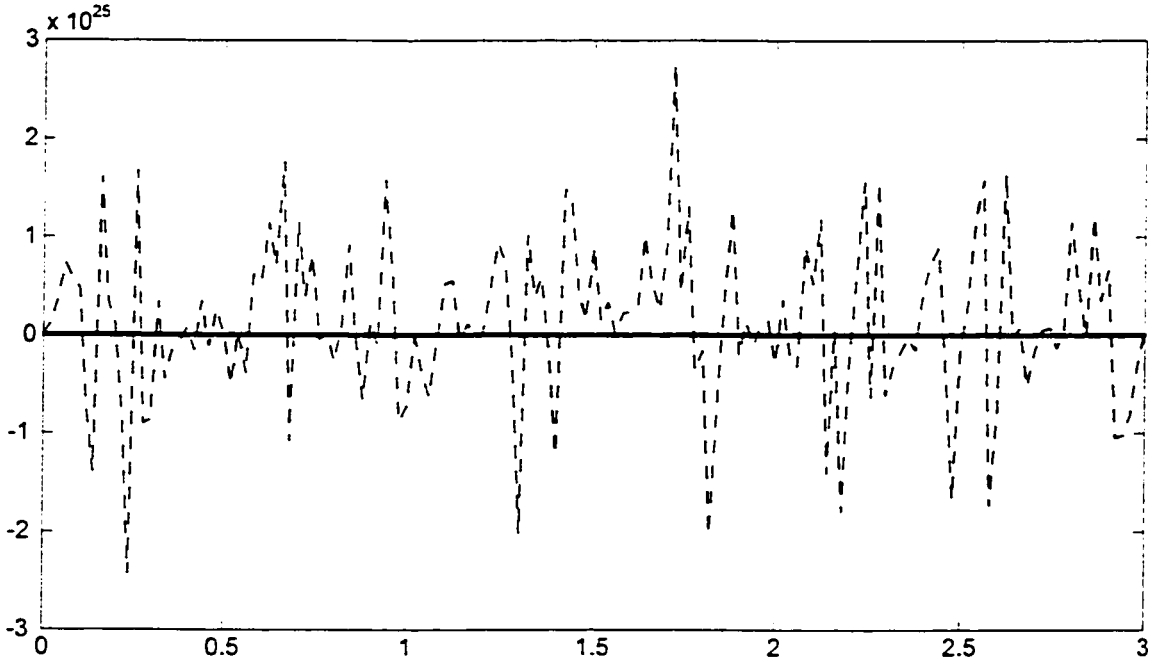

Figure 2.17: Response of the classical heat model in the case of noisy data with SNR=20 dB. $N = 8. T = 1. m = 8.$

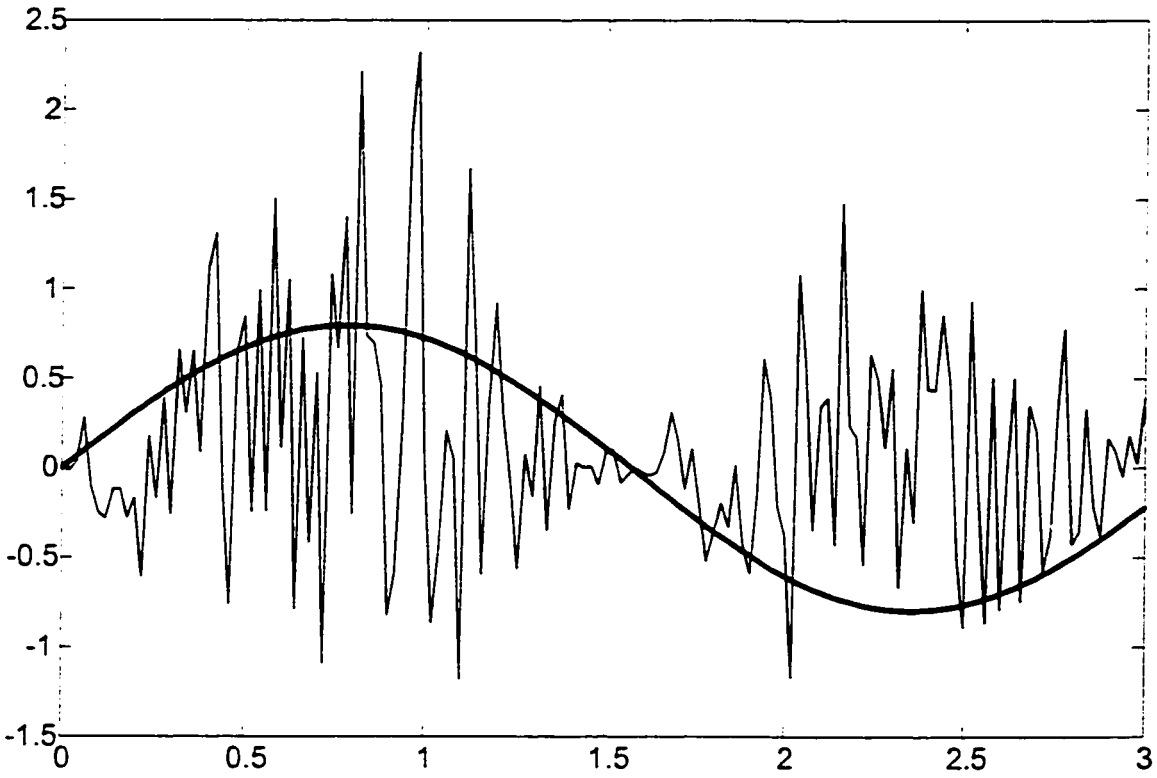

Figure 2.18: Response of the damped model in the case of noisy data with SNR=20 dB, $N = 3$, $m = 2$, $T = 2$, $\delta = 0.14$.

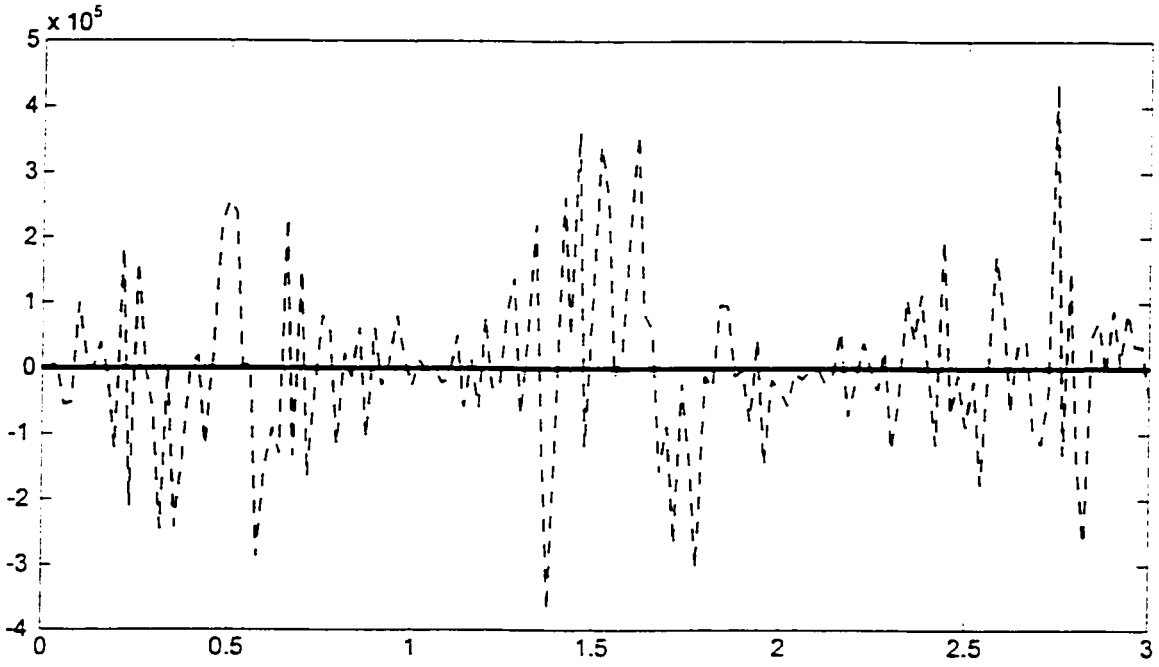

Figure 2.19: Response of the classical heat model in the case of noisy data with SNR=20 dB. $N = 3$. $m = 2$. $T = 2$.

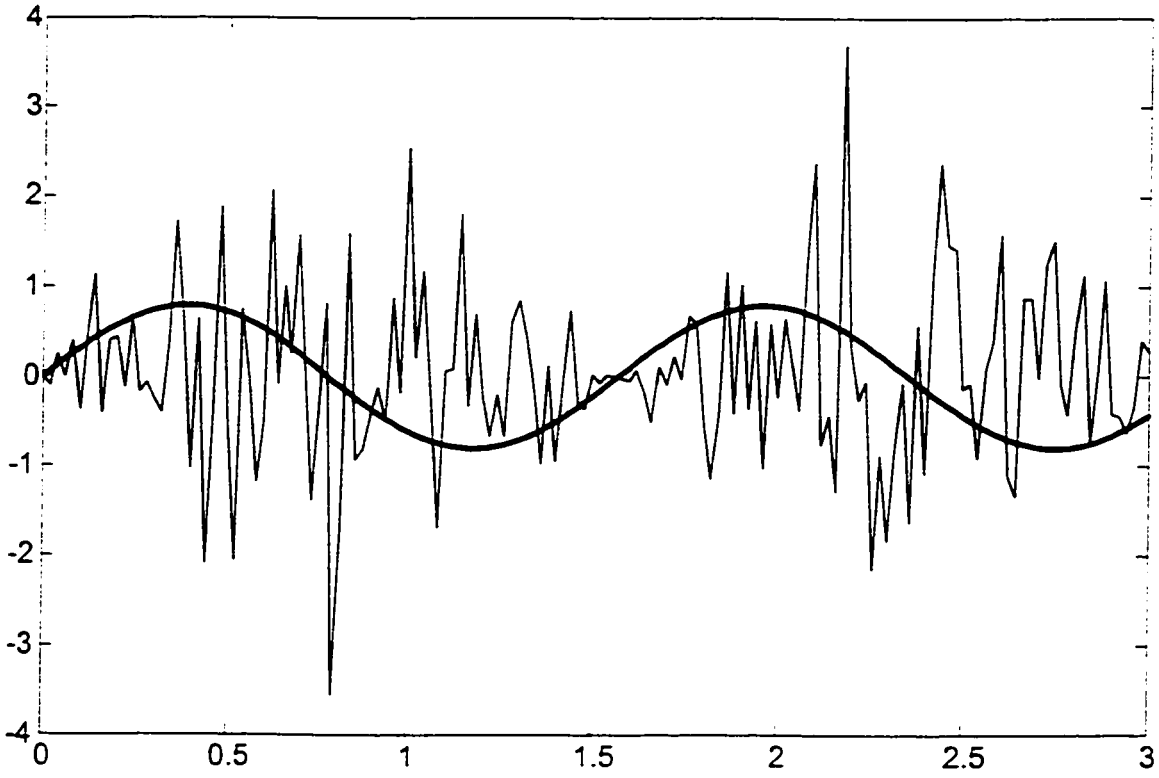

Figure 2.20: Response of the damped model in the case of noisy data with SNR=20 dB. $N = 4$. $m = 4$. $T = 2$, $\delta = 0.11$.

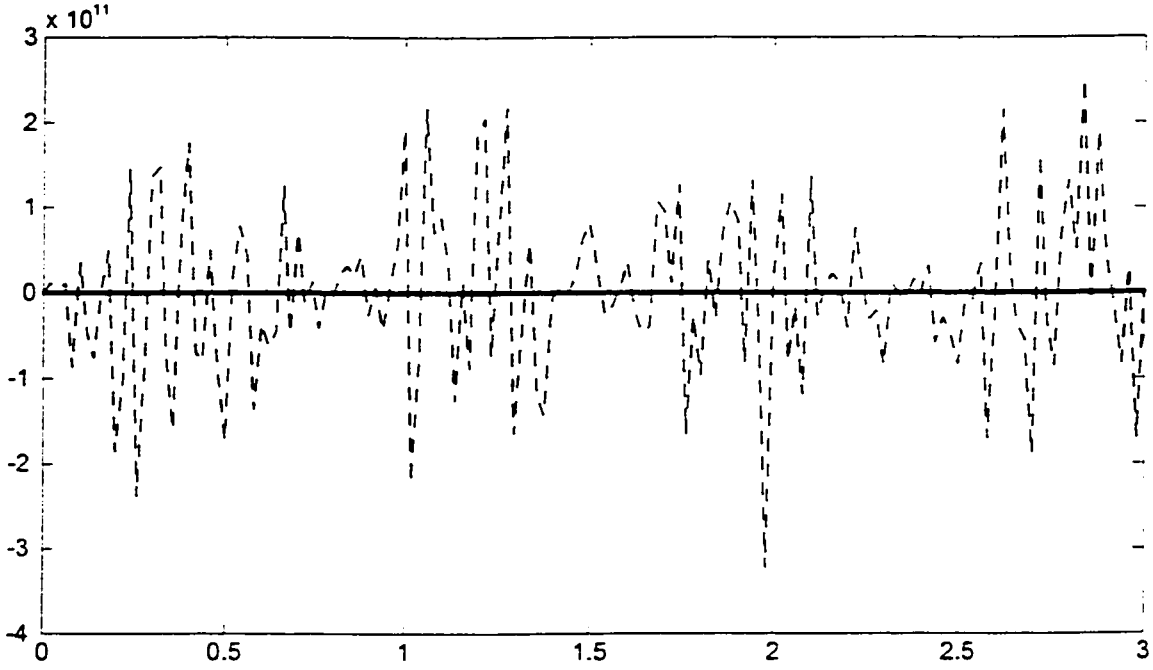

Figure 2.21: Response of the classical heat model in the case of noisy data with SNR=20 dB. $N = 4$. $m = 4$. $T = 2$.

which will give an appropriate choice of δ. For example, in Fig. 2.14, the signal starts to appear for $\delta = 0.08$ and is amplifies to a significant level for $\delta = 0.05$. So the appropriate choice of δ is approximately 0.065 and it may be refined further by checking neighboring values of 0.065 for which the spikes are milder. We have observed that the same procedure of finding δ works for higher modes as well as for lower modes.

2.4 Conclusions

It has been shown here by classical techniques that damping of the medium, indeed, play a role in the initial profile reconstruction. The reconstructed initial profile by using damped data without taking into account the damping of the medium in the inversion formula is compared with the exact initial profile. In this chapter we have demonstrated with the help of numerical examples that neglecting damping of the medium is not a suitable approximation. It is also shown that how the magnitude of damping affects the reconstruction of the initial profile.

It is shown that a complete reformulation of the heat conduction problem as a damped wave equation produces meaningful results. We applied the method to one-dimensional problems but it can be applied to higher dimensions as well by applying exactly the same procedure. The damped model with a small damping parameter closely approximates the heat conduction equation. It is also shown that in case of noisy data, the damped model approximates the exact initial profile better than the heat conduction model. Further, in the case of noisy data, the information about the initial profile cannot even be recovered for higher modes by the heat conduction

model but -the damped model may give some useful information about the initial profile if the value of damping parameter δ is chosen appropriately.

We have presented a method to estimate the damping parameter δ. It remains to find an analytical formula to estimate an appropriate value of the damping parameter δ which best regularizes the heat conduction model. At least our method may motivate and suggest. where to look for it.

Chapter 3

THE GELFAND-LEVITAN AND MARCHENKO METHOD APPLIED TO AN INVERSE PROBLEM IN LOVE WAVES

3.0.1 Abstract

The Gelfand-Levitan and Marchenko (GLM) procedure is used for the development of an inversion formalism for estimating parameter changes across inhomogeneities. The shear velocity is assumed to have a small variation across the inhomogeneity and we consider the inverse problem of recovering a one-dimensional shear velocity variation. The Love waves, traveling in a layer overlying a half space, incident upon delta function potential, are considered. The equation of motion for Love waves is transformed to the Schrödinger equation by assuming a small variation in shear velocity which leads to the potential term in the governing equation of Love waves and then the potential is recovered by applying the GLM procedure.

3.1 Introduction

The general problem can be simplified if the scattering object is assumed to be an inhomogeneous region whose material parameter has only one-dimensional spatial variations. Such inverse problems are of interest in geophysics and seismology and underground acoustics due to their various applications in determination of inhomogeneities and exploration of minerals. see e.g. Claerbout [23]. Liner [53]. Gray [43]. Bleistein et al. [17] among others.

A discrete model by Gerver and Kazdan [38] addressed the problem of finding a velocity profile from the Love wave dispersion curve. Also. a discrete model by Barcilon [8]. considered the question of unique determination of density from the dispersion relation of Love waves. There are some authors who worked on the inverse problem of determining phase velocity of surface waves. see for example Cara [20] and van Heijst et al. [68]. Our aim here is to consider an analytic procedure to determine the variation in shear velocity.

The analytic solution is obtained by transforming the equation of motion for Love wave propagation into a one-dimensional Schrödinger equation. The basic underlying assumption in transforming the equation of motion is that the unknown coefficient can be written as small perturbation from a known reference value, see e.g. Cohen and Bleistein [15,27]. A further assumption for one-dimensional case is that the coefficient varies in one direction only. We study the inverse problem arising from the Love wave propagating in a layer of uniform thickness overlying a homogeneous, isotropic half space. The layer is assumed to undergo a change in terms of its elastic properties and

thus gives rise to a potential term in the Schrödinger equation corresponding to the surface wave motion. Using the formulation proposed by Gelfand-Levitan [36] and independently by Marchenko [55], we recover the potential function which in turn determines the change in the surface layer. In the previously introduced methods, see e.g. Keller et al. [51] and Kay et al. [50], the Helmholtz equation is transformed to the Schrödinger equation by first transforming the independent variable via Liouville transformation followed by a transformation of the dependent field variable. Once this has been done, the recovered potential must be used to solve the Riccati equation, followed by the coordinate stretching process which converts the profile back to the geometric space. Each of these operations individually provide a veritable minefield of problems and pitfalls and application to Love wave problems does not seem to be apparent. As opposed to this, we use a simpler and more direct transformation, which avoids such problems.

3.1.1 Organization of the Chapter

In this chapter we present an analytical solution to the inverse scattering problem for Love wave propagation in an inhomogeneous medium. In the second section the details of the problem are spelled out and the governing equations of Love waves are transformed to the Schrödinger equation. In the third section the GLM procedure is applied to the problem we formulated in the second section. Finally in the last section conclusions are presented. The details of the GLM procedure are relegated to Appendix B.

3.2 Formulation of the Problem

We consider Love waves travelling from right to left in a layer overlying a half space. The geometry of the problem is shown in the fig. 3.1.

The incident Love wave of the nth mode has the displacements

$$u_1 = A\cos\left[(z+h)\,\sigma_{1n}\right] V(x)\,. \tag{3.1}$$

$$u_2 = A\cos\left[\sigma_{1n}h\right]\exp\left[-\sigma_{2n}z\right] V(x)\,. \tag{3.2}$$

where A is undetermined constant and

$$\sigma_{1n} = \sqrt{\frac{\omega^2}{\beta_{10}^2} - k_n^2}, \qquad \sigma_{2n} = \sqrt{k_n^2 - \frac{\omega^2}{\beta_{20}^2}}. \tag{3.3}$$

with β_{10}, β_{20} as background shear velocities. The constant k_n is the nth root of the Love wave dispersion relation

$$\tan\left[\left(\sqrt{\frac{\omega^2}{\beta_{10}^2} - k^2}\right)h\right] = \nu\frac{\sqrt{k^2 - \frac{\omega^2}{\beta_{20}^2}}}{\sqrt{\frac{\omega^2}{\beta_{10}^2} - k^2}}, \qquad \nu = \frac{\mu_1}{\mu_2}, \tag{3.4}$$

corresponding to the layer of thickness h. The displacements, u_i, $i = 1, 2$, satisfy the following governing equations (Aki and Richards [4], Achenbach [2])

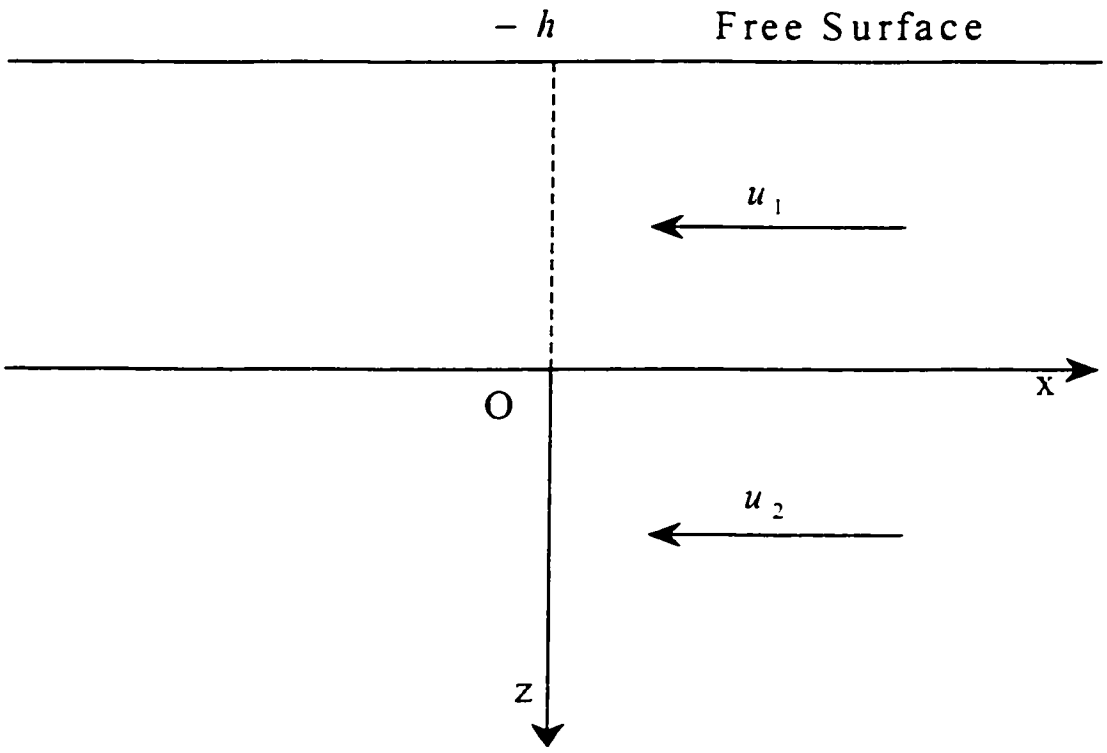

Figure 3.1: Geometry of the problem.

$$\frac{\partial^2 u_i}{\partial x^2} + \frac{\partial^2 u_i}{\partial z^2} = \frac{1}{\beta_i^2}\frac{\partial^2 u_i}{\partial t^2}, \qquad i = 1, 2. \tag{3.5}$$

We use equations (3.1) and (3.2) in equation (3.5) to get

$$\frac{\partial^2 V}{\partial x^2} - \sigma_{1n}^2 V = -\frac{\omega^2}{\beta_1^2} V, \qquad -h \le z \le 0. \tag{3.6}$$

$$\frac{\partial^2 V}{\partial x^2} + \sigma_{2n}^2 V = -\frac{\omega^2}{\beta_2^2} V, \qquad z \ge 0. \tag{3.7}$$

Suppose there is some inhomogeneity in the x-direction in the layer. So we consider equation (3.6) and assume that β_1 is small variation in the background shear velocity β_{10} across the inhomogeneity, i.e.

$$\beta_1 = \beta_{10}\left[1 + \alpha(x)\right], \quad \alpha(x) \ll 1. \tag{3.8}$$

$$\frac{1}{\beta_1^2} = \frac{1}{\beta_{10}^2}\left[1 - 2\alpha(x)\right]. \tag{3.9}$$

where in equation (3.9), we have neglected higher powers of $a(x)$. Therefore by using (3.9) we can write

$$\begin{aligned} \frac{\omega^2}{\beta_1^2} - \sigma_{1n}^2 &= \frac{\omega^2}{\beta_{10}^2}[1 - 2a(x)] - \left(\frac{\omega^2}{\beta_{10}^2} - k_n^2\right) = k_n^2 - \frac{2\omega^2}{\beta_{10}^2}a(x) \\ &= k_n^2 - q(x). \end{aligned} \tag{3.10}$$

We use equation (3.10) in equation (3.6) to get

$$\frac{\partial^2 V}{\partial x^2} + [k_n^2 - q(x)]V = 0. \tag{3.11}$$

So equation (3.6) is transformed to the Schrödinger equation (3.11) with potential $q(x)$. Now we proceed to solve the inverse problem of recovering the potential by GLM method.

3.3 Solution of the Inverse Problem

We are concerned here only to find discontinuities in the shear velocity, i.e. , to seek the reflectors of the unknown medium. The discontinuities of the medium can therefore be modeled by the delta function, peaking at the point of discontinuity. So we consider the delta function potential

$$q(x) = q_0\delta(x). \tag{3.12}$$

where q_0 is the strength of the potential. According to the inverse scattering technique, the first step is to solve the direct problem. In this case, the direct problem satisfies the equation

$$\frac{\partial^2 V}{\partial x^2} + \left[k_n^2 - q_0 \delta(x)\right] V = 0. \tag{3.13}$$

It is reasonable to assume that $\frac{\partial^2 V}{\partial x^2}$ behaves like a delta function at $x = 0$. Therefore, the first derivative must undergo a jump discontinuity at that point. Integrating equation (3.13) over the interval $[-\epsilon, \epsilon]$ and then letting $\epsilon \to 0$, we obtain the jump as

$$\left.\frac{\partial V}{\partial x}\right|_{-\epsilon}^{\epsilon} = q_0 V(0). \qquad \text{as } \epsilon \to 0. \tag{3.14}$$

Let a plane wave $\exp(-ik_n x)$ be incident on the delta function potential from the right. For the potential under consideration, the fundamental solutions of the scattering equation (3.13) are

$$\begin{aligned} \phi(x, k_n) &= \exp(-ik_n x) + \frac{q_0}{k_n} \sin(k_n x), && x \geq 0, \\ &= \exp(-ik_n x). && x \leq 0. \end{aligned} \tag{3.15}$$

$$\begin{aligned} \psi(x,k_n) &= \exp(ik_n x) - \frac{q_0}{k_n}\sin(k_n x), && x \le 0. \\ &= \exp(ik_n x). && x \ge 0. \end{aligned} \tag{3.16}$$

The reflection coefficient $R(k_n)$ can calculated as follows

$$R(k_n) = \frac{c_{11}(k_n)}{c_{12}(k_n)}. \tag{3.17}$$

where

$$c_{11}(k_n) = \frac{W(\phi(x,-k_n), v(x,k_n))}{2ik_n}. \qquad c_{12}(k_n) = \frac{W(\phi(x,k_n), v(x,k_n))}{-2ik_n}. \tag{3.18}$$

and $W(\phi(x,k_n), v(x,k_n))$ denote the Wronskian. From equation (3.17) the reflection coefficient is given by

$$R(k_n) = \frac{-iq_0}{[2k_n + iq_0]}. \tag{3.19}$$

The Fourier transform of the reflection coefficient can be calculated from the integral (Kay and Moses [50])

$$R(\zeta) = \frac{-iq_0}{4\pi}\int_{-\infty}^{\infty} \frac{\exp(ik_n\zeta)}{k_n + \frac{iq_0}{2}} dk_n. \tag{3.20}$$

The pole of the integrand is at $k_n = -\frac{iq_0}{2}$. If $\zeta > 0$, the contour can be closed in the upper half plane and since there is no singularity lying inside the contour, by Cauchy's theorem the integral will be zero. If, on the other hand, $\zeta < 0$, then the contour will be closed in the lower half plane and by Cauchy's theorem we have

$$R(\zeta) = -\frac{q_0}{2} \exp\left(\frac{q_0 \zeta}{2}\right) H(-\zeta). \tag{3.21}$$

where $H(\zeta)$ is the Heaviside function. The bound state solutions occur if the poles of the reflection coefficient lie in the upper half plane. So the potential $q(x)$ appearing in equation(3.13) has no bound state solutions as should be expected. To recover the potential, all we need is the impulse response function $R(\zeta)$ given by equation (3.21). The Gelfand-Levitan and Marchenko [50] integral equation is given by

$$K(x,\xi) + R(x+\xi) + \int_x^\infty K(x,\theta) R(\xi+\theta)\, d\theta = 0. \tag{3.22}$$

Now we use equation (3.21) in (3.22) to get

$$K(x,\xi) - \frac{q_0}{2} \exp\left[\frac{q_0 (x+\xi)}{2}\right] H[-(x+\xi)] - \frac{q_0}{2} \int_x^{-\xi} K(x,\theta) \exp\left[\frac{q_0 (\xi+\theta)}{2}\right] d\theta = 0. \tag{3.23}$$

If $x > -\xi$, then $K(x,\xi) = 0$ identically. In the opposite case $x + \xi < 0$, the integral

equation (3.23) can be satisfied by taking $K(x,\xi)$ to be a constant which equals $\frac{q_0}{2}$. This then gives

$$K(x,\xi) = \frac{q_0}{2} H[-(x+\xi)]. \tag{3.24}$$

$$\begin{aligned} q(x) &= -2\frac{d}{dx}[K(x,x)]. \\ &= q_0\delta(x). \end{aligned} \tag{3.25}$$

It may be noted that we can transform equation (3.7) to the Schrödinger equation in a way similar to that used to transform equation (3.6). We can then apply a similar procedure to recover the inhomogeneity in the half space.

3.4 Conclusions

It has been established that the governing equation for the Love wave can be transformed to one-dimensional Schrödinger equation in a more direct and straightforward manner provided that there are small variations in the propagation speed across the inhomogeneity. The method outlined here can be applied to problems where the material parameter is known up to a small perturbation, and varies in one direction only. We have used the GLM procedure to recover the shear velocity variation in the surface layer and have mentioned that the same procedure can be used to recover the shear velocity variation in the half space.

Chapter 4

VELOCITY INVERSION IN THE PRESENCE OF DAMPING BASED ON BORN'S INVERSION THEORY

4.0.1 Abstract

The inverse problems are important in seismic exploration and underground geology. The frequently used earth model for such a purpose is that of a homogeneous and isotropic medium. This may not be an accurate description of many practical situations. We consider a model that incorporates the effects of damping in the medium and develop an inversion procedure in this case. It is hoped that the results based upon this model will prove to be more realistic in some situations of interest.

We exploit the high frequency character of seismic data. We consider the one-dimensional inverse problem of determining variations in propagation speed, taking into account damping of the medium. We also consider the inverse problem of recovering variations in damping from observations of signals which pass through the medium

of interest. Our method is based on the linearized inversion associated with Born's inversion theory. Thus we assume that damping and sound speed are well approximated by the background plus the perturbation. The application of the method leads to a linear integral equation involving variations in sound speed and damping. Our aim is to recover these variations in velocity and damping. which in turn yields a map of the interfaces in the interior of the earth. We also consider the three-dimensional inverse problem and follow a parallel line. as laid down for the one-dimensional problem. to derive an integral equation and present the process of high frequency inversion.

4.1 Introduction

The objective here is to study the problem of mapping the interior of the earth as an inverse problem and to develop methods which yield increasingly more accurate results of that inverse problem. The methods we use are classical, employing perturbation techniques. transform methods and asymptotic analysis to get information about the interior of the earth. We assume the perturbation in wave speed and damping have parallel form and it is this perturbation we seek to recover. One or more signals are introduced near the surface of the earth in a region of interest and responses from irregularities in the interior of the earth are recorded. Under the assumption of constant density, an approximate solution to this inverse problem for the velocity was demonstrated by Claerbout [23].

The objective of seismic inversion is to estimate earth parameters. such as velocity and density from seismic data. In a seismic experiment. a source is set off at a point on the surface of earth, and the upward propagating wave is then measured at an array

of receivers near the source. The image of a subsurface, so constructed, is important, either for theoretical purposes or for the purpose of interpretation by a geologist for the identification of likely subsurface regions for resource extraction. These inverse problems form a class of problems in which unknown coefficients of wave equation represent internal parameters of a medium and the known information consists of boundary measurements. As mentioned above, an inverse problem can be simplified if the scattered field is approximated as a linear functional of the object. There are several conditions under which the problem could be linearized. These conditions, for example, are those of the Born and the Rytov approximations [19,49,58,66]. For instance, in the Born approximation, the scattered field amplitude is assumed to be a linear functional of the object, whereas in the Rytov approximation, the phase perturbation is assumed to be a linear functional of the object. Furthermore, another way of obtaining a linearized relationship between data and the object is to use high frequency waves. In this case the concepts of reflection and refraction of plane waves at plane interface carry over to inhomogeneous media i.e. the rules of "geometric optics". If the primary concern is seismic inversion, then the real objective is to obtain a reflector map of the earth's interior and devise means for estimating the changes in earth parameters across those reflectors.

The one-dimensional problem has been discussed in detail by Gerver [37]. He demonstrated that velocity of propagation can be determined uniquely from the observations at one point. An inverse problem of determining small variations in propagation speed through the medium of interest was considered by Cohen and Bleistein [13,25,27]. They have shown that closed form approximate solutions for the

velocity profile can be obtained for a wide variety of wave propagation equations. In a series of papers by Mager and Bleistein [54], Armstrong and Bleistein [6], Cohen and Bleistein [26], a theory was developed to extract information from a high frequency band-limited Fourier transform of a piecewise constant function. It was shown in these studies of references how to locate the discontinuities of such a function and how to estimate the magnitude of the discontinuity. To achieve higher order accuracy Gray [42] presented an inversion technique based on perturbation theory. There is a rich literature on travel-time method in the continuous case (Ware and Aki [70], Gopinath and Sondhi [40]), these authors were primarily concerned with the case of discontinuous velocity profiles. Raz [63] provided extension to the three-dimensional case. He showed how observations at different offsets can be used to invert a tilted stratified earth. An approach to the fully three-dimensional problem was presented in Clayton and Stolt [24]. The most recent results following Born approximation applied to three-dimensional problems are due to Bleistein [14, 17, 18], Liner [53], Hanitzsch [46], Gardner et al. [35], Berkhout et al. [11], Black et al. [12], Artley and Hale [7], Gray [43, 44], de Hoop et al. [29], Tygel et al. [67], Xu [73] among others.

In this chapter we introduce a damping term in the wave equation (Stakgold [65]) and study its effect on inversion. The damping may be caused due to impurities in the medium, the presence of fluid saturated rocks in the medium, distributed boundary frictions or small viscous effects. We will consider the procedure for high frequency inversion. The starting point is an integral equation based on the Born approximation for modelling the direct scattering problem. The major steps of the derivation of a high frequency inversion technique are as follows:

- Derive the forward modelling formula (written in terms of unknown material parameters).
- Find a way to invert the modeling formula to solve for unknown material parameters.
- If a satisfactory result is not obtained, begin the process again by deriving a new forward model.

4.1.1 Organization of the Chapter

In the second section of this chapter, we consider the recovery of wave speed and damping for one dimensional damped wave equation. The velocity inversion without damping is summarized in the first subsection and is based upon Bleistein et al. [18]. The velocity inversion in the presence of damping is discussed in the second subsection. The damping parameter is recovered in the third subsection, and an iteration procedure to improve the results is also described.

The three-dimensional problem is considered in the third section of this chapter. We present the procedure for velocity inversion in this case. We consider the simplest case, that is to recover the wave speed for constant background and zero-offset data. Nevertheless, this will provide a launching pad to attack more complicated problems.

The background material and complicated calculations are summarized in Appendix C.

4.2 Inversion in the One-dimension

In this section we study the one-dimensional damped wave equation. Our aim is to recover variations in velocity and damping, which in turn yields a map of interfaces in the interior of the earth. The work presented in this section had been reported. see Zaman and Masood [75].

4.2.1 Inversion Without Damping

Assume that the propagation of the field $u(x,\omega)$ is governed by the scalar Helmholtz equation

$$\pounds u = \frac{d^2u}{dx^2} + \frac{\omega^2}{v^2(x)}u = -\delta(x). \tag{4.1}$$

together with the Sommerfeld radiation condition

$$\frac{du}{dx} \mp \frac{i\omega}{v(x)}u \to 0. \quad \text{as } x \to \pm\infty. \tag{4.2}$$

Suppose $v(x)$ is a perturbation on some reference or background velocity, $c(x)$

$$\frac{1}{v^2(x)} = \frac{1}{c^2(x)}\left[1+\alpha(x)\right], \quad \alpha(x) << 1. \tag{4.3}$$

The total field $u(x,\omega)$ can be separated into the incident part $u_I(x,\omega)$ in the absence

of the perturbation and $u_S(x,\omega)$ in the presence of the perturbation, $a(x)$. Thus, set

$$u(x,\omega) = u_I(x,\omega) + u_S(x,\omega). \tag{4.4}$$

and require that $u_I(x,\omega)$ and $u_S(x,\omega)$ are solutions of the following problems:

$$\mathcal{L}_0 u_I = \frac{d^2 u_I}{dx^2} + \frac{\omega^2}{c^2} u_I = -\delta(x). \tag{4.5}$$

$$\mathcal{L}_0 u_S = -\frac{\omega^2}{c^2}\left[u_I(x,\omega) + u_S(x,\omega)\right]. \tag{4.6}$$

Next, we use the Green function representation to write down the solution of equation (4.6) as

$$u_S(\zeta,\omega) = \omega^2 \int_0^\infty \frac{a(x)}{c^2(x)}\left[u_I(x,\omega) + u_S(x,\omega)\right] g(x,\zeta,\omega)\, dx. \tag{4.7}$$

The product, $a(x)\, u_S(x,\omega)$, appearing under the integral in (4.7) is significantly smaller than the product, $a(x)\, u_I(x,\omega)$, and this leads to the Born approximation

$$u_S(\zeta,\omega) = \omega^2 \int_0^\infty \frac{a(x)}{c^2(x)} u_I(x,\omega)\, g(x,\zeta,\omega)\, dx. \tag{4.8}$$

Since for the inverse problem, the total field is observed at the origin, i.e. $\zeta = 0$

$$u_S(0,\omega) = \omega^2 \int_0^\infty \frac{a(x)}{c^2(x)} u_I(x,\omega)\, g(x,0,\omega)\, dx. \tag{4.9}$$

The WKBJ approximation of the Green function has the following form

$$g(x,0,\omega) = -\frac{A(x)}{2i\omega} \exp\left[i\omega\varphi(x,0)\right] \quad , \quad \varphi(x,y) = \int_y^x \frac{dt}{c(t)}. \tag{4.10}$$

In the simplest case, when $c(x)$ is continuous, the WKBJ amplitude $A(x)$ is given by

$$A(x) = \sqrt{c(0)\, c(x)}.$$

Since we are concerned here entirely with high frequency solutions, we need to use $u_I(x,\omega) = F(\omega)\, g(x,0,\omega)$, where $F(\omega)$ is some frequency domain (high-pass) filter. With this modification for $u_I(x,\omega)$, and using (4.10) for $g(x,0,\omega)$ in (4.9) leads to the integral equation

$$u_S(0,\omega) = -\int_0^\infty F(\omega)\, \frac{a(x)\, A^2(x)}{4c^2(x)} \exp\left[2i\omega\varphi(x,0)\right] dx. \tag{4.11}$$

Since $a(x) = 0$ for $x < 0$, this is Fourier type integral because lower limit can be extended to $-\infty$. However, the amplitude in this more general Fourier integral should be calculated separately, see Appendix C. The inversion operator corresponding to this has the form (with $F(\omega) = 1$)

$$\alpha(y) = -\frac{4c(y)}{\pi A^2(y)} \int_{-\infty}^{\infty} u_S(0,\omega) \exp[-2i\omega\phi(y,0)]\, d\omega. \tag{4.12}$$

The reflectivity function $\beta(y)$ can be obtained by differentiating (4.12) with respect to 'y' and dividing by -4. Thus multiplying (4.12) by the factor $\frac{i\omega}{2c(y)}$ we obtain the result

$$\beta(y) = -\frac{2}{\pi A^2(y)} \int_{-\infty}^{\infty} i\omega u_S(0,\omega) \exp[-2i\omega\phi(y,0)]\, d\omega. \tag{4.13}$$

4.2.2 Velocity Inversion in the Presence of Damping

In this section, the one-dimensional problem for variable velocity in the presence of variable damping will be considered. Consider the propagation of the field governed by the scalar Helmholtz equation

$$\mathcal{L}u = \frac{d^2u}{dx^2} + \left[\frac{\omega^2 + i\omega\gamma(x)}{v^2(x)}\right] u = -\delta(x - x_s). \tag{4.14}$$

with damping $\gamma(x)$ and source placed at point x_s. It is assumed that the source point is to the left of the region where $v(x)$ and $\gamma(x)$ are unknown. The impulse response will be observed at a point x_g also to the left of the region of unknown $v(x)$ and $\gamma(x)$. The objective will be to see what can be determined about the perturbations from the observed response.

Introduce variations in damping and sound speed to have the parallel form

$$\gamma(x) = \gamma_0(x) + \epsilon\gamma(x). \tag{4.15}$$

$$v(x) = v_0(x) + \epsilon v(x). \qquad \frac{1}{v^2(x)} = \frac{1}{v_0^2(x)}\left[1 - \frac{2\epsilon v(x)}{v_0(x)}\right]. \tag{4.16}$$

We have used same ϵ for both $\gamma(x)$ and $v(x)$, because if it is ϵ_1 for $\gamma(x)$ and ϵ_2 for $v(x)$ then we set $\epsilon = \max(\epsilon_1, \epsilon_2)$. These representations are substituted into (4.14) and only linear terms in ϵ are retained. The resulting equation is

$$\begin{aligned} \mathcal{L}_0 u &= \frac{d^2u}{dx^2} + \left[\frac{\omega^2 + i\omega\gamma_0(x)}{v_0^2(x)}\right] u = -\delta(x - x_s) \\ &+ \left[-i\epsilon\omega\gamma(x) + \frac{2\epsilon\omega^2 v(x)}{v_0(x)} + \frac{2i\epsilon\omega\gamma_0(x)\, v(x)}{v_0(x)}\right] \frac{u}{v_0^2(x)}. \end{aligned} \tag{4.17}$$

Introduce $u_I(x, x_s, \omega)$ as the response to the delta function in the unperturbed medium and $u_S(x, x_s, \omega)$ as everything else. we can write $u = u_I + u_S$ with

$$\mathcal{L}_0 u_I(x, x_s, \omega) = -\delta(x - x_s). \tag{4.18}$$

and

$$\mathcal{L}_0 u_S(x, x_s, \omega) = \left[-i\epsilon\omega\gamma(x) + \frac{2\epsilon\omega^2 v(x)}{v_0(x)} + \frac{2i\epsilon\omega\gamma_0(x)\, v(x)}{v_0(x)}\right] \frac{u_I(x, x_s, \omega)}{v_0^2(x)}. \tag{4.19}$$

We now construct a Green's function representation of (4.19), observed at a point x_g (geophone location). It satisfies the following equation

$$\mathcal{L}_0 g\left(x, x_g, \omega\right) = -\delta\left(x - x_g\right). \tag{4.20}$$

Note that this Green's function differs from u_I, defined by (4.18), only by subscripts s and g. Since we are concerned only with high frequency inversion, we will use WKBJ approximations for u_I and g to the leading order in ω. These leading order approximations are given by

$$u_I\left(x, x_s, \omega\right) = -\frac{F\left(\omega\right) A\left(x_s, x\right)}{2i\omega} \exp\left[i\omega\phi\left(x_s, x\right) - \frac{1}{2}\psi\left(x_s, x\right)\right], \tag{4.21}$$

$$g\left(x, x_g, \omega\right) = -\frac{A\left(x_g, x\right)}{2i\omega} \exp\left[i\omega\phi\left(x_g, x\right) - \frac{1}{2}\psi\left(x_g, x\right)\right], \tag{4.22}$$

where for the case of continuous $v_0\left(x\right)$ and $\gamma_0\left(x\right)$ the WKBJ amplitude and phase are given by

$$A\left(x_g, x\right) = \sqrt{v_0\left(x_g\right) v_0\left(x\right)}. \qquad \phi\left(x_g, x\right) = \int_{x_g}^{x} \frac{dt}{v_0\left(t\right)}, \text{ and } \psi\left(x_g, x\right) = \int_{x_g}^{x} \frac{\gamma_0\left(t\right) dt}{v_0\left(t\right)}. \tag{4.23}$$

The solution of (4.19) in terms of Green's function is given by

$$u_S(x_g, x_s, \omega) = -\int_0^\infty \left[-i\epsilon\omega\gamma(x) + \frac{2\epsilon\omega^2 v(x)}{v_0(x)} + \frac{2i\epsilon\omega\gamma_0(x)v(x)}{v_0(x)}\right] \frac{u_j(x, x_s, \omega)\, g(x, x_g, \omega)}{v_0^2(x)} dx. \tag{4.24}$$

Now using the WKBJ representations (4.21) and (4.22) in (4.24), and retaining only the leading order terms in ω, we get

$$u_S(x_g, x_s, \omega) = \frac{\epsilon}{2}\int_0^\infty F(\omega)\frac{v(x)}{v_0^3(x)} A(x_g, x) A(x_s, x) \exp\{i\omega[\varphi(x_g, x) + \varphi(x_s, x)]\} \exp\left\{-\frac{1}{2}[v(x_g, x) + v(x_s, x)]\right\} dx. \tag{4.25}$$

This can be treated as a Fourier transform of $\epsilon v(x)$ and inversion can be performed in the same way as (4.11), see Appendix C. The result is

$$\epsilon v(y) = \frac{2v_0^2(y)\exp\left\{\frac{1}{2}[v(x_g, y) - v(x_s, y)]\right\}}{\pi A(x_g, y) A(x_s, y)} \int_{-\infty}^{\infty} u_S(x_g, x_s, \omega) \exp\{-i\omega[\varphi(x_g, y) + \varphi(x_s, y)]\} d\omega. \tag{4.26}$$

The reflectivity function $\beta(y)$ can be computed in the same way as in (4.12) and is given by

$$\beta(y) = \frac{-2\exp\left\{\frac{1}{2}\left[\psi(x_g,y)+\psi(x_s,y)\right]\right\}}{\pi A(x_g,y)A(x_s,y)}\int_{-\infty}^{\infty} i\omega u_S(x_g,x_s,\omega)$$
$$\exp\left\{-i\omega\left[\phi(x_g,y)+\phi(x_s,y)\right]\right\}d\omega. \tag{4.27}$$

From expressions (4.26) and (4.27), it is clear that perturbation in velocity and reflectivity function also depend on background damping $\gamma_0(x)$. Hence these results demonstrate an improvement on previous results. These expressions reduce to (4.12) and (4.13), if we take $\gamma(x)=0$ and $x_s=x_g=0$.

4.2.3 Recovery of the Damping Effect

Consider (4.24) again and retain terms of order $\frac{1}{\omega}$ to get

$$u_S(x_g,x_s,\omega) = -\int_0^{\infty} F(\omega)\left[\frac{i\epsilon\gamma(x)}{4\omega}-\frac{\epsilon v(x)}{2v_0(x)}-\frac{i\epsilon\gamma_0(x)v(x)}{2\omega v_0(x)}\right]$$
$$\frac{A(x_g,x)A(x_s,x)}{v_0^2(x)}\exp\left\{i\omega\left[\phi(x_g,x)+\phi(x_s,x)\right]\right\}$$
$$\exp\left\{-\frac{1}{2}\left[\psi(x_g,x)+\psi(x_s,x)\right]\right\}dx. \tag{4.28}$$

Since $\epsilon v(x)$ is known from (4.26), therefore set

$$V(x_g,x_s,\omega) = \int_0^{\infty} F(\omega)\left[\frac{\epsilon v(x)}{2v_0(x)}+\frac{i\epsilon\gamma_0(x)v(x)}{2\omega v_0(x)}\right]\frac{A(x_g,x)A(x_s,x)}{v_0^2(x)} \tag{4.29}$$
$$\exp\left\{i\omega\left[\phi(x_g,x)+\phi(x_s,x)\right]\right\}\exp\left\{-\frac{1}{2}\left[\psi(x_g,x)+\psi(x_s,x)\right]\right\}dx,$$

and

$$W(x_g, x_s, \omega) = 4i\omega \left[u_S(x_g, x_s, \omega) - V(x_g, x_s, \omega) \right]. \tag{4.30}$$

Using (4.29) and (4.30) in (4.28), we get the following integral equation

$$\begin{aligned} W(x_g, x_s, \omega) &= \int_0^\infty F(\omega) \frac{\epsilon\gamma(x) A(x_g, x) A(x_s, x)}{v_0^2(x)} \exp\{i\omega [\phi(x_g, x) + \phi(x_s, x)]\} \\ &\quad \exp\left\{ -\frac{1}{2} [v(x_g, x) + v(x_s, x)] \right\} dx. \end{aligned} \tag{4.31}$$

Since $\epsilon\gamma(x) = 0$ for $x < 0$, therefore lower integral limit can be extended to $-\infty$. This is Fourier integral and it can be inverted in the same way as in (4.11), see Appendix C. The result is

$$\begin{aligned} \epsilon\gamma(y) &= \frac{v_0(y) \exp\left\{ \frac{1}{2} [v(x_g, y) + v(x_s, y)] \right\}}{\pi A(x_g, y) A(x_s, y)} \int_{-\infty}^{\infty} W(x_g, x_s, \omega) \\ &\quad \exp\{-i\omega [\phi(x_g, y) + \phi(x_s, y)]\} d\omega. \end{aligned} \tag{4.32}$$

Substitute the approximation obtained for $\epsilon\gamma(y)$ from (4.32) in expression (4.28), and set

$$X(x_g, x_s, \omega) = \int_0^\infty F(\omega) \left[\frac{i\epsilon\gamma(x)}{4\omega}\right] \frac{A(x_g, x) A(x_s, x)}{v_0^2(x)} \exp\{i\omega[\phi(x_g, x) + \phi(x_s, x)]\}$$
$$\exp\left\{-\frac{1}{2}[\psi(x_g, x) + \psi(x_s, x)]\right\} dx. \tag{4.33}$$

Assume constant background damping, that is, $\gamma_0(x) = \gamma_0$, and write

$$Y(x_g, x_s, \omega) = \frac{2\omega}{(\omega + i\gamma_0)} [X(x_g, x_s, \omega) + u_S(x_g, x_s, \omega)]. \tag{4.34}$$

Therefore the improved value of $\epsilon v(y)$ is given by

$$\epsilon v(y) = \frac{v_0^2(y) \exp\left\{\frac{1}{2}[\psi(x_g, y) + \psi(x_s, y)]\right\}}{\pi A(x_g, y) A(x_s, y)} \int_{-\infty}^{\infty} Y(x_g, x_s, \omega)$$
$$\exp\{-i\omega[\phi(x_g, y) + \phi(x_s, y)]\} d\omega. \tag{4.35}$$

Now from (4.35), $\epsilon v(y)$ can be computed and the above procedure from (4.29) to (4.35) can be repeated to get the next approximations for $\epsilon\gamma(y)$ and $\epsilon v(y)$. The results of this section demonstrate the dependence of perturbation in wave speed on perturbation in damping and vice versa. We have derived an approximate solution to the inverse problem for the wave speed in the presence of damping. The perturbation in damping is also recovered in an inhomogeneous medium. Finally, an iterative procedure is presented to get increasingly better approximations.

4.3 Inversion in Higher Dimensions

In the previous section a procedure was presented for high frequency inversion of impulse response data. Here, we consider the three-dimensional inverse problem and follow a similar procedure to derive an integral equation and begin the process of high frequency inversion. As in the previous section, the starting point is an inverse scattering integral equation based on the Born approximation for modeling of the direct scattering problem. Now, however, an added richness to the problem arises from the extra dimensions. Because now the sources and receivers need no longer to be coincident or in a line and changes in background propagation speed and damping now lead to refraction and other higher dimensional phenomena. As in the one-dimensional case, much insight will be gained from considering the constant background and zero-offset problem.

4.3.1 The Scattering Problem

We introduce a three-dimensional coordinate system, (x_1, x_2, x_3), with x_3 positive in the downward direction. The propagation speed and damping is assumed to be known in some portion of the region $x_3 \geq 0$ and unknown outside that portion of the region. We consider a bandlimited impulsive point source at x_s and response to this source will be observed at one or more geophones x_g. The objective is to obtain information about the propagation speed, $v(x)$, from observations of the wavefield. Now instead of the one-dimensional Helmholtz equation (4.14), the signal propagation is governed by the three-dimensional Helmholtz equation

$$\mathcal{L}u(x, x_s, \omega) = \left[\nabla^2 + \frac{\omega^2 + i\omega\gamma(x)}{v^2(x)}\right] u(x, x_s, \omega) = -F(\omega)\,\delta(x - x_s), \qquad (4.36)$$

where $F(\omega)$ is some frequency domain filter. The function $u(x, x_s, \omega)$ satisfies the Sommerfeld radiation condition

$$ru \text{ bounded}, \quad r\left(\frac{\partial u}{\partial r} - \frac{i\sqrt{\omega^2 + i\omega\gamma}}{v}u\right) \to 0 \quad \text{as} \quad r \to \infty, \quad r = |x|. \quad (4.37)$$

We introduce variations in damping and propagation speed to have parallel form. that is the background plus the perturbation. and therefore these profiles have the following representations

$$\gamma(x) = \gamma_0(x) + \epsilon\gamma(x). \qquad (4.38)$$

$$v(x) = v_0(x) + \epsilon v(x), \qquad \frac{1}{v^2(x)} = \frac{1}{v_0^2(x)}\left[1 - \frac{2\epsilon v(x)}{v_0(x)}\right]. \qquad (4.39)$$

where we have retained only first order terms of ϵ. These representations are substituted into (4.36) and only linear terms in ϵ are retained. The resulting equation is

$$\mathcal{L}_0 u(x, x_s, \omega) = \left[\nabla^2 + \frac{\omega^2 + i\omega\gamma_0(x)}{v_0^2(x)}\right] u(x, x_s, \omega) = -F(\omega)\,\delta(x - x_s) + \left[-i\epsilon\omega\gamma(x) + \frac{2\epsilon\omega^2 v(x)}{v_0(x)} + \frac{2i\epsilon\omega\gamma_0(x)\,v(x)}{v_0(x)}\right] \frac{u(x, x_s, \omega)}{v_0^2(x)}. \quad (4.40)$$

Following the footsteps of the one-dimensional problem, the wavefield can be decomposed into a reference field $u_I(x, x_s, \omega)$ and a scattered field $u_S(x, x_s, \omega)$:

$$u(x, x_s, \omega) = u_I(x, x_s, \omega) + u_S(x, x_s, \omega). \quad (4.41)$$

Now we substitute (4.41) into (4.40) and require that $u_I(x, x_s, \omega)$ is a solution of the unperturbed equation

$$\mathcal{L}_0 u_I(x, x_s, \omega) = -F(\omega)\,\delta(x - x_s). \quad (4.42)$$

subject to the radiation condition (4.37). It now follows that $u_S(x, x_s, \omega)$ satisfies the following equation

$$\mathcal{L}_0 u_S(x, x_s, \omega) = \left[-i\epsilon\omega\gamma(x) + \frac{2\epsilon\omega^2 v(x)}{v_0(x)} + \frac{2i\epsilon\omega\gamma_0(x)\,v(x)}{v_0(x)}\right] \frac{u_I(x, x_s, \omega)}{v_0^2(x)}. \quad (4.43)$$

As in the one dimensional case, we write $u_S(x, x_s, \omega)$ in terms of the Green function

$$u_S(x_g, x_s, \omega) = \int_D \left[-i\epsilon\omega\gamma(x) + \frac{2\epsilon\omega^2 v(x)}{v_0(x)} + \frac{2i\epsilon\omega\gamma_0(x)\, v(x)}{v_0(x)} \right] \frac{[u_I(x, x_s, \omega) + u_S(x, x_s, \omega)]\, g(x, x_g, \omega)}{v_0^2(x)} d^3x. \quad (4.44)$$

Here, the domain D of integration must contain the support of $\alpha(x)$ and $\gamma(x)$ assumed to be some finite subdomain of $x_3 > 0$.

4.3.1.1 The Born Approximation

As in the one-dimensional case for small perturbations ($\epsilon v(x)$ and $\epsilon\gamma(x)$), we would like to argue that the scattered field $u_S(x, x_s, \omega)$ is small. So that we can neglect the products of $\epsilon v(x)$ and $\epsilon\gamma(x)$ with $u_S(x, x_s, \omega)$ as compared to the products with $u_I(x, x_s, \omega)$ under the integral sign of the integral equation (4.44). Unfortunately, this is not always true in three dimensions if the reflected field is observed beyond the critical angle of reflection. In this case the reflection coefficient has unit magnitude and the scattered field is comparable to the incident field, at least in that subdomain of D. Thus we cannot neglect the former product as compared to the latter in three dimensions, as it was in the one-dimensional problem. However, for near zero-offset or backscattered observations, it is true that small $\epsilon v(x)$ and $\epsilon\gamma(x)$ imply small $u_S(x, x_s, \omega)$. Since this is the problem to be considered, we proceed to make the Born approximation to obtain the integral equation

$$u_S(x_g, x_s, \omega) = \int_D \left[-i\epsilon\omega\gamma(x) + \frac{2\epsilon\omega^2 v(x)}{v_0(x)} + \frac{2i\epsilon\omega\gamma_0(x)v(x)}{v_0(x)} \right] \frac{u_I(x, x_s, \omega)\, g(x, x_g, \omega)}{v_0^2(x)} d^3x. \tag{4.45}$$

The equation (4.45) is the fundamental integral equation for acoustic inversion.

4.3.2 The Constant Background Zero-Offset Equation

The simplest problem to deal with is one in which the source and receiver are coincident, that is $x_s = x_g$, on a flat surface $x_3 = 0$, the background speed and damping are constant, $v_0(x) = v_0$, $\gamma_0(x) = \gamma_0$. In this case it is convenient to introduce

$$\zeta = (\zeta_1, \zeta_2, 0) = x_s = x_g. \tag{4.46}$$

Assuming a high frequency, we can make following approximation

$$\sqrt{\frac{\omega^2 + i\omega\gamma_0}{v_0^2}} \approx \frac{\omega}{v_0}\left(1 + \frac{i\gamma_0}{2\omega}\right). \tag{4.47}$$

So, we would have following representations for the Green function and the incident field

$$g(\zeta, x, \omega) = \frac{\exp\left[\frac{\omega\left(1+\frac{i\gamma_0}{2\omega}\right)r}{v_0}\right]}{4\pi r}. \tag{4.48}$$

$$u_I(\zeta, x, \omega) = F(\omega) \frac{\exp\left[\frac{\omega\left(1+\frac{i\gamma_0}{2\omega}\right)r}{v_0}\right]}{4\pi r}, \qquad r = |x - \zeta|. \tag{4.49}$$

Therefore we can rewrite (4.45) as

$$u_S(\zeta, \omega) = \frac{F(\omega)}{(4\pi v_0)^2} \int_{x_3>0} \left[-i\epsilon\omega\gamma(x) + \frac{2\epsilon\omega^2 v(x)}{v_0} + \frac{2i\epsilon\omega\gamma_0 v(x)}{v_0}\right] \frac{\exp\left[\frac{2i\omega\left(1+\frac{i\gamma_0}{2\omega}\right)r}{v_0}\right]}{r^2} d^3x. \tag{4.50}$$

4.3.2.1 One Experiment, One Degree of Freedom in $\epsilon v(x)$ and $\epsilon\gamma(x)$

Suppose that data is collected for one zero-offset experiment. In this case, we seek an inversion only for $\epsilon v(x) = \epsilon v(x_3)$ and $\epsilon\gamma(x) = \epsilon\gamma(x_3)$, i.e. the wavespeed and damping vary from constant backgrounds as functions of depth only. Furthermore, the coordinates of that single experiment might as well be taken to be $(0, 0, 0)$, so that (4.50) becomes

$$u_S(0, 0, 0, \omega) = \frac{F(\omega)}{(4\pi v_0)^2} \int_{x_3>0} \left[-i\epsilon\omega\gamma(x_3) + \frac{2\epsilon\omega^2 v(x_3)}{v_0} + \frac{2i\epsilon\omega\gamma_0 v(x_3)}{v_0}\right] \frac{\exp\left[\frac{2i\omega\left(1+\frac{i\gamma_0}{2\omega}\right)r}{v_0}\right]}{r^2} d^3x, \qquad r = \sqrt{x_1^2 + x_2^2 + x_3^2}. \tag{4.51}$$

The dependence of the integrand on x_1 and x_2 is only through r. Therefore

integration in these variables can be carried out. Introducing polar coordinates (ρ, θ) in place of (x_1, x_2). So, the integral equation (4.51) takes the form

$$u_S(0,0,0,\omega) = \frac{F(\omega)}{8\pi v_0^2}\int_{x_3>0}\left[-i\epsilon\omega\gamma(x_3) + \frac{2\epsilon\omega^2 v(x_3)}{v_0} + \frac{2i\epsilon\omega\gamma_0 v(x_3)}{v_0}\right] \frac{\exp\left[\frac{2i\omega\left(1-\frac{i\gamma_0}{2\omega}\right)r}{v_0}\right]}{r^2}\rho d\rho dx_3. \qquad r=\sqrt{\rho^2+x_3^2}. \tag{4.52}$$

While it may not be possible to evaluate the integral over ρ exactly, it is possible to find an approximation to this integral that is consistent with the high frequency assumption. To do this we require that $\mathrm{Im}\,\omega > 0$, and integrate by parts with respect to ρ. The term to be integrated is $\exp\left[\frac{i(2\omega+i\gamma_0)r}{v_0}\right]\frac{\rho}{r}$, and noting that $\frac{d\rho}{dr} = \frac{\rho}{r}$, we obtain

$$\begin{aligned} u_S(0,0,0,\omega) = \frac{F(\omega)}{8\pi v_0^2}\Bigg\{ & \int_{x_3>0}\left[-i\epsilon\omega\gamma(x_3) + \frac{2\epsilon\omega^2 v(x_3)}{v_0} + \frac{2i\epsilon\omega\gamma_0 v(x_3)}{v_0}\right] \\ & \frac{v_0}{2i\omega\left(1+\frac{i\gamma_0}{2\omega}\right)r}\exp\left[\frac{2i\omega\left(1+\frac{i\gamma_0}{2\omega}\right)r}{v_0}\right]\Bigg|_0^\infty dx_3 \\ & + \int_{x_3>0}\left[-i\epsilon\omega\gamma(x_3) + \frac{2\epsilon\omega^2 v(x_3)}{v_0} + \frac{2i\epsilon\omega\gamma_0 v(x_3)}{v_0}\right] \\ & \frac{v_0}{2i\omega\left(1+\frac{i\gamma_0}{2\omega}\right)r^3}\exp\left[\frac{2i\omega\left(1+\frac{i\gamma_0}{2\omega}\right)r}{v_0}\right]\rho d\rho dx_3\Bigg\}. \end{aligned} \tag{4.53}$$

We keep only the leading order terms in ω and set $F(\omega) = 1$, to get

$$u_S(0,0,0,\omega) = \frac{i\omega}{8\pi v_0^2} \int_{x_3>0} \frac{\epsilon v(x_3)}{\left(1 + \frac{i\gamma_0}{2\omega}\right) x_3} \exp\left[\frac{2i\omega x_3}{v_0}\right] \exp\left[\frac{-\gamma_0 x_3}{v_0}\right] dx_3. \qquad (4.54)$$

This equation represents the observed data as some multiple of the Fourier transform of $(\epsilon v(x_3) \exp[-\gamma_0 x_3/v_0])/x_3$ and the solution is obtained by Fourier inversion. Here the transform variable is $2\omega/v_0$, therefore the Fourier inversion formula must be with respect to this transform variable. Consequently

$$\epsilon v(x_3) = 8x_3 v_0 \exp\left[\frac{\gamma_0 x_3}{v_0}\right] \int_{-\infty}^{\infty} \frac{u_S(0,0,\omega)}{i\omega} \left(1 + \frac{i\gamma_0}{2\omega}\right) \exp\left[\frac{-2i\omega x_3}{v_0}\right] d\omega. \qquad (4.55)$$

Now we compare this result with the one-dimensional inversion formula (4.26). While there are certain similarities, there are differences as well. Here the observed field is three dimensional, so we should expect some change like the x_3 factor on the right hand side of (4.55) due to the geometrical spreading.

4.3.2.1.1 Recovery of Damping and an Iterative Procedure to Improve Velocity and Damping Profiles We consider (4.53) and integrate by parts with respect to ρ the second integral. Now we also include terms of order ω^0 and ω and set $F(\omega) = 1$, which yields

$$
\begin{aligned}
u_S(0,0,0,\omega) &= \frac{\omega}{8\pi v_0^2}\int_{x_3>0}\frac{\epsilon\gamma(x_3)\,v_0}{2\left(1+\frac{i\gamma_0}{2\omega}\right)x_3}\exp\left[\frac{2i\omega x_3}{v_0}\right]\exp\left[\frac{-\gamma_0 x_3}{v_0}\right]dx_3 + \\
&\quad \frac{\omega}{8\pi v_0^2}\int_{x_3>0}\frac{\epsilon v(x_3)}{\left(1+\frac{i\gamma_0}{2\omega}\right)x_3}\left(i\omega-\gamma_0+\frac{v_0}{2\left(1+\frac{i\gamma_0}{2\omega}\right)x_3}\right) \\
&\quad \exp\left[\frac{2i\omega x_3}{v_0}\right]\exp\left[\frac{-\gamma_0 x_3}{v_0}\right]dx_3 \\
&= X_1(\omega)+Y_1(\omega)\,. \qquad (4.56)
\end{aligned}
$$

where

$$
X_1(\omega)=\frac{\omega}{8\pi v_0^2}\int_{x_3>0}\frac{\epsilon\gamma(x_3)\,v_0}{2\left(1+\frac{i\gamma_0}{2\omega}\right)x_3}\exp\left[\frac{2i\omega x_3}{v_0}\right]\exp\left[\frac{-\gamma_0 x_3}{v_0}\right]dx_3.
$$

and

$$
\begin{aligned}
Y_1(\omega) &= \frac{\omega}{8\pi v_0^2}\int_{x_3>0}\frac{\epsilon v(x_3)}{\left(1+\frac{i\gamma_0}{2\omega}\right)x_3}\left(i\omega-\gamma_0+\frac{v_0}{2\left(1+\frac{i\gamma_0}{2\omega}\right)x_3}\right) \\
&\quad \exp\left[\frac{2i\omega x_3}{v_0}\right]\exp\left[\frac{-\gamma_0 x_3}{v_0}\right]dx_3.
\end{aligned}
$$

Now we can write (4.56) in the form

$$
u_S(0,0,0,\omega)-Y_1(\omega)=\frac{\omega}{8\pi v_0^2}\int_{x_3>0}\frac{\epsilon\gamma(x_3)\,v_0}{2\left(1+\frac{i\gamma_0}{2\omega}\right)x_3}\exp\left[\frac{2i\omega x_3}{v_0}\right]\exp\left[\frac{-\gamma_0 x_3}{v_0}\right]dx_3. \qquad (4.57)
$$

This equation represents the observed data and the recovered velocity profile from

(4.55) as some multiple of the Fourier transform of $(\epsilon\gamma(x_3)\exp[-\gamma_0 x_3/v_0])/x_3$, and the solution is obtained by Fourier inversion. Here the transform variable is $2\omega/v_0$, therefore Fourier inversion must be made with respect to this transform variable. Consequently

$$\epsilon\gamma(x_3) = 16x_3\exp\left[\frac{\gamma_0 x_3}{v_0}\right]\int_{-\infty}^{\infty}\frac{u_S(0.0,\omega)-X_1(\omega)}{\omega}\left(1+\frac{i\gamma_0}{2\omega}\right)\exp\left[\frac{-2i\omega x_3}{v_0}\right]d\omega. \tag{4.58}$$

Once $\epsilon\gamma(x_3)$ is recovered from (4.58), we can get next approximation to $\epsilon\gamma(x_3)$ from (4.56) as follows

$$\begin{aligned}\epsilon\gamma(x_3) &= 8x_3 v_0\exp\left[\frac{\gamma_0 x_3}{v_0}\right]\int_{-\infty}^{\infty}[u_S(0.0,\omega)-X_1(\omega)] \\ &\left(i\omega-\gamma_0+\frac{v_0}{2\left(1+\frac{i\gamma_0}{2\omega}\right)x_3}\right)\left(1+\frac{i\gamma_0}{2\omega}\right)\exp\left[\frac{-2i\omega x_3}{v_0}\right]d\omega. \end{aligned}\tag{4.59}$$

Expressions (4.58) and (4.59) describe an iterative procedure to improve the velocity and damping profiles.

4.3.3 Zero-Offset Constant Background Inversion in Three-dimensions

We again consider integral equation (4.50) and assume that the vector ζ ranges over the entire upper surface. When $F(\omega)=1$, this equation admits an exact solution

and this solution will be derived in this subsection. So first consider (4.50) with $F(\omega)$ replaced by unity

$$u_S(\zeta,\omega) = \frac{1}{(4\pi v_0)^2}\int_{x_3>0}\left[-i\epsilon\omega\gamma(x)+\frac{2\epsilon\omega^2 v(x)}{v_0}+\frac{2i\epsilon\omega\gamma_0 v(x)}{v_0}\right] \frac{1}{r^2}\exp\left[\frac{2i\omega r}{v_0}\right]\exp\left[\frac{-\gamma_0 r}{v_0}\right]d^3x. \tag{4.60}$$

where $\zeta = x_s = x_g$, and $r = |x-\zeta|$. Since the source and receiver are coincident, in the last expression we have modified the notation and set $u_S(x_g,x_s,\omega) = u_S(\zeta,\omega)$. We exploit the high frequency nature of the data and keep leading order terms of ω in the last integral equation. The result is

$$u_S(\zeta,\omega) = \frac{\omega^2}{8\pi^2 v_0^3}\int_{x_3>0}\frac{\epsilon v(x)}{r^2}\exp\left[\frac{(2i\omega-\gamma_0)r}{v_0}\right]. \tag{4.61}$$

The integral equation (4.61) is of convolution form, the function $\epsilon v(x)$ being convolved with the function $r^{-2}\exp[(2i\omega-\gamma_0)r/v_0]$. Thus, a Fourier transform will replace the integration in x_1 and x_2 by the multiplication of two transformed functions. Unfortunately, the Fourier transform of $r^{-2}\exp[(2i\omega-\gamma_0)r/v_0]$ is unknown. On the other hand, if there were only one power of r in the denominator, that is $r^{-1}\exp[(2i\omega-\gamma_0)r/v_0]$. then the Fourier transform would be known in closed form. Thus to get one power of r in the denominator we differentiate integral equation (4.61) with respect to ω. The result is

$$\int_D \epsilon v(x)\, g_1(\zeta - x.\omega)\, d^3x = -i\pi v_0^4 \frac{\partial}{\partial \omega}\left[\frac{u_S(\zeta.\omega)}{\omega^2}\right], \tag{4.62}$$

where g_1 is the free-space Green function for a medium.

$$g_1(\zeta - x.\omega) \equiv \frac{\exp\left[\frac{(2i\omega - \gamma_0)r}{v_0}\right]}{4\pi r}. \qquad r \equiv |\zeta - x|. \tag{4.63}$$

Now we define the spatial Fourier transform for this problem with a factor of two in the exponent. The forward spatial transform

$$\widetilde{f}(\kappa) = \int_{-\infty}^{\infty}\int_{-\infty}^{\infty} \exp[-2i\kappa.\rho]\, f(\rho)\, d^2\rho. \tag{4.64}$$

and the inverse transform

$$f(\rho) = \frac{1}{\pi^2}\int_{-\infty}^{\infty}\int_{-\infty}^{\infty} \exp[2i\kappa.\rho]\, \widetilde{f}(\rho)\, d^2\kappa. \tag{4.65}$$

are defined with the convention $\rho \equiv (x_1.x_2)$. The wave vector κ is defined in terms of two wave numbers k_1 and k_2 by $\kappa \equiv (k_1.k_2)$. Application of the spatial Fourier transform equation (4.64) to (4.62), converts the convolution to a multiplication in the κ domain and the result is

$$\int_0^{\infty} \epsilon\widetilde{v}(x)\, \widetilde{g}_1(\kappa.x_3.\omega)\, dx_3 = -i\pi v_0^4 \frac{\partial}{\partial \omega}\left[\frac{\widetilde{u}_S(\kappa.\omega)}{\omega^2}\right], \tag{4.66}$$

with the Transverse Fourier transform of $g_1(x.\omega)$ being given by

$$\widetilde{g}_1(\kappa.x_3.\omega) = \int_{-\infty}^{\infty}\int_{-\infty}^{\infty} \frac{\exp\left[-2i\kappa.\rho + \frac{(2i\omega-\gamma_0)r}{v_0}\sqrt{\rho^2+x_3^2}\right]}{4\pi\sqrt{\rho^2+x_3^2}} d^2\rho. \tag{4.67}$$

One way to find $\widetilde{g}_1(\kappa.x_3.\omega)$ is by directly performing the above integration. But the most physically enlightening way of finding the expression is by considering (4.63) as being Green's function for the Helmholtz equation

$$\left[\nabla^2 - \left(\frac{2i\omega-\gamma_0}{v_0}\right)^2\right] g_1(x_1.x_2.x_3.\omega) = -\delta(x_1)\,\delta(x_2)\,\delta(x_3). \tag{4.68}$$

The Fourier transform of this Helmholtz equation yields

$$\left[\frac{d^2}{dx_3^2} - 4\kappa^2 + \frac{4\omega^2}{v_0^2} - \frac{\gamma_0^2}{v_0^2} + \frac{4i\gamma_0\omega}{v_0^2}\right]\widetilde{g}_1(\kappa.x_3.\omega) = -\delta(x_3). \tag{4.69}$$

Note that the factor of 4 multiplying κ^2 is a result of having a factor of 2 in the exponent of the transform kernel. Since $k^2 = \frac{\omega^2}{v_0^2} - \frac{\gamma_0^2}{4v_0^2} + \frac{i\gamma_0\omega}{v_0^2} = k_1^2 + k_2^2 + k_3^2$, so rewriting the last equation by using the following definition for the vertical wave number k_3

$$k_3^2 = \frac{\omega^2}{v_0^2} - \frac{\gamma_0^2}{4v_0^2} + \frac{i\gamma_0\omega}{v_0^2} - \kappa^2, \tag{4.70}$$

allows us to write

$$\left[\frac{d^2}{dx_3^2} + (2k_3)^2\right] \widetilde{g}_1(\kappa, x_3, \omega) = -\delta(x_3). \tag{4.71}$$

It is now clear that $\widetilde{g}_1(\kappa, x_3, \omega)$ is just the Green function for the one-dimensional wave equation. Therefore we may write the result

$$\widetilde{g}_1(\kappa, x_3, \omega) = -\frac{\exp[2ik_3|x_3|]}{4ik_3}. \tag{4.72}$$

The real and imaginary parts of k_3 are given by

$$\mathrm{Re}(k_3) = \sqrt{\frac{1}{2}\left(\frac{\omega^2}{v_0^2} - \frac{\gamma_0^2}{4v_0^2} - \kappa^2 + \sqrt{\left(\frac{\omega^2}{v_0^2} - \frac{\gamma_0^2}{4v_0^2} - \kappa^2\right)^2 + \frac{\gamma_0^2\omega^2}{v_0^4}}\right)},$$

$$\mathrm{Im}(k_3) = \frac{\gamma_0\omega}{2v_0^2\,\mathrm{Re}(k_3)}.$$

On substitution of (4.72) in (4.66), we obtain

$$\int_0^\infty \epsilon\widetilde{v}(x)\exp[2ik_3|x_3|]\,dx_3 = -4\pi k_3 v_0^4 \frac{\partial}{\partial\omega}\left[\frac{\widetilde{u}_S(\kappa,\omega)}{\omega^2}\right]. \tag{4.73}$$

The integral equation (4.73) is nearly a forward Fourier transform in x_3. To make this similarity exact, first we observe that $x_3 = |x_3|$ on the domain of integration. Furthermore, the lower limit of integration can be extended to $-\infty$, since by assumption $\epsilon v(x) = 0$ for $x_3 < 0$ and hence $\epsilon\widetilde{v}(x)$ is also zero for $x_3 < 0$. We may thus

write (4.73) as

$$\int_{-\infty}^{\infty} \epsilon\widetilde{v}(x) \exp[2ik_3x_3]\, dx_3 = -4\pi k_3 v_0^4 \frac{\partial}{\partial\omega}\left[\frac{\widetilde{u}_S(\kappa,\omega)}{\omega^2}\right]. \tag{4.74}$$

Application of the inverse transform to the equation (4.74) leads to

$$\begin{aligned} &\frac{1}{\pi}\int_{-\infty}^{\infty}\left\{\int_{-\infty}^{\infty}\epsilon\widetilde{v}(x)\exp[2ik_3x_3]\,dx_3\right\}\exp[-2ik_3x_3]\,dk_3 \\ = &-\int_{-\infty}^{\infty} 4k_3v_0^4\frac{\partial}{\partial\omega}\frac{\widetilde{u}_S(\kappa,\omega)}{\omega^2}\exp[-2ik_3x_3]\,dk_3. \end{aligned} \tag{4.75}$$

This yields the following equation

$$\epsilon\widetilde{v}(x) = -4v_0^4\int_{-\infty}^{\infty} k_3\frac{\partial}{\partial\omega}\left[\frac{\widetilde{u}_S(\kappa,\omega)}{\omega^2}\right]\exp[-2ik_3x_3]\,dk_3. \tag{4.76}$$

Now apply the inverse Fourier transform (4.65) to (4.76). we find that

$$\epsilon v(x) = -\frac{4v_0^4}{\pi^2}\int_{-\infty}^{\infty} k_3\frac{\partial}{\partial\omega}\left[\frac{\widetilde{u}_S(\kappa,\omega)}{\omega^2}\right]\exp[2i(\kappa.\rho - k_3x_3)]\,d^3k. \tag{4.77}$$

In the right hand side of (4.77) the ζ dependence is not explicit, and to make this dependence explicit we write $\widetilde{u}_S(\kappa,\omega)$ in its spatial Fourier representation (that is to apply (4.64)). Thus we have

$$\begin{aligned} \epsilon v(x) = &-\frac{4v_0^4}{\pi^2}\int_{-\infty}^{\infty} k_3 d^3k\int_{-\infty}^{\infty} d^2\zeta\frac{\partial}{\partial\omega}\left[\frac{u_S(\zeta,\omega)}{\omega^2}\right] \\ &\exp[2i(\kappa.(\rho-\zeta) - k_3x_3)]. \end{aligned} \tag{4.78}$$

Since the data are recorded in the time domain, the inversion formula should be written as a function of time. Rewriting $u_S(\zeta,\omega)$ in its temporal Fourier representation

$$\begin{aligned} \epsilon v(x) &= -\frac{4iv_0^4}{\pi^2}\int_{-\infty}^{\infty} d^2\zeta \int_{-\infty}^{\infty} k_3 d^3k \exp\left[2i\left(\kappa\cdot(\rho-\zeta)-k_3x_3\right)\right] \\ &\quad \frac{1}{\omega_0^2}\int_0^{\infty} u_S(\zeta,t)\left[1+\frac{2i}{\omega_0 t}\right] t\exp\left[i\omega_0 t\right] dt. \end{aligned} \tag{4.79}$$

This is an exact solution to the integral equation (4.61). More precisely, (4.61) is an equation in the space-frequency domain, meaning that (4.78) is a solution of (4.61) and the last expression is the result of reexpressing the observed data in space-time.

4.3.3.0.2 Recovery of the Damping and an Iterative Procedure to Improve Velocity and Damping Profiles We consider the expression (4.60), and writing it in the form

$$\begin{aligned} \frac{u_S(\zeta,\omega)}{\omega} &= \frac{1}{(4\pi v_0)^2}\int_{x_3>0}\frac{2\epsilon v(x)}{v_0 r^2}(\omega+i\gamma_0)\exp\left[\frac{2i\omega r}{v_0}\right]\exp\left[\frac{-\gamma_0 r}{v_0}\right] d^3x \\ &\quad -\frac{i}{(4\pi v_0)^2}\int_{x_3>0}\frac{\epsilon\gamma(x)}{r^2}\exp\left[\frac{2i\omega r}{v_0}\right]\exp\left[\frac{-\gamma_0 r}{v_0}\right] d^3x \\ &= X_2(\zeta,\omega)+Y_2(\zeta,\omega), \end{aligned} \tag{4.80}$$

where

$$X_2(\zeta,\omega)=\frac{1}{(4\pi v_0)^2}\int_{x_3>0}\frac{2\epsilon v(x)}{v_0 r^2}(\omega+i\gamma_0)\exp\left[\frac{2i\omega r}{v_0}\right]\exp\left[\frac{-\gamma_0 r}{v_0}\right] d^3x.$$

and

$$Y_2(\zeta,\omega) = -\frac{i}{(4\pi v_0)^2}\int_{x_3>0}\frac{\epsilon\gamma(x)}{r^2}\exp\left[\frac{2i\omega r}{v_0}\right]\exp\left[\frac{-\gamma_0 r}{v_0}\right]d^3x.$$

Since $\epsilon\gamma(x)$ can be recovered from (4.79), therefore $X_2(\zeta,\omega)$ can be treated as known function. Expression (4.80) can be written in the form

$$-\frac{i}{(4\pi v_0)^2}\int_{x_3>0}\frac{\epsilon\gamma(x)}{r^2}\exp\left[\frac{(2i\omega-\gamma_0)r}{v_0}\right]d^3x = \left(\frac{u_S(\zeta,\omega)}{\omega} - X_2(\zeta,\omega)\right). \quad (4.81)$$

The integral equation (4.81) is of convolution form, the function $\epsilon\gamma(x)$ being convolved with the function $r^{-2}\exp[(2i\omega-\gamma_0)r/v_0]$. As in the case of (4.61) to get Fourier transform in the closed form, we differentiate (4.81) with respect to ω. The result is

$$\int_{x_3>0}\epsilon\gamma(x)\,g_1(\zeta-x,\omega)\,d^3x = 2\pi v_0^3\frac{\partial}{\partial\omega}\left(\frac{u_S(\zeta,\omega)}{\omega} - X_2(\zeta,\omega)\right), \quad (4.82)$$

where $g_1(\zeta-x,\omega)$ is given by (4.63). Now we apply exactly the same procedure as applied to (4.62) to yield

$$\begin{aligned}\epsilon\gamma(x) &= -\frac{8iv_0^3}{\pi^2}\int_{-\infty}^{\infty}k_3d^3k\int_{-\infty}^{\infty}d^2\zeta\frac{\partial}{\partial\omega}\left[\frac{u_S(\zeta,\omega)}{\omega} - X_2(\zeta,\omega)\right]\\ &\quad \exp[2i(\kappa.(\rho-\zeta)-k_3x_3)]. \quad (4.83)\end{aligned}$$

Since, the data are recorded in the time domain, therefore writing $u_S(\zeta,\omega)$ and $X_2(\zeta,\omega)$ in their causal temporal Fourier representation further modifies the inversion formula (4.83) to be

$$\begin{aligned}\epsilon\gamma(x) &= \frac{8v_0^3}{\pi^2}\int_{-\infty}^{\infty} d^2\zeta \int_{-\infty}^{\infty} d^3k k_3 \exp\left[2i\left(\kappa.(\rho-\zeta)-k_3x_3\right)\right] \\ &\int_0^{\infty}\left[u_S(\zeta,t)\left(\frac{1}{\omega_0}+\frac{i}{\omega_0^2 t}\right)-X_2(\zeta,\omega_0)\right] t\exp\left[i\omega_0 t\right] dt. \qquad (4.84)\end{aligned}$$

Now the velocity and damping profiles can be improved by an iterative procedure. We substitute the damping profile from (4.84) in (4.80) and repeat all the steps of this subsection to get next approximation to the velocity profile. This velocity profile can then be used to get next approximation to the damping profile.

4.4 Conclusions

We have derived approximate solutions to the inverse problem of finding the velocity and damping from the observed wavefield. The approximations made are often used in modeling the inverse problem in seismic exploration. It is established in this work that the damping of the medium plays a role in getting a more accurate map of the subsurface. An iterative procedure to improve velocity and damping profiles is also presented.

We have presented a procedure to determine wavespeed and damping profiles of a medium with one dimension of parameter variability when the source and receiver are located at the same place for both one-dimensional and three-dimensional problems.

We also have assumed constant-background wavespeed and damping. Nevertheless, the inversion procedure presented in this chapter may provide a launching pad to attack more general problems:

- The derivation of inversion formulas for a variety of source-receiver geometries.
- The derivation of inversion formulas for two-dimensional parameter variability.
- The derivation of inversion formulas for variable-background and a variety of source-receiver geometries.

APPENDICES

Appendix A

Appendix for Chapter 2

A.1 Some Preliminaries

This Appendix contains the background material needed to study the contents of this Thesis, in particular, Chapter 2.

Definition 4 (Norm) *A norm is a mapping* $\|.\| : X \rightarrow R$ *on a vector space* X *and which has the following properties:*

- $\|x\| \geq 0$.
- $\|x\| = 0 \Longleftrightarrow x = 0$,
- $\|\alpha x\| = |\alpha| \, \|x\|$,
- $\|x + y\| \leq \|x\| + \|y\|$.

for all $x, y \in X$ *and any scalar* α.

The space X together with the norm defined above is called a **normed space.**

Definition 5 (Inner product) *Let* X *be a vector space over a field* F. *A mapping* $\langle ... \rangle : X \times X \rightarrow F$ *is called an inner product if it satisfies the following properties:*

1. $\langle u, v \rangle = \overline{\langle v, u \rangle}$ *where* $\overline{\langle v, u \rangle}$ *is the complex conjugate of* $\langle u, v \rangle$.

2. $\langle \alpha u + \beta v, w \rangle = \alpha \langle u, w \rangle + \beta \langle v, w \rangle$.

3. $\langle u, u \rangle \geq 0$. *equality holds iff* $u = 0$.

A vector space together with the inner product defined above is called an **inner product space**. An inner product on X defines a norm on X given by

$$\|u\| = \sqrt{\langle u, u \rangle}. \tag{A.1}$$

Hence inner product spaces are normed spaces. A **Hilbert space** is a complete inner product space. An important Hilbert space is $L^2[a, b]$, which consists of all measurable and square integrable function on $[a, b]$ in Lebesgue sense. A sequence of elements $\{f_n\}$ in H is said to be **orthonormal** if $\langle f_n, f_m \rangle = 1$ for $n = m$ and $\langle f_n, f_m \rangle = 0$ otherwise.

Definition 6 (Linear operator) *An operator* $T : X \to Y$, *where* X *and* Y *are vector spaces over the same field* F, *is said to be a linear operator if it satisfies*

$$T(\alpha u + \beta v) = \alpha T(u) + \beta T(v), \quad \text{for all } u, v \in X \text{ and } \alpha, \beta \in F. \tag{A.2}$$

In particular, if $Y = F$ then T is said to be a **linear functional**. If X and Y are normed spaces, then T is said to be a **bounded operator** if there exist $M > 0$, such that $\|Tx\| \leq M \|x\|$ for all $x \in X$. A linear operator $T : H \to H$ on a Hilbert space H is said to be **compact** if it maps every bounded subset S of H into relatively compact subset $T(S)$ of H, that is, $\overline{T(S)}$ is compact in H.

Definition 7 (Fredholm integral equations) *The integral equation of first kind can be written as*

$$g(x) = \lambda \int_a^b K(x,t) f(t)\, dt. \tag{A.3}$$

and the integral equation of second kind can be written as

$$g(x) = f(x) - \lambda \int_a^b K(x,t) f(t)\, dt. \tag{A.4}$$

where $f(x)$ is unknown. $g(x)$ and $K(x,t)$ are given and λ is a parameter. $K(x,t)$ is called kernel of the integral equations.

A.2 Singular Value Decomposition

Let X and Y be Hilbert spaces and $K : X \longrightarrow Y$ be a compact linear operator. Let $K^* : Y \longrightarrow X$ be **adjoint** of K i.e. for all $x \in X$ and $y \in Y$, $\langle Kx, y\rangle = \langle x, K^* y\rangle$. If K is densely defined and $K = K^*$, then K is said to be **self adjoint**. The nonnegative square roots of the eigenvalues of the nonnegative self adjoint compact operator $K^*K : X \rightarrow X$ are called **singular values** of K.

Definition 8 (Singular system) *A singular system $(\sigma_n; v_n, u_n)$ of the operator K is defined as follows:*

Let the non-zero eigenvalues $\{\sigma_n^2\}_{n\in N}$ of the selfadjoint operator K^*K (and also of KK^*) be written down in decreasing order with multiplicity. $\sigma_n > 0$. Then there exists a complete orthonormal sequence $\{v_n\}_{n\in N}$ of eigenvectors of K^*K (which spans

$\overline{R(K^*)} = \overline{R(K^*K)}$). *and the* $\{u_n\}_{n\in N}$ *are defined via the vectors*

$$u_n \doteq \frac{Kv_n}{\|Kv_n\|} \ . \tag{A.5}$$

The $\{u_n\}_{n\in N}$ *are complete orthonormal system of eigenvectors of* KK^* *and span* $\overline{R(K)} = \overline{R(KK^*)}$. *Also, the following formulae hold:*

$$Kv_n = \sigma_n u_n. \tag{A.6}$$

$$K^* u_n = \sigma_n v_n. \tag{A.7}$$

$$Kx = \sum_{n=1}^{\infty} \sigma_n \langle x, u_n \rangle v_n. \qquad x \in X. \tag{A.8}$$

$$K^* y = \sum_{n=1}^{\infty} \sigma_n \langle y, u_n \rangle v_n. \qquad y \in Y. \tag{A.9}$$

where these infinite series converge in the Hilbert space norm of X *and* Y.

Theorem 9 (Picard) *Let* $(\sigma_n; v_n, u_n)$ *be a singular system for the compact linear operator* $K : X \longrightarrow Y$. *Then the equation of first kind* $Kx = y$ *is solvable iff*

$$y \in N(K^*)^{\perp} = \overline{K(X)} \text{ and } \quad \sum_{n=1}^{\infty} \frac{|\langle y, u_n \rangle|^2}{\sigma_n^2} < \infty. \tag{A.10}$$

In this case the solution is given by

$$x = \sum_{n=1}^{\infty} \frac{\langle y, u_n \rangle}{\sigma_n} v_n. \tag{A.11}$$

The condition (A.10) for the existence of solution is called Picard criterion. It says that solution of $Kx = y$ exists only if the Fourier coefficients $\langle y, u_n \rangle$ decay fast enough relative to the singular values σ_n [45].

Appendix B

Appendix for Chapter 3

This Appendix contains the background material needed to study the contents of this Thesis. in particular, Chapter 3.

B.1 Direct Scattering

Consider the Schrödinger's equation

$$\frac{d^2u}{dx^2} + (\lambda - q(x))\,u = 0. \tag{B.1}$$

The properties of this equation are easy to discuss. although explicit solutions are nearly impossible to obtain. Since $q(x)$ is assumed to be absolutely integrable, $\int_{-\infty}^{\infty} |q(x)|\,dx < \infty$. we use variation of parameters to find integral equations for fundamental solutions of this equation. For example. solution of $u' + \lambda u = f$ can be written as

$$u = \frac{1}{2ik}\int_{x_0}^{x} e^{ik(x-y)} f(y)\,dy - \frac{1}{2ik}\int_{x_1}^{x} e^{-ik(x-y)} f(y)\,dy. \quad \lambda = k^2, \tag{B.2}$$

where x_0 and x_1 are arbitrary constants. We take $f(x) = q(x)u(x)$ and obtain

$$\phi(x,k) = e^{ikx} - \frac{1}{k}\int_x^\infty \sin k(x-y)\,q(y)\,\phi(y,k)\,dy. \tag{B.3}$$

$$w(x,k) = e^{-ikx} + \frac{1}{k}\int_{-\infty}^x \sin k(x-y)\,q(y)\,w(y,k)\,dy. \tag{B.4}$$

as two solutions of the Schrödinger's equation. Notice that $\phi(x,k)$ behaves like $\exp(ikx)$ as $x \to \infty$ and $w(x,k)$ behaves like $\exp(-ikx)$ as $x \to -\infty$.

These statements do not prove the existence of $\phi(x,k)$ and $w(x,k)$. The existence of these solutions can be proved by using contraction mapping theorem. The choice of $\exp(ikx)$ and $\exp(-ikx)$ as the asymptotic behavior of $\phi(x,k)$ and $w(x,k)$ are motivated by both mathematical and physical reasoning. For k in the upper half of the complex plane (which it is since $\lambda = k^2$ and we take k to be the principal square root of λ), $\exp(ikx)$ is square integrable for large positive x and $\exp(-ikx)$ is square integrable for large negative x. If we examine carefully the wave equation and its solutions, we see that the solution with spatial dependence $\exp(ikx)$ correspond to rightward moving waves, and those with spatial dependence $\exp(-ikx)$ correspond to leftward moving waves. Given this nomenclature, we see that the two solutions of Schrödinger's equation $\phi(x,k)$ and $\psi(x,k)$ are right moving as $x \to \infty$ and left moving as $x \to -\infty$, respectively. Also, it is easy to see that $\phi(x,-k)$ and $\psi(x,-k)$ are solutions of Schrödinger's equation as well.

We know that any second order differential equation can have at most two linearly

independent solutions, and that any solution can be represented as a linear combination of a linearly independent pair. Therefore we can express solutions $\varphi(x,k)$ and $\psi(x,k)$ as

$$\psi(x,k) = c_{11}(k)\,\varphi(x,k) + c_{12}(k)\,\varphi(x,-k). \tag{B.5}$$

$$\varphi(x,k) = c_{21}(k)\,\psi(x,-k) + c_{22}(k)\,\psi(x,k). \tag{B.6}$$

In expression $(B.5)$, $c_{12}(k)$ is the amplitude of an incoming wave from $x \to \infty$. $c_{11}(k)$ is the amplitude of wave reflected back to $x \to \infty$. We denote

$$T_r = \frac{1}{c_{12}(k)}. \qquad R_r = \frac{c_{11}(k)}{c_{12}(k)}. \tag{B.7}$$

as the **Transmission and Reflection Coefficients** for waves incident from the right. Similarly

$$T_L = \frac{1}{c_{21}(k)}. \qquad R_L = \frac{c_{22}(k)}{c_{21}(k)}. \tag{B.8}$$

are the transmission and reflection coefficients, respectively, for waves incident from the left.

There are some important consistency relationships between the coefficients $c_{ij}(k)$.

The definitions of $c_{ij}(k)$ hold if and only if

$$\begin{aligned} c_{11}(k)\,c_{21}(k) + c_{21}(k)\,c_{22}(-k) &= 0. \\ c_{11}(k)\,c_{22}(k) + c_{12}(k)\,c_{21}(-k) &= 1. \\ c_{11}(k)\,c_{22}(k) + c_{21}(k)\,c_{12}(-k) &= 1. \\ c_{11}(-k)\,c_{12}(k) + c_{22}(k)\,c_{12}(k) &= 0. \end{aligned} \tag{B.9}$$

We can calculate the Wronskian

$$\begin{aligned} W(\phi(x,k),\psi(x,k)) &= c_{12}(k)\,W(\phi(x,k),\phi(x,-k)) = -2ikc_{12}(k). \\ W(\phi(x,k),\psi(x,-k)) &= c_{22}(k)\,W(\psi(x,k),\psi(x,-k)) = 2ikc_{22}(k). \\ W(\phi(x,-k),\psi(x,k)) &= 2ikc_{11}(k). \end{aligned} \tag{B.10}$$

A zero of $c_{12}(k)$ with $\operatorname{Im} k > 0$, if it exists, has an important physical interpretation. If $c_{12}(k_0) = 0$, then $W(\phi(x,k_0),\psi(x,k_0)) = 0$ so that $\psi(x,k_0) = \alpha\phi(x,k_0)$ for some nonzero constant α. Since $\phi(x,k_0) \sim \exp(ik_0x)$ as $x \to \infty$ and $\psi(x,k_0) \sim \exp(-ik_0x)$ as $x \to -\infty$, we see that $\psi(x,k_0)$ is a square integrable solution of the Schrödinger's equation. Square integrable solutions, if they exist, are called **Bound States** and are analogous to eigenfunctions of the Sturm-Liouville problems. The term "bound state" refers to the fact that these wave functions are "bound" to the scattering center by the potential. It can be shown easily that the roots of $c_{12}(k) = 0$ in the upper half plane occur only on the imaginary axis and are always simple.

B.2 Inverse Scattering

We define the function $K(x,y)$ by

$$\varphi(x,k) = e^{ikx} + \int_x^\infty K(x,y)\, e^{iky} dy. \tag{B.11}$$

Although we know that $\varphi(x,k)$ is well defined, it is not immediately clear that $K(x,y)$ exists. To check its existence we substitute $\varphi(x,k)$ into the Schrödinger's equation and find after integration by parts that,

$$\begin{aligned} \frac{d^2\varphi}{dx^2} - q(x)\,\varphi + k^2\varphi \;=\; & \int_x^\infty \left[\frac{\partial^2 K(x,y)}{\partial x^2} - \frac{\partial^2 K(x,y)}{\partial y^2} - q(x)\,K(x,y)\right] e^{iky} dy \\ & + \lim_{y\to\infty}\left[\frac{\partial K(x,y)}{\partial y} - ikK(x,y)\right] e^{iky} \\ & - \left[2\frac{dK(x,x)}{dx} + q(x)\right] e^{ikx}. \end{aligned} \tag{B.12}$$

We require the kernel $K(x,y)$ to satisfy

$$\frac{\partial^2 K(x,y)}{\partial x^2} - \frac{\partial^2 K(x,y)}{\partial y^2} - q(x)\,K(x,y) = 0. \tag{B.13}$$

$$q(x) = -2\frac{dK(x,x)}{dx}, \tag{B.14}$$

$$\lim_{y\to\infty} \frac{\partial K(x,y)}{\partial y} = \lim_{y\to\infty} K(x,y) = 0. \tag{B.15}$$

It was proved by Gelfand and Levitan [36] that the function $K(x,y)$ exists and is unique.

From equation $(B.5)$, it follows that

$$\frac{1}{2\pi}\int_C T(k)\,\psi(x,k)\,e^{iky}dk = \frac{1}{2\pi}\int_C R(k)\,\phi(x,k)\,e^{iky}dk - \frac{1}{2\pi}\int_C \phi(x,-k)\,e^{iky}dk. \tag{B.16}$$

where C is the contour in the upper half k plane starting at $k = -\infty + i0^-$ and ending at $k = \infty + i0^-$ and it passes above all zeroes of $c_{12}(k)$. It is easy to show the following asymptotic relationship

$$\frac{\psi(x,k)}{c_{12}(k)}e^{ikx} = 1 - O\left(\frac{1}{k}\right), \qquad \text{as } k \to \infty. \tag{B.17}$$

where the notation $O\left(\frac{1}{k}\right)$, called "**Big O**", means a term which is bounded by $M\left|\frac{1}{k}\right|$ for some positive constant M and all sufficiently large k. Therefore, since $\psi(x,k)\,e^{ikx}$ is analytic in the upper half plane

$$\begin{aligned}\frac{1}{2\pi}\int_C T(k)\,\psi(x,k)\,e^{iky}dk &= \frac{1}{2\pi}\int_C \frac{\psi(x,k)\,e^{ikx}}{c_{12}(k)}e^{ik(y-x)}dk \\ &= \delta(x-y) + \frac{1}{2\pi}\int_C O\left(\frac{1}{k}\right)e^{ik(y-x)}dk. \end{aligned} \tag{B.18}$$

Using Jordan's lemma for $y > x$ we see that

$$\frac{1}{2\pi}\int_C T(k)\,\psi(x,k)\,e^{iky}dk = 0. \tag{B.19}$$

Now we use expressions $(B.11)$ and $(B.19)$ in $(B.16)$ to get

$$\begin{aligned} 0 &= \frac{1}{2\pi}\int_C R(k)\, e^{ik(x+y)}dk + \frac{1}{2\pi}\int_x^\infty \int_C R(k)\, K(x,s)\, e^{ik(s+y)}dkds \\ &\quad + \frac{1}{2\pi}\int_x^\infty \int_C K(x,s)\, e^{-ik(s-y)}dkds. \end{aligned} \tag{B.20}$$

provided $y > x$. We define

$$R(z) = \frac{1}{2\pi}\int_C R(k)\, e^{ikz}dk, \tag{B.21}$$

and finally obtain the equation

$$0 = R(x+y) + \frac{1}{2\pi}\int_x^\infty R(s+y)\, K(x,s)\, ds + K(x,y). \qquad \text{provided } y > x. \tag{B.22}$$

This equation is called Gelfand-Levitan and Marchenko (GLM) equation. The GLM equation is important because, if we can solve it for $K(x,y)$, then $q(x)$ can easily be computed from $(B.14)$. In other words, given the reflection coefficient $R(k)$, we can reconstruct the potential $q(x)$ whenever we can solve the GLM equation for $K(x,y)$. A good account of the material presented in this Appendix can be found in Lamb [52].

Appendix C

Appendix for Chapter 4

C.1 The Reflection Seismic Experiment

The essential features of an exploration seismic experiment are:

- Using controlled sources of seismic energy.
- Illumination of a subsurface target area with the downward propagating waves.
- Reflection, refraction, and diffraction of the seismic waves by subsurface heterogeneities.
- Detection of the back-scattered seismic energy on seismometers spread out on the Earth's surface.

On land, seismometers are called geophones. Generally they work by measuring the motion of a magnet relative to a coil attached to the housing and implanted in the Earth. The motion of the magnet relative to the coil produces a voltage which is proportional to the velocity of the displacement on the earth's surface. Seismic sources include, for example, dynamite, weight drops, and vibrators. Explosives like dynamite require some sort of hole to be drilled to contain the blast and the holes are then often filled with heavy mud in order to direct the energy of the blast downward. Weight drops involve a crane, from which

the weight is dropped from a considerable height. Small dynamite blasts and hydraulic vibrators are popular sources for very high-resolution near-surface studies.

C.1.1 Source-Receiver Configurations

Seismic surveys are limited to ensembles of experiments with a nonzero offset between sources and their respective receivers. Each of the experiments composing the ensemble usually consists of an arrangement involving one source and several receivers, all in a line, called a shot profile. Data may be grouped into several possible categories based on the particular source-receiver configuration that was used to acquire the individual shot profiles.

1. **Zero-Offset Data:** consist of seismograms recorded when source and receiver are placed next to each other on the surface of the earth; so close in fact they are effectively at the same location. With this arrangement we can record the seismic echoes from the same point whence they originated.

2. **Common Source (Shot) Profiles:** It consist of seismograms recorded at positions of increasing range from a given source. The geometry of such an experiment is shown in Fig. C.1.a.

3. **Common Offset Profiles:** It consist of seismograms recorded at positions along the surface of the earth with the distance between the source and receiver held constant. Its scheme is shown in Fig. C.1.b.

The world-widely used arrangement in practice is the "common midpoint" geometry, which can be used to approximate zero-offset profiles after proper processing steps.

C.2 Bandlimited Data and its Causes

Consider the set of points x where $f(x) \neq 0$: the **support** of f is the closure of this set. A function whose Fourier transform has a bounded support is said to be **bandlimited** and in this case the support is called band of the function. For instance, consider the function defined by $f(x) = \sin(\pi x)/\pi x$. it is bandlimited because it is the inverse Fourier transform of the characteristic function of the interval $[-\pi, \pi]$. In this case we call π the bandwidth of the function f. A basic property of a bandlimited function is the possibility of representing such a function, without any loss of information, by means of its samples taken at equidistant points.

Bandlimiting of observed data has a variety of causes. We list a few major causes below:

- The frequency of the seismic source is related to the finite nonzero action time and physical geometry of the source mechanism. Equally important is the coupling between the source and the propagating medium.

- The presence of small heterogeneities, randomly distributed in the interior of the earth, scatter the high frequency energy in an incoherent fashion, preventing an image of gross structure being constructed with waves of too high a frequency. Thus higher-frequency signals do not always guarantee better resolution.

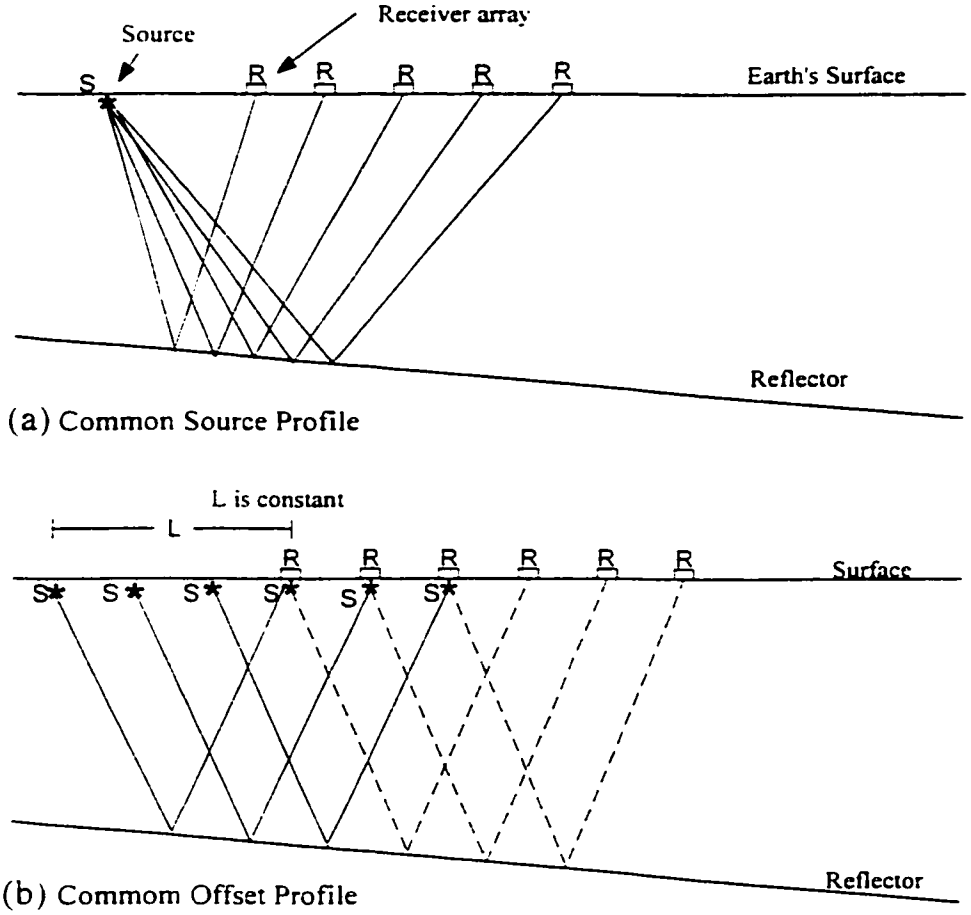

Figure C.1: Geometry of the source receiver array.

- The geophone is not rigidly attached to the earth, bandlimiting associated with natural resonances of the soil-geophone system exists.

- The seismic detectors and recorders contain built-in filter to limit ambient noise level.

Although the causes of bandlimiting are clearly complicated, it is satisfactory to treat these processes as the action of a single filter, $F(\omega)$, which may be assumed to have necessary properties (such as a symmetric real part and antisymmetric imaginary part to produce a real valued output).

C.2.1 Reflectivity Function

The reflectivity function of a surface is defined to be the normal reflection strength multiplied by the singular function. The reflectivity function locates the boundary of the scattering object and characterizes the change in medium properties through the normal reflection coefficient. If the discontinuities are our primary interest then bandlimited delta functions are easier to identify than bandlimited step functions.

C.3 WKBJ Approximation and Amplitude Calculation of the Inverse Fourier Integral

C.3.1 WKBJ Approximation

WKBJ theory is a powerful tool for obtaining a global approximation to the solution of a linear differential equation whose highest derivative is multiplied by a

small parameter ϵ. This theory is suitable for linear differential equations of any order, for initial value and boundary value problems, and for eigenvalue problems.

Dissipative and dispersive phenomena are both characterized by exponential behavior, where the exponent is real in the former case and imaginary in the latter case. Thus for a differential equation that exhibits either or both kinds of such behavior, it is natural to seek an approximate solution of the form

$$u(x) \sim \exp\left[\frac{1}{\delta}\sum_{n=0}^{\infty}\delta^n S_n(x)\right]. \qquad \delta \to 0. \tag{C.1}$$

This expression is the starting formula from which all WKBJ approximations are derived. The WKBJ theory is singular perturbation theory because it is used to solve a differential equation whose highest order derivative is multiplied by a small parameter. When the small parameter vanishes, the order of differential equation changes abruptly.

Example 10 *Consider the boundary value problem*

$$\epsilon u_{xx} + a(x)\,u_x + b(x)\,u = 0, \quad u(0) = A, \quad u(1) = B, \tag{C.2}$$

where we assume that $a(x) > 0$ *for* $0 \le x \le 1$ *and* $\epsilon \to 0^+$. *We begin by substituting* (C.1) *in* (C.2) *and neglecting terms which vanish as* $\delta \to 0$. *The result is*

$$\frac{\epsilon}{\delta^2}\left(\frac{dS_0}{dx}\right)^2 + 2\frac{\epsilon}{\delta}\frac{dS_0}{dx}\frac{dS_1}{dx} + \frac{\epsilon}{\delta}\frac{d^2S_0}{dx^2} + \frac{1}{\delta}\frac{dS_0}{dx}a + \frac{dS_1}{dx}a + b + \ldots = 0. \tag{C.3}$$

The largest term in this expression is the first term and the second largest is fourth term. By dominant balance these two terms must be of equal magnitude and this can be achieved if δ is proportional to ϵ and for simplicity we choose $\delta = \epsilon$. So in (C.3) let us compare coefficients of ϵ^{-1} and ϵ^0. The resulting equations

$$\left(\frac{dS_0}{dx}\right)^2 + \frac{dS_0}{dx}a = 0. \tag{C.4}$$

and

$$2\frac{dS_0}{dx}\frac{dS_1}{dx} + \frac{d^2S_0}{dx^2} + \frac{dS_1}{dx}a + b = 0. \tag{C.5}$$

are easy to solve. The two independent solutions of (C.4) and (C.5) are

$$u_1(x) \sim c_1 \exp\left[-\int_0^x \frac{b(t)}{a(t)}dt\right]. \quad \epsilon \to 0^-. \tag{C.6}$$

$$u_2(x) \sim \frac{c_2}{a(x)} \exp\left[\int_0^x \frac{b(t)}{a(t)}dt - \frac{1}{\epsilon}\int_0^x a(t)\,dt\right]. \quad \epsilon \to 0^+. \tag{C.7}$$

where c_1 and c_2 are constants which can be determined from the boundary conditions given in (C.2). The general solution is given by

$$\begin{aligned} u(x) \sim\ & B\exp\left[\int_x^1 \frac{b(t)}{a(t)}dt\right] + \frac{a(0)}{a(x)}\left[A - B\exp\left(\int_0^1 \frac{b(t)}{a(t)}dt\right)\right] \\ & \exp\left[\int_0^x \frac{b(t)}{a(t)}dt - \frac{1}{\epsilon}\int_0^x a(t)\,dt\right]. \end{aligned}$$

C.3.2 Amplitude Calculation of the Inverse Fourier Integral

The inversion operator for (4.11) has the form

$$a(y) = \int_{-\infty}^{\infty} b(y,\omega)\, u_S(0,\omega) \exp[2i\omega\phi(y,0)]\, d\omega. \tag{C.8}$$

where $b(y,\omega)$ is to be determined. To see the form of $b(y,\omega)$, substitute (4.11) in the above expression to get

$$\begin{aligned} a(y) &= -\int_0^{\infty} dx \frac{a(x) A^2(x)}{4c(x)} \int_{-\infty}^{\infty} F(\omega)\, b(y,\omega) \exp[2i\omega\phi(x,y)]\, d\omega \\ &= \int_0^{\infty} a(x) f(x,y)\, dx. \end{aligned} \tag{C.9}$$

Equation (C.9) will be at least approximately satisfied if we set

$$f(x,y) = \delta_B(x-y) = \frac{1}{2\pi} \int_{-\infty}^{\infty} F(\omega) \exp[i\omega(x-y)]\, d\omega. \tag{C.10}$$

where $\delta_B(x-y)$ is bandlimited delta function. If $b(y,\omega)$ is independent of ω, that is, $b(y,\omega) = b(y)$, then

$$\begin{aligned} f(x,y) &= -\frac{2\pi A^2(x)\, b(y)}{4c^2(x)} \delta_B[2\phi(x,y)] \\ &= -\frac{\pi A^2(y)\, b(y)}{4c(y)} \delta_B(x-y). \end{aligned} \tag{C.11}$$

The second line in the above expression follows from the first because $\frac{2}{c(x)}$ is the derivative of the argument of the delta function and the support of the delta function is $x = y$. These are asymptotic equalities depending upon sufficiently high frequencies.

The choice of $b(y)$ to make $(C.9)$ true is now apparent

$$b(y) = -\frac{4c(y)}{\pi A^2(y)}. \tag{C.12}$$

This leads to inversion formula given by (4.12).

The inversion amplitude for (4.25) can easily be deduced by comparing it with (4.11). We have to make the following replacements

- replace $-A^2(x)/4c^2(x)$ by

  $A(x_g, x)\, A(x_s, x) \exp\left\{-\frac{1}{2}\left[w(x_g, x) + w(x_s, x)\right]\right\} / 2v_0^3(x).$

- replace the argument $2\varphi(x, 0)$ by $\left[\varphi(x_g, x) + \varphi(x_s, x)\right]$.

With these changes in place the amplitude $b(y)$ is given by

$$b(y) = \frac{2v_0^2(y) \exp\left\{\frac{1}{2}\left[w(x_g, y) + w(x_s, y)\right]\right\}}{\pi A(x_g, y)\, A(x_s, y)}. \tag{C.13}$$

Similarly inversion amplitude for (4.31) can be found by making appropriate changes.

Bibliography

[1] Abel, N. H. Resolution d' un probleme de mecanique. *Journal fur die reine und angewandte Mathematik*. Bd 1(97). (1826).

[2] Achenbach. J. D. *Wave Propagation in Elastic Solids*. North-Holland Publishing Company, Amsterdam. 1980.

[3] Adorf, H. -M. Hubble space telescope image reconstruction in its fourth year. *Inverse Problems*, 11:639–653. (1995).

[4] Aki, K., and Richards. P. G. *Quantitative Seismology: Theory and Methods*. W. H. Freeman and Company. San Francisco. 1980.

[5] Al-Khalidy, N. On the solution of parabolic and hyperbolic inverse heat conduction problems. *Int. J. Heat Mass Transf.*, 41:3731–3740. (1998).

[6] Armstrong, J. A., and Bleistein, N. An analysis of the aperture limited Fourier inversion of characteristic functions. Technical Report MS-R-7812, Univ. of Denver Math. Dept., (1978).

[7] Artley, C., and Hale, D. Dip moveout processing for depth-variable velocity. *Geophysics*, 59(4):610–622, (1994).

[8] Barcilon, V. A discrete model of the inverse Love wave problem. *Geophysics J. R. Astron. Soc.*, 44:61–76, (1976).

[9] Beck, J. V., Blackwell, B., and Clair, C. R. St. *Inverse Heat Conduction: Ill-Posed Problems.* Wiley Intersc., New York, 1985.

[10] Bender, C. M., and Orszag, S. A. *Advanced Mathematical Methods for Scientists and Engineers.* McGraw-Hill Book Company, New York, 1978.

[11] Berkhout, A. J., and Verschuur, D. J. Estimation of multiple scattering by iterative inversion, i. Theoretical considerations. *Geophysics*, 62:1586–1595, (1997).

[12] Black, J. L., Schleicher, K. L., and Zhang, L. True amplitude imaging and dip moveout. *Geophysics*, 58:47–66, (1993).

[13] Bleistein, N. *Mathematical Methods for Wave Phenomena.* Academic Press Inc., New York, 1984.

[14] Bleistein, N. On imaging of reflectors in the earth. *Geophysics*, 52:931–942, (1987).

[15] Bleistein, N., and Cohen, J. K. Nonuniqueness in the inverse source problem in acoustics and electromagnetic. *J. Math. Phy.*, 18:194–201, (1977).

[16] Bleistein, N., Cohen, J. K., and Hagin, F. G. Computational and asymptotic aspects of velocity inversion. *Geophysics*, 50:1253–1265, (1985).

[17] Bleistein, N., Cohen, J. K., and Jaramillo, H. True amplitude transformation to zero offset of data from curved reflectors. *Geophysics*, 64:12–129, (1999).

[18] Bleistein, N., Cohen, J. K., and Stockwell, J. W. *Mathematics of Multi-dimensional Seismic Inversion.* Springer Verlag, New York, 2000.

[19] Born, M., and Wolf, E. *Principles of Optics.* Pergamon Press, 6th edition, 1980.

[20] Cara, M. Regional variations of higher mode phase velocities: A spatial filtering method. *Geophys. J. R. Astron. Soc.*, 54:439–460, (1978).

[21] Carslaw, H. S., and Jaeger, J. C. *Conduction of Heat in Solids.* Oxford Univ. Press, London, 1959.

[22] Chadan, K., and Sabatier. P. C. *Inverse Problems in Quantum Scattering Theory.* Springer Verlag, New York, 1977.

[23] Claerbout. J. F. Towards the unified theory of reflector mapping. *Geophysics.* 36:467–481, (1971).

[24] Clayton, R. W., and Stolt, R. H. A Born WKBJ inversion method for acoustic reflection data. *Geophysics.* 46:1559–1568. (1981).

[25] Cohen. J. K., and Bleistein. N. An inverse method for determining small variations in propagation speed. *SIAM J. Appl. Math.*, 32(4):784–799. (1977).

[26] Cohen. J. K., and Bleistein. N. The singular function of a surface and physical optics inverse scattering. *Wave Motion.* 1:153–161. (1979).

[27] Cohen, J. K., and Bleistein, N. Velocity inversion procedure for acoustic waves. *Geophysics*, 44(6):1077–1087. (1979).

[28] Cormack. A. M. Early two-dimensional reconstruction and recent topics stemming from it. (Noble Prize Lecture). *Science*, 209:1482–1486. (1980).

[29] de Hoop, M., and Bleistein, N. Generalised Radon transform inversions for reflectivity in anisotropic elastic media. *Inverse Problems*, 13:669–690, (1997).

[30] Devaney, A. J. Nonuniqueness in the inverse scattering problem. *J. Math. Phys.*, 19(7):1526–1531, (1978).

[31] Devaney, A. J., and Sherman, G. C. Nonuniqueness in inverse source and scattering problems. *IEEE Trans. Biomed. Eng.*, 30:377–386, (1982).

[32] L. Elden. Modified equations for approximating the solution of a Cauchy problem

for the heat equation. In H. W. Engl and C. W. Groetsch, editors. *Inverse and Ill-Posed Problems*, pages 345–350. Academic Press, Inc., Orlando, 1987.

[33] Engl, H. W., and Groetsch, C. W. *Inverse and Ill-posed Problems*. Academic Press, Orlando, 1987.

[34] Engl, H. W., Hanke, M., and Neubauer, A. *Regularization of Inverse Problems*, Kluwer, Dordrecht, 1996.

[35] Gardner, G. H. F., and Forel, D. Amplitude preservation equations for dip moveout. *Geophysics*, 55:485–487, (1995).

[36] Gel'fand, I. M., and Levitan, B. M. On the determination of a differential equation by its spectral function. *American Math. Soc. Transl.*, 1:253–304, (1955).

[37] Gerver, M. L. Inverse problem for the one-dimensional wave equation. *Geophys. J. Roy. Astron. Soc.*, 21:337–357, (1970).

[38] Gerver, M. L., and Kazdan, D. A. Finding a velocity profile from a Love wave dispersion curve: problems of uniqueness. In V. I. Keilis-Borok, editor, *Computational Seismology*. Consultant Bureau, New York, 1972.

[39] Gerver, M. L., and Markushevitch, V. Determination of a seismic wave velocity from the travel time curve. *Geophys. J. Royal astron. Soc.*, 11:165–173, (1966).

[40] Gopinath, B., and Sondhi, M. M. Inversion of the telegraph equation and synthesis of nonuniform lines. *Proc. IEEE*, 59:383, (1971).

[41] Gratzke, U., Kapadia, P. D., and Dowden, J. Heat conduction in high-speed laser welding. *J. Phys. D: Appl. Phys.*, 24:2125–2134, (1991).

[42] Gray, S. H. A second order procedure for one dimensional velocity inversion. *SIAM J. Appl. Math.*, 39:456–462, (1980).

[43] Gray, S. H. Frequency-selective design of the Kirchhoff migration operator. *Geophysics*, 40:565–572. (1992).

[44] Gray, S. H. Kirchhoff migration using Eikonal equation traveltime. *Geophysics*. 59(5):810–817. (1994).

[45] Groetsch. C. W. *Generalized Inverses of Linear Operators: Representation and Approximation*. Dekker, New York, 1977.

[46] Hanitzsch. C. Comparison of weights in prestack amplitude-preserving Kirchhoff depth migration. *Geophysics*, 62:1812–1816. (1997).

[47] Hensel. E. *Inverse Theory and Applications for Engineers*. Prentice Hall. New Jersey. 1991.

[48] Herglotz. G. Über das Benndorfsche Problem des Fortpflanzungsgeschwindigkeit der Erdbebenstrahlen. *Zeitschrift für Geophys.*, 8:145–147. (1907).

[49] Hopcraft. K. I., and Smith. P. R. *An Introduction to Electromagnetic Inverse Scattering*. Kluwer, Dordrecht, 1992.

[50] Kay, I., and Moses, H. E. *Inverse Scattering Papers 1955-1963 (Lie Groups: History, Frontiers and Applications Vol. 12)*,. Math. Sci. Press, Brookline. M. A.. 1983.

[51] Keller, J. B., Kay, I., and Shmoys, J. Determination of potential from scattering data. *Phys. Rev.*. 102:557–559, (1956).

[52] Lamb, G. L. Jr. *Elements of Soliton Theory*. John Wiley and Sons, New York, 1980.

[53] Liner, C. L. Born theory of wave equation dip moveout. *Geophysics*, 56:182–189, (1991).

[54] Mager. R. D., and Bleistein, N. An examination of the limited aperture problem of physical optics inverse scattering. *IEEE Trans. Ant. Prop.*. AP-25:695–699. (1978).

[55] Marchenko. V.A. Concerning the theory of a differential operator of second order. *Doklady Acad. Nauk. SSSR.* 72:457–460. (1950).

[56] Masood. K.. and Zaman. F. D. An initial inverse problem of heat conduction in a plate with a hyperbolic model. *Intern. Math. Journal.* 2(3):237–251. (2002).

[57] Masood. K., Messaoudi. S.. and Zaman. F. D. Initial inverse problem in heat equation with Bessel operator. *Int. Journal of Heat and Mass Transfer.* 45(14): 2959–2965. May 2002.

[58] Morse. P. M.. and Feshbach. H. *Methods of Theoretical Physics.* McGraw-Hill. New York. 1953.

[59] Nakamura. G., Saitoh. S.. and Syarif. A. Representation of initial heat distribution by means of their heat distribution as a function of time. *Inverse Problems.* 15:1255–1261. (1999).

[60] Newton. R.G. Inverse scattering. i. One dimension. *J. Math. Phys.*. 21(3):493–505. (1980).

[61] Newton. R.G. Inverse scattering. ii. Three dimensions. *J. Math. Phys.*. 21(7): 1698–1715. (1980).

[62] Newton, R.G. Inverse scattering. iii. Three dimension, continued. *J. Math. Phys.*, 22(10):2191–2200, (1981).

[63] Raz, S. Three dimensional velocity profile inversion from finite offset scattering data. *Geophysics*, 46, (1981).

[64] Rutherford, E. The scattering of alpha and beta particles by matter and the structure of the atom. *Phil. Mag. Ser.*, 21:669–688, (1911).

[65] Stakgold. I. *Boundary Value Problems of Mathematical Physics*. volume 2. The Macmillan Company. New York, 1968.

[66] Tatarski. V. I. *Wave Propagation in a Turbulent medium*. McGraw-Hill. New York, 1961.

[67] Tygel. M.. Schleicher. J.. Hubral. P.. and Santos. L. T. 2.5-D true-amplitude Kirchhoff migration to zero offset in laterally inhomogeneous media. *Geophysics*. 63(2):557–573. (1998).

[68] van Heijst. H. J.. and Woodhouse. J. H. Measuring surface wave overtone phase velocities using a mode-branch stripping technique. *Geophys. J. Int.*. 131:209–230. (1997).

[69] Vedavarz. A.. Mitra. K.. and Kumar. S. Hyperbolic temperature profiles for laser surface interactions. *J. Appl. Phys.*. 76(9):5014–5021. (1994).

[70] Ware. J. A.. and Aki. K. Continuous and discrete inverse scattering problems in a stratified elastic medium. i. Plane waves at normal incidence. *J. Acoust. Soc. Am.*. 45:911–921. (1969).

[71] Weber. C. F. Analysis and solution of ill-posed inverse heat conduction problems. *Int. J. Heat mass transfer*. 24:1783–1792. (1981).

[72] Wiechert. E. Über Erdbebenwellen. I. Theoretisches über die Ausbreitung der Erdbedenwellen. *Nachr. Ges. Wiss. Göttingen, Math.-Phys. Klasse*. pages 415–529. (1907).

[73] Xu. M. Amplitude calculation for 3-d common offset v(z) inversion. Technical Report CWP-213. Colorado School of Mines. (1996).

[74] Zaman. F. D.. and Masood. K. An inverse problem in hyperbolic heat equation. In *The First Saudi Science Conference*. pages 377–386. Dhahran. Saudi Arabia. April (2001). KFUPM Press.

[75] Zaman, F. D., and Masood, K. An inversion procedure for the recovery of propagation speed and damping of the medium. *IL Nuovo Cimento 'C'*, (in press).

VITA

- Joined the Ph. D. program at King Fahd University of Petroleum & Minerals in Sep. 1997.
- Worked as a senior teacher in different institutions in United Arab Emirates from 1994 to 1997
- Received the Master of Arts degree in Mathematics from the State University of New York at Buffalo, New York, USA in Feb. 1993.
- Received the M. Phil. degree in Applied Mathematics from the Quaid-i-Azam University, Islamabad, Pakistan in Feb. 1990.
- Received the Master of science degree in Applied Mathematics from the Government College, Lahore, Pakistan in 1987.
- **Research Interests:** Direct and Inverse Boundary Value Problems, Applied Mathematics.